

AD-A080 894

RAYTHEON CO SUDBURY MASS EQUIPMENT DEVELOPMENT LABS
DIGITAL TRANSMISSION SYSTEM.(U)

F/8 9/2

OCT 79 M UNKAUF, P DANIS, C ALEMEYER

F30602-76-C-0217

UNCLASSIFIED

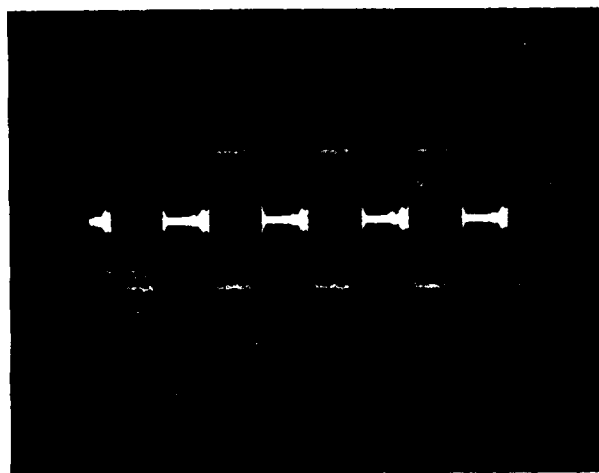
RADC-TR-79-250

ML

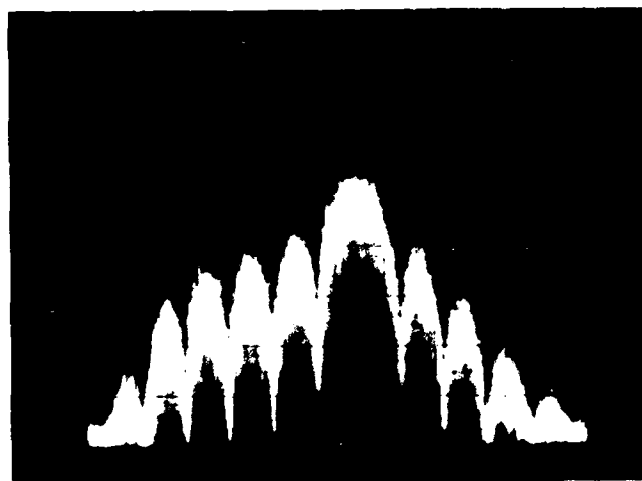
2 3

AD-A080894





DAR-IV TRANSMISSION WAVESHAPE



DAR-IV TRANSMISSION WAVEFORMS
1.75 MB/S

FIGURE 4-3. DAR-IV Transmission Waveforms

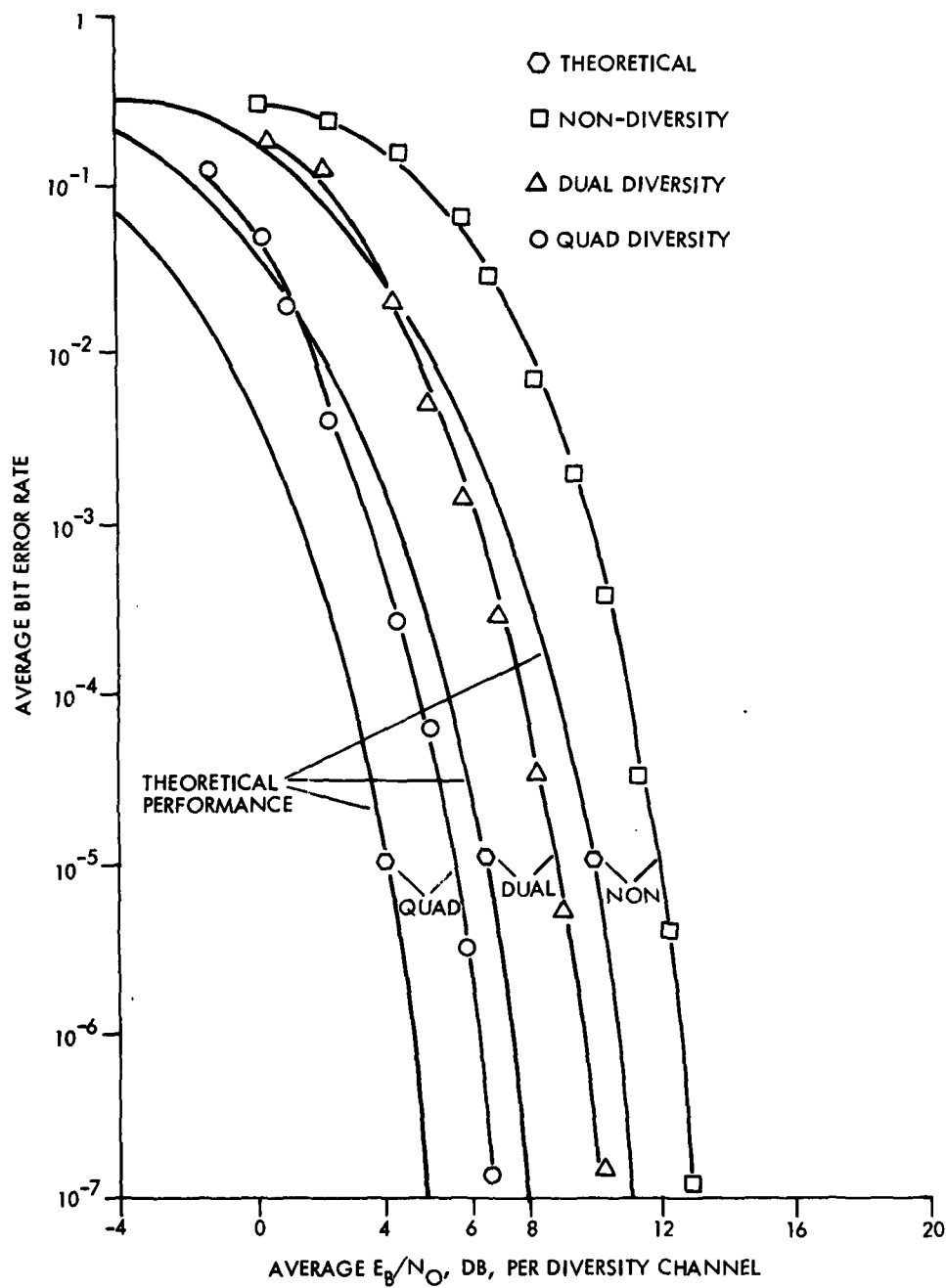


Figure 4-4. Back-To-Back Performance 1.75 MB/S
Non, Dual and Quad Diversity

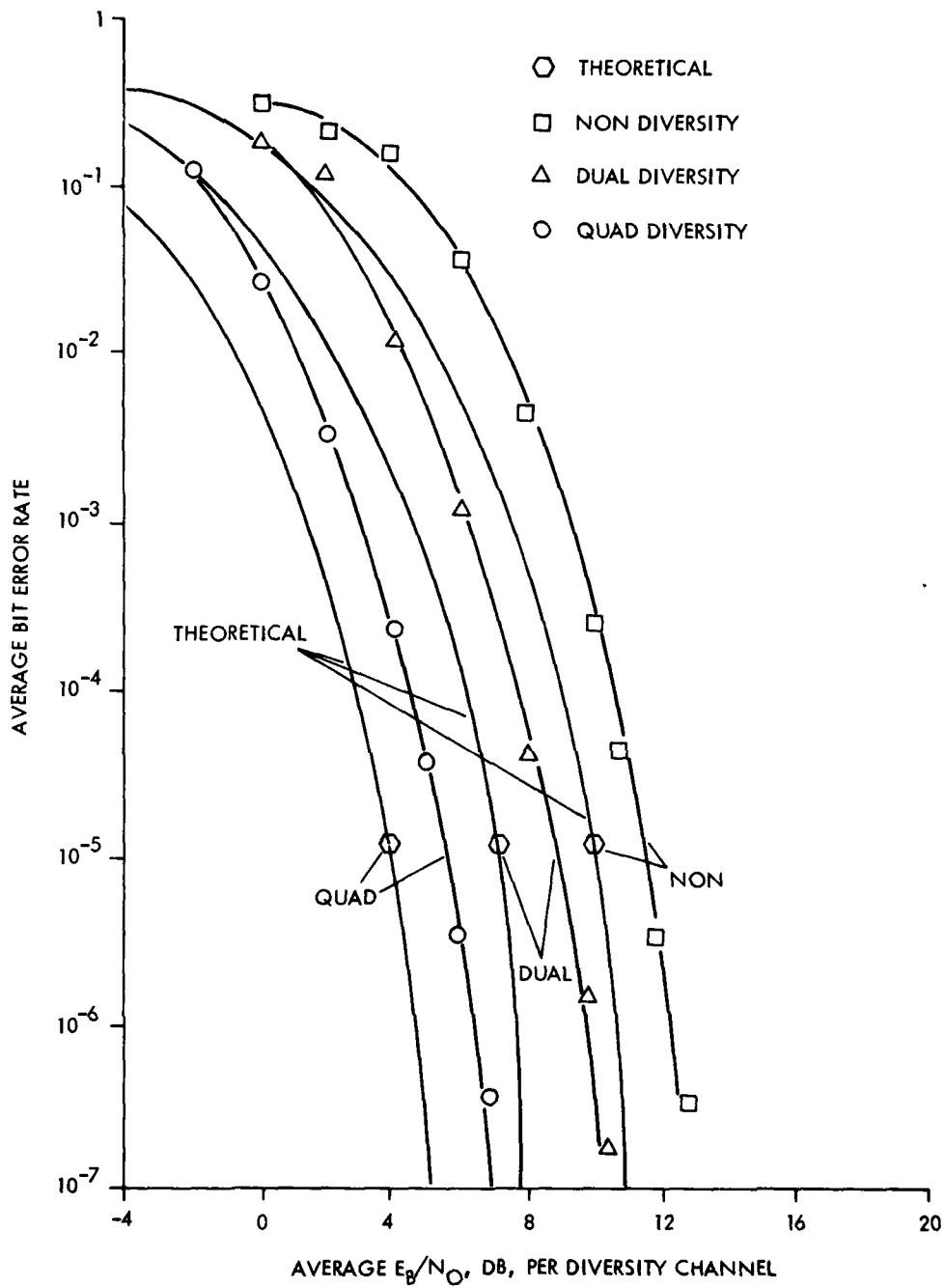


Figure 4-5. Back-To-Back Performance 3.5 MB/S
Non, Dual and Quad Diversity

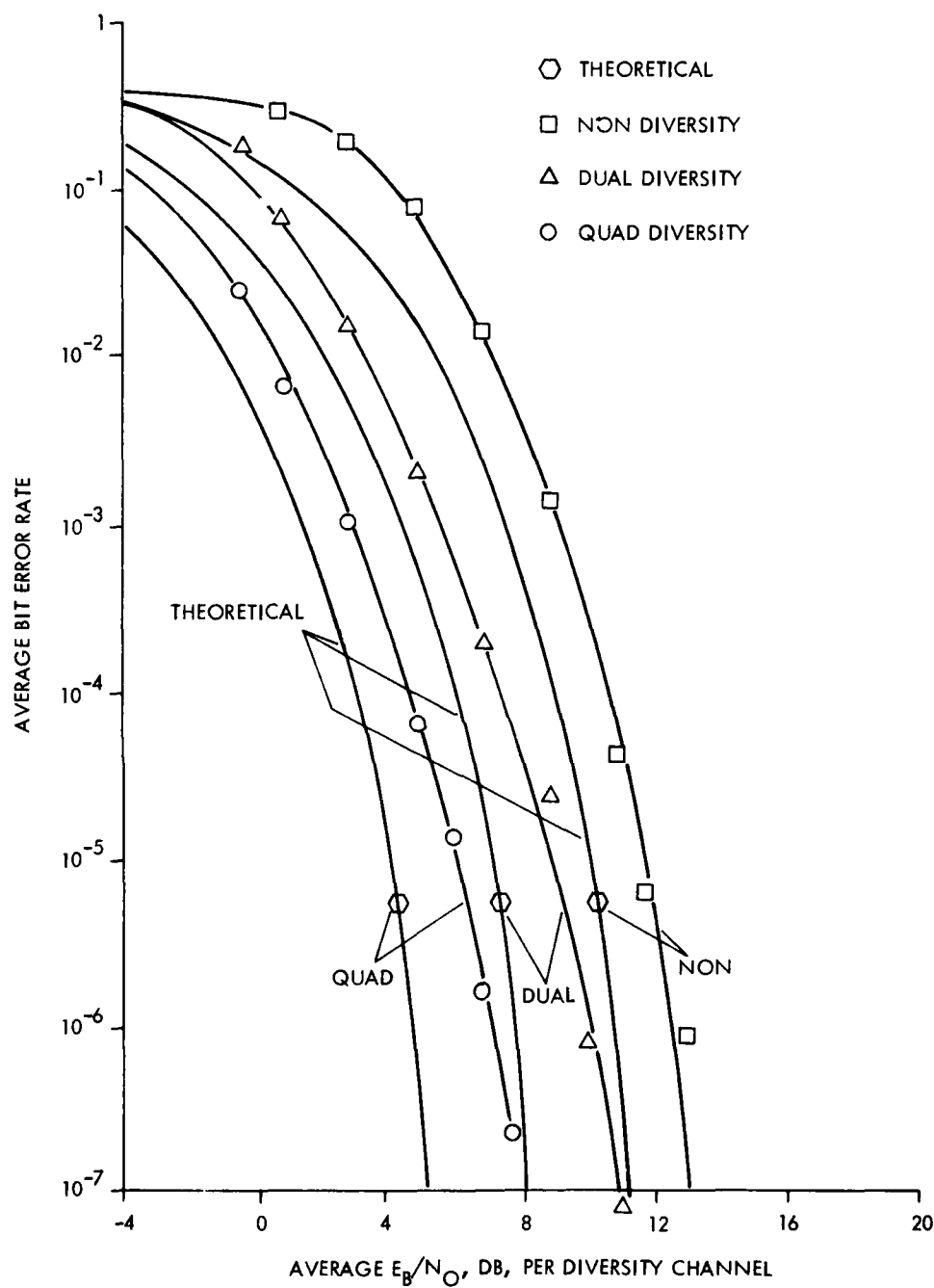


Figure 4-6. Back-To-Back Performance 7.0 MB/S
Non, Dual and Quad Diversity

0.5 to 1.0 dB was observed which is to be expected in the absence of multipath. The resultant overall implementation loss (at 10^{-5} BER) was then approximately 2 to 3 dB depending on the order of explicit diversity when the DFE was employed. Without multipath the DFE losses are created by the fact that the DFE will make minor corrections for intersymbol interference even when none is present due to the presence of a noisy signal and quantization errors in the DFE loop. The DFE thus introduces a jitter or additional noise term and is, therefore, only employed when intersymbol interference is likely to be a more important performance limitation than thermal noise.

Figure 4-7, 4-8 and 4-9 show the effect of the equalizer in the back-to-back configuration for 1.75 Mb/s, 3.5 Mb/s and 7.0 Mb/s, respectively.

4.7.4 Operation Over Temperature

The temperature effect on back-to-back performance is shown in Figure 4-10 for three temperatures; 60°F, 105°F and room temperature which was 78°F. Data was taken at 7.0 Mb/s quad diversity. At a BER of 10^{-5} , the BER E_b/N_0 curve is degraded by only 0.4 dB over the temperature range. The test was run with the transmitter in one oven and the receiver in another.

4.7.5 Demodulator Interchangeability

Demodulator interchangeability was measured by swapping Channel #1 with Channel #4 and Channel #2 with Channel #3. The results are plotted in Figure 4-11, 4-12 and 4-13. As expected, there is little difference in the results.

4.7.6 On-Line Performance Assessments

The DTS modem contains an on-line BER monitor. The error rate displayed is determined by counting the number of frame errors committed in a given interval. Table 4-1 is a comparison of the displayed error rate with an actual BER measurement under non-fading conditions.

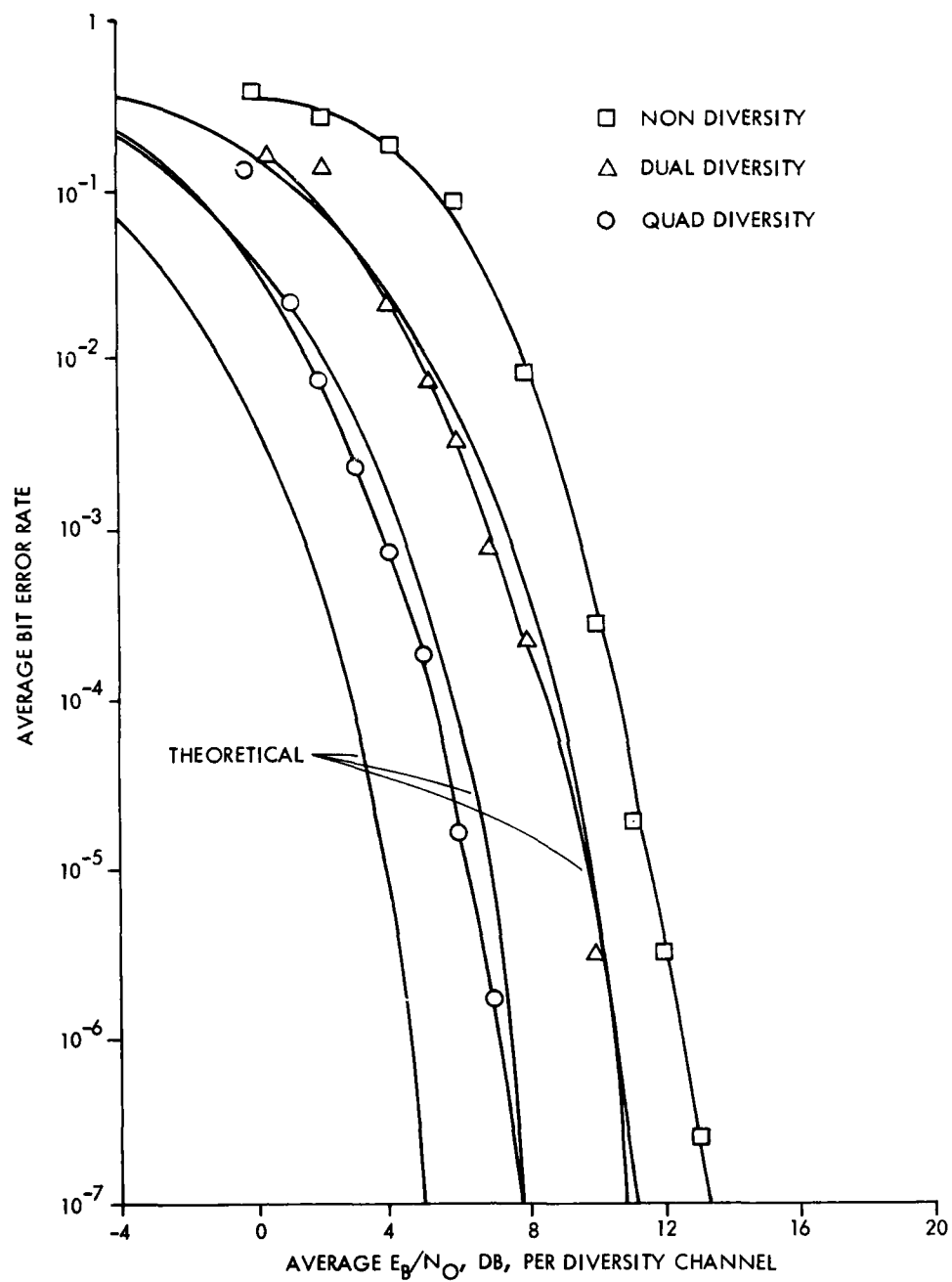


Figure 4-7. Back-to-Back Performance 1.75 MB/S Non, Dual and Quad Diversity with Equalizer On

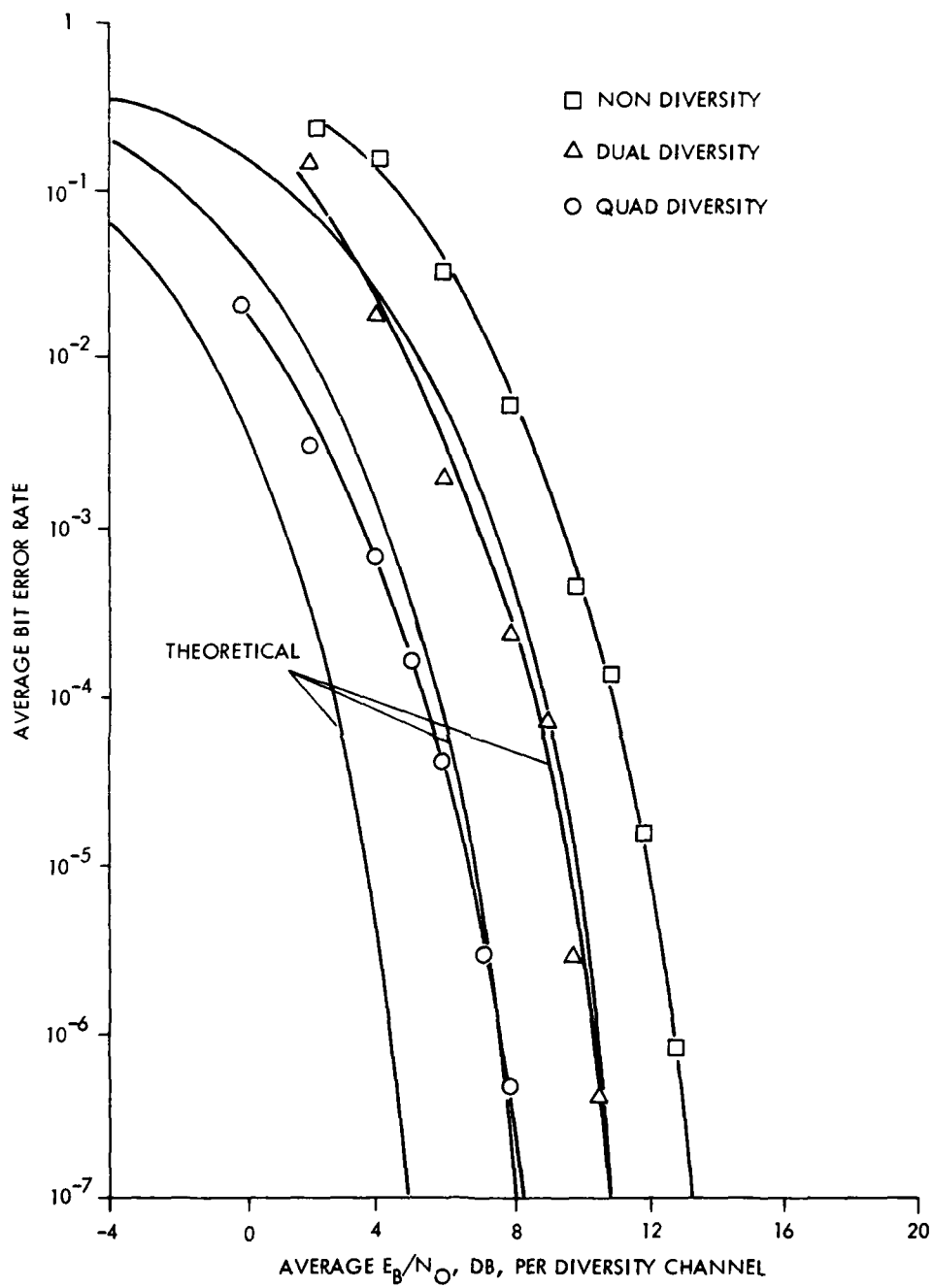


Figure 4-8. Back-to-Back Performance 3.5 MB/S Non, Dual and Quad Diversity with Equalizer On

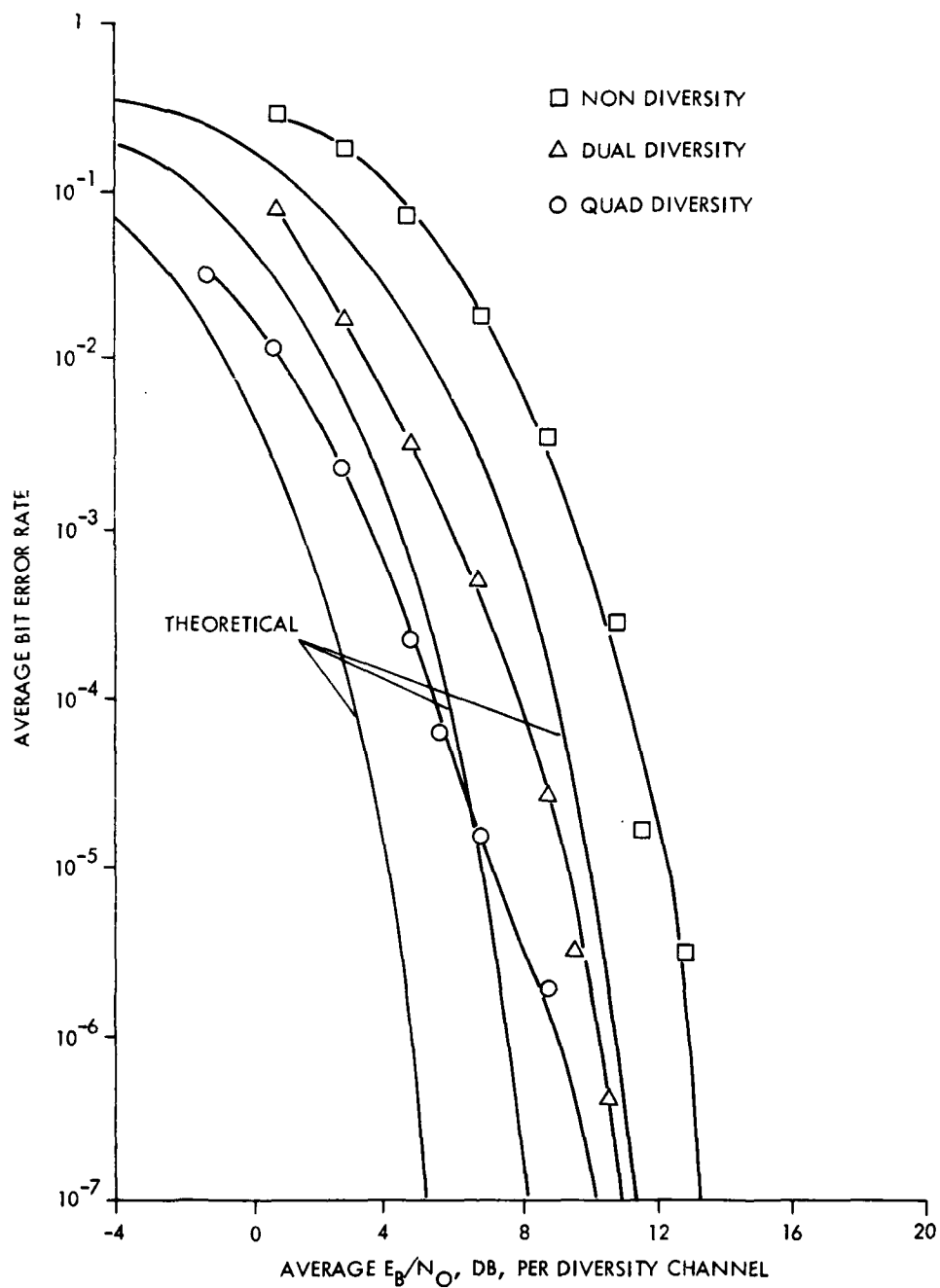


Figure 4-9. Back-to-Back Performance 7.0 MB/s Non, Dual and Quad Diversity with Equalizer On

Data was taken at the 1.75 Mb/s transmission rate with a range of 0.0 to 8.0 in E_b/N_o in 1 dB steps. The frame error display of the modem receiver agreed within 0.4×10^{-3} from 2.0×10^{-2} down to 1.2×10^{-4} BER. At this lower BER, the performance assessment display switches to a different count format that requires 10 times as many frames to obtain an update on the display. At this transition region, the discrepancy between the display and actual BER will be the largest, but it still is an excellent approximation of BER.

TABLE 4-1. BER DISPLAY VERSUS ACTUAL

E_b/N_o	Frame Error Rate Display	Measured BER
0.0	2.9×10^{-2}	2.8×10^{-2}
2.0	5.6×10^{-3}	5.6×10^{-3}
3.0	1.3×10^{-3}	1.2×10^{-3}
4.0	6.4×10^{-4}	6.0×10^{-4}
5.0	1.5×10^{-4}	1.2×10^{-4}
6.0	1.4×10^{-4}	3.5×10^{-5}
7.0	6.0×10^{-6}	7.5×10^{-6}
8.0	* 0.0×10^{-6}	1.2×10^{-6}

*Indicates lowest reading of display meter.

4.7.7 Analog Orderwire Performance

A measure of the performance of the analog orderwire card was made by inserting a 1 KHz sine wave into the TX modem orderwire input and observing the quality of the receiver output.

The analog orderwire input and output are shown in Figure 4-14. The transmission rate was set at 7.0 Mb/s.

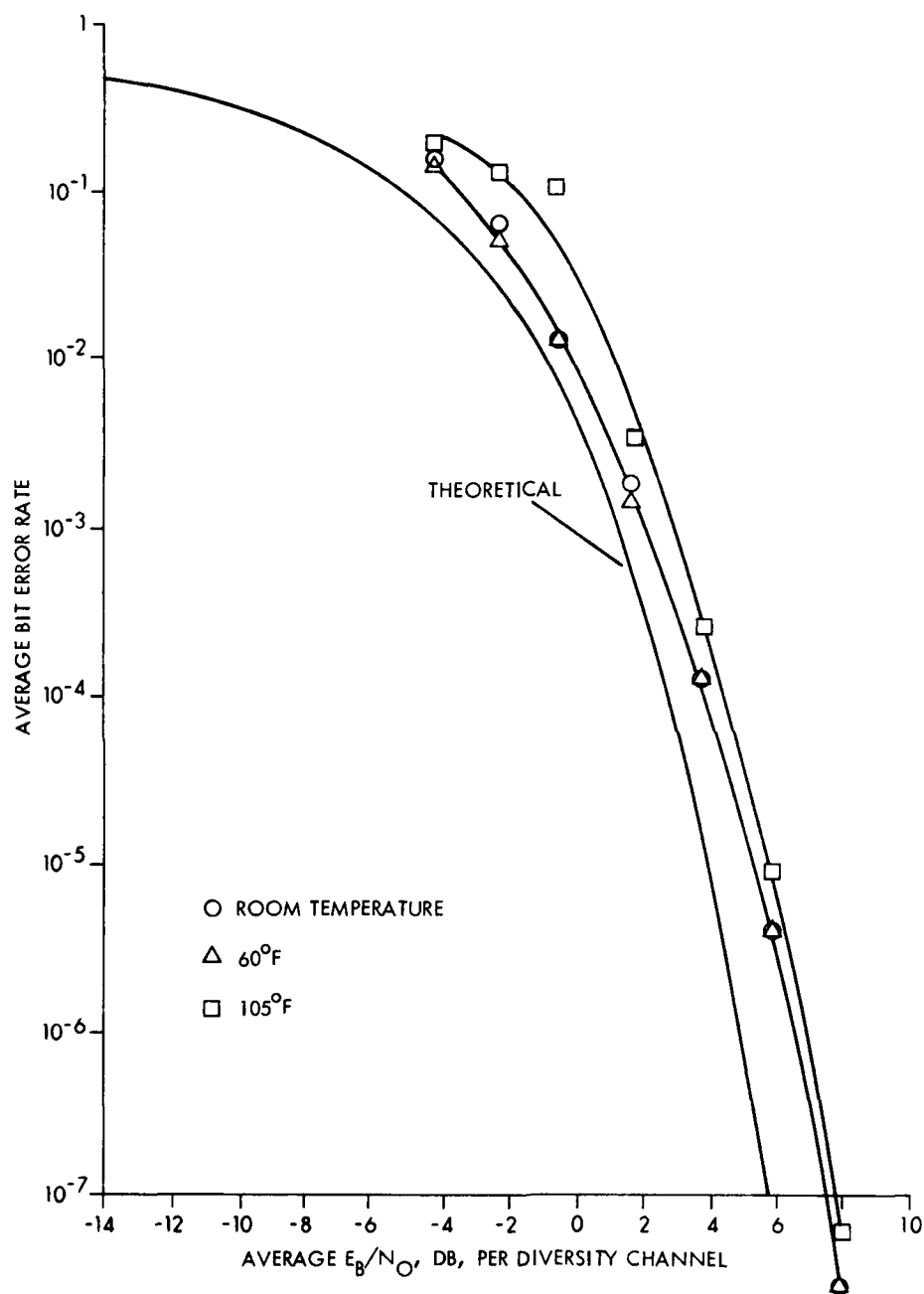


Figure 4-10. Back-to-Back Performance Over Temperature
7.0 MB/S Quad Diversity

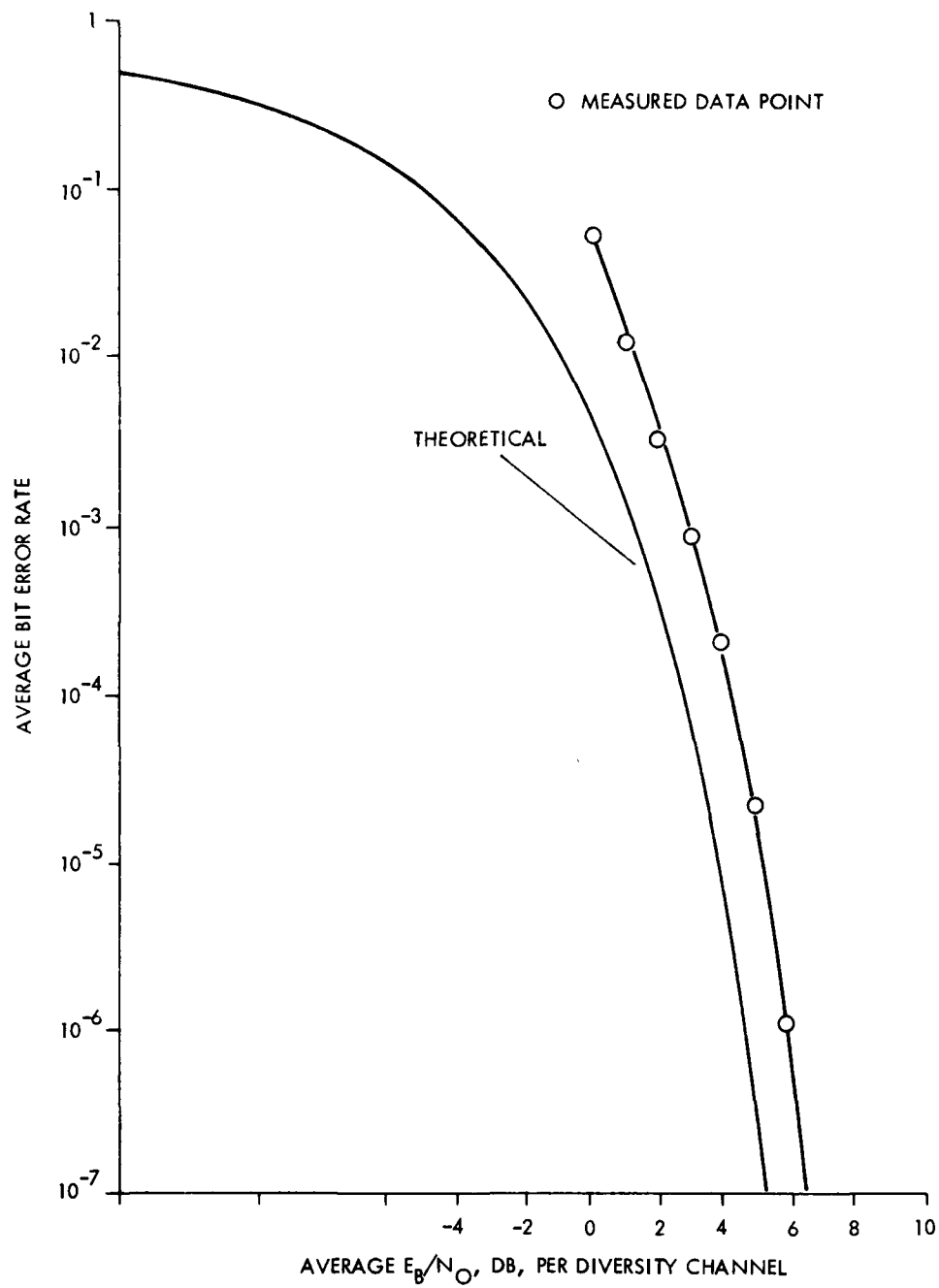


Figure 4-11. Back-to-Back Performance Demods Interchanged
1.75 MB/S Quad Diversity

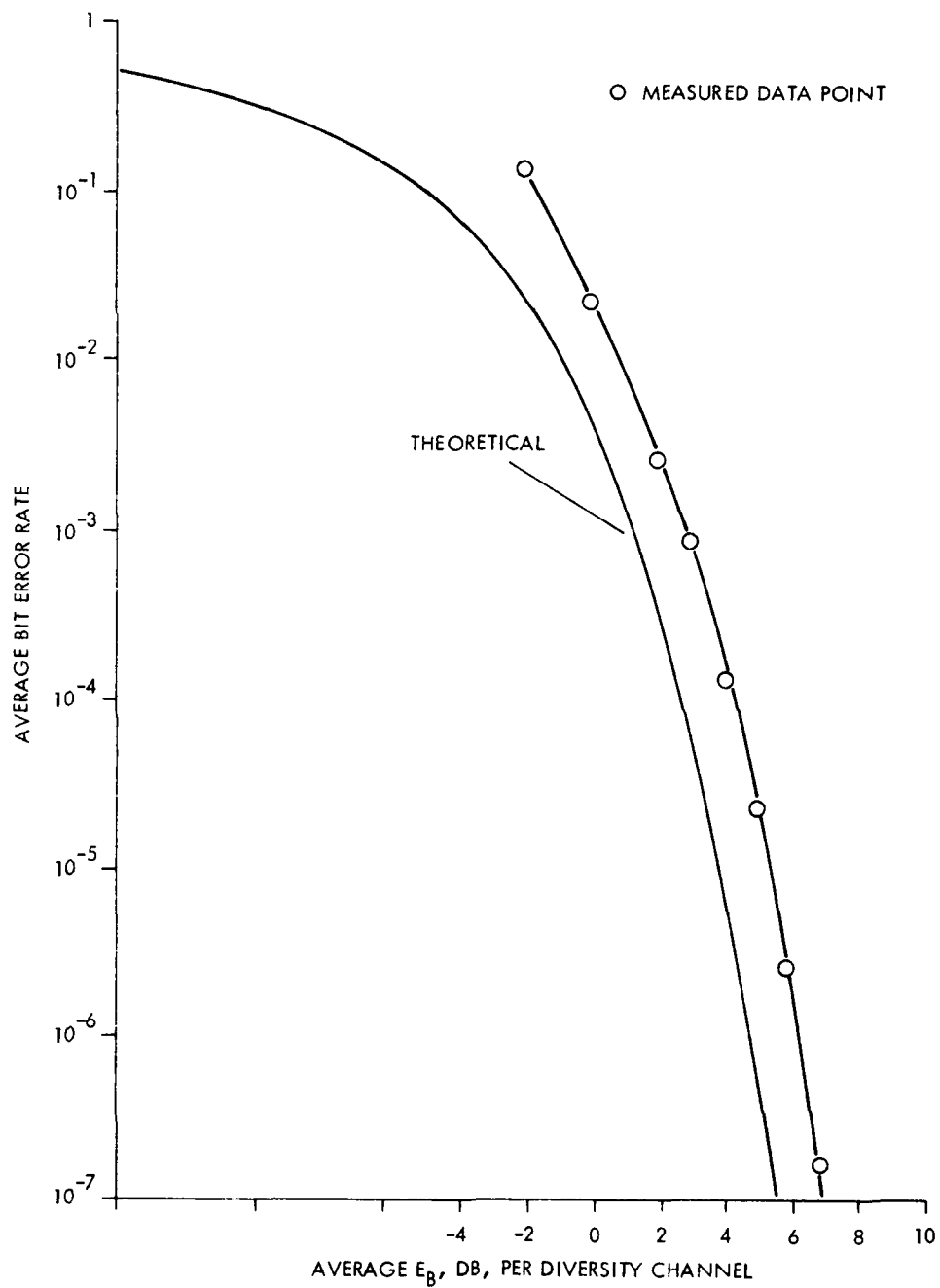


Figure 4-12. Back-to-Back Performance Demods Interchanged
3.5 MB/S Quad Diversity

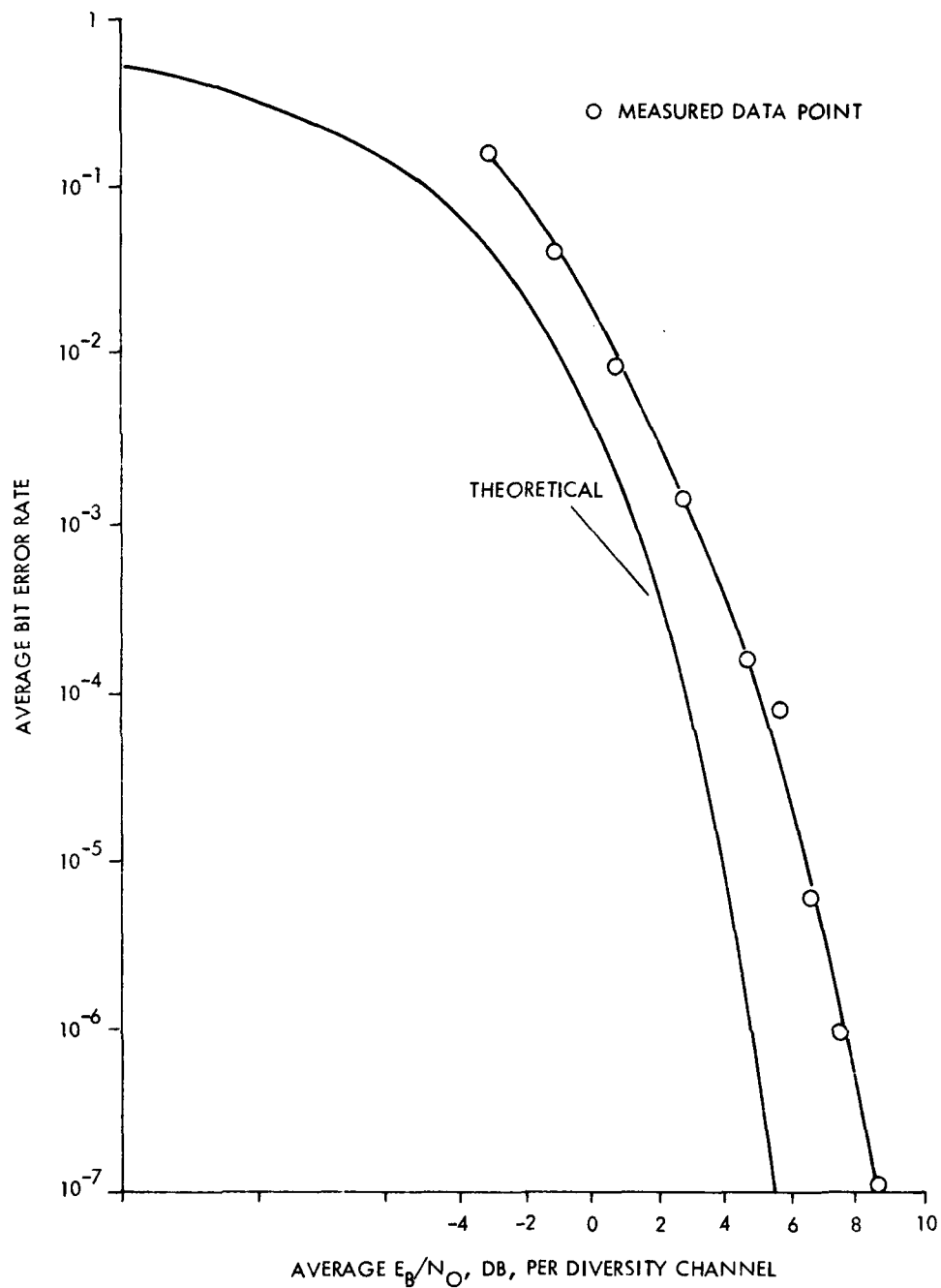
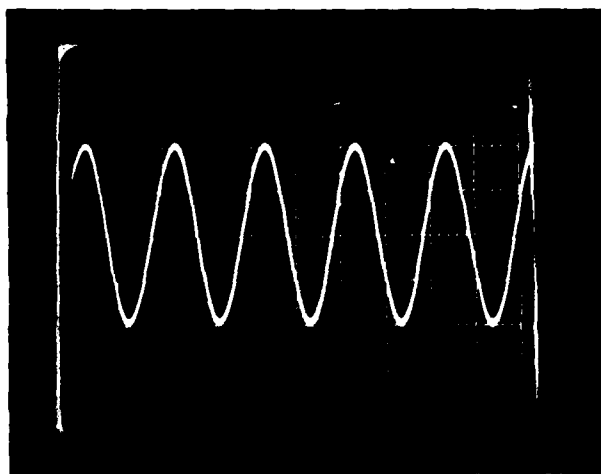
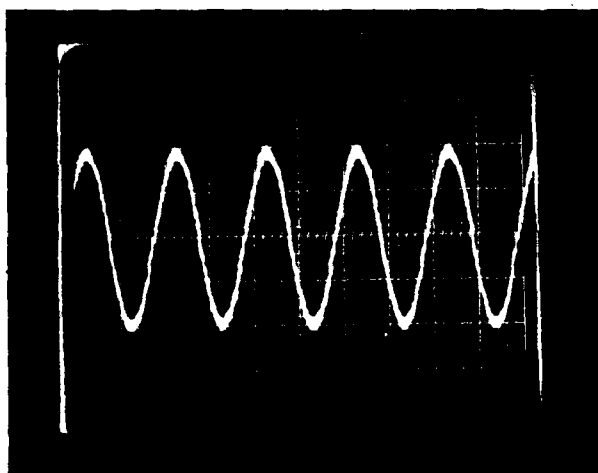


Figure 4-13. Back-to-Back Performance Demods Interchanged
7.0 MB/S Quad Diversity



INPUT
H = 0.5 MSEC/DIV
V = 1V/DIV



OUTPUT
H = 0.5 MSEC/DIV
V = 1V/DIV

Figure 4-14. Analog Orderwire

5.0 CHANNEL SIMULATOR TESTS

5.1 General

The tropospheric scatter media simulator tests are described below. These tests were concentrated on the median and "worst case" multipath conditions for a 168 mile tropo path using the AN/MRC-98 radio at 880 MHz or the AN/TRC-132 radio at C-band. Tests were conducted at 1.75 Mbps, 3.5 Mbps and 7.0 Mbps and for all orders of diversity. Emphasis in the test program was placed on the higher orders of diversity and higher data rates typical of the potential DCS strategic applications. The test results show good agreement with theoretical predictions and verify the potential of the DAR-IV modem technique in satisfying future requirements of an all digital DCS given the bandwidth necessary to support the time gating technique.

Section 5.4 provides a performance summary of the simulator testing. Comparison of the results with theoretical shows that the DAR, after subtraction of implementation losses, provides ideal adaptive matched filter performance within its design limits. A simple mathematical expression is fitted to these results which allows the prediction of the required E_b/N_0 for a 10^{-5} average BER within ± 0.5 dB given only the channel RMS multipath delay spread and the 3 dB bandwidth of the transmitted spectrum.

5.2 DAR DCS Tropo Simulator Testing

5.2.1 Test Conditions

Figure 5-1 shows the basic setup used for media simulator testing of the DAR-IV modem. A set of Hewlett-Packard test data pattern generators HP 3760A were used to simulate random binary data and determine the occurrence of errors. In all the tests performed, a repetitive pseudorandom data pattern of approximately 2^{15} bits in length was employed which models random data to high accuracy.

The RADC four-channel troposcatter simulator was employed to create multipath propagation effects similar to

those encountered on a real link. This simulator can provide up to four independently fading and multipath corrupted channels to examine the diversity performance of a modem. The channel simulator is basically transversal filter (or tapped delay-line filter) whose tap outputs are multiplied by weighted gaussian noise and linearly added. The noise weighting of the TAPs (or the average power of the signal from each tap) is adjusted to reflect the desired multipath delay power spectrum.

A series of tests were performed on the RADC laboratory channel simulator to evaluate the potential applicability of the DAR-IV modem technique to the future DCS troposcatter links. Tests were conducted at data rates of 1.75 Mbps, 3.5 Mbps and 7.0 Mbps in dual and quad diversity with and without the benefit of a "tail cancelling" circuit. Channel multipath conditions representative of the "average" and "worst case" conditions (refractive indices of 1.33 and 0.75, respectively), were simulated for the 168 mile AN/MRC-98 tropo radio at 880 MHz and the 168 mile AN/TRC-132 tropo radio at C-band. Also simulated was the multipath conditions of a 250 mile path with 0.6° beamwidth antennas. The tests were concentrated on the higher orders of diversity and higher data rate modes consistent with possible future DCS applications.

Section 5.2.2 describes the multipath profiles simulated and their relation to the paths to be employed for over-the-air testing. Section 5.2.2.2 describes results of a series of tests which were used to establish a baseline for the long AN/MRC-98 tropo link. Section 5.3.3.2 describes the results of the tests for the long AN/TRC-132 tropo link as well as the model of a 250 mile link with 0.6° beamwidths.

5.2.2 Multipath Profiles for Simulator Testing

To employ the RADC tropo channel simulator, it is necessary to specify a multipath delay power spectrum, $Q(\xi)$ and a two-sided RMS doppler spread. The doppler spread is related to the fade rate of the channel and doppler spreads between 0.1 Hz and 10 Hz are selectable on the simulator. Based on preliminary simulator tests of the DAR-IV in the Raytheon Laboratory and theoretical consideration, it has been found

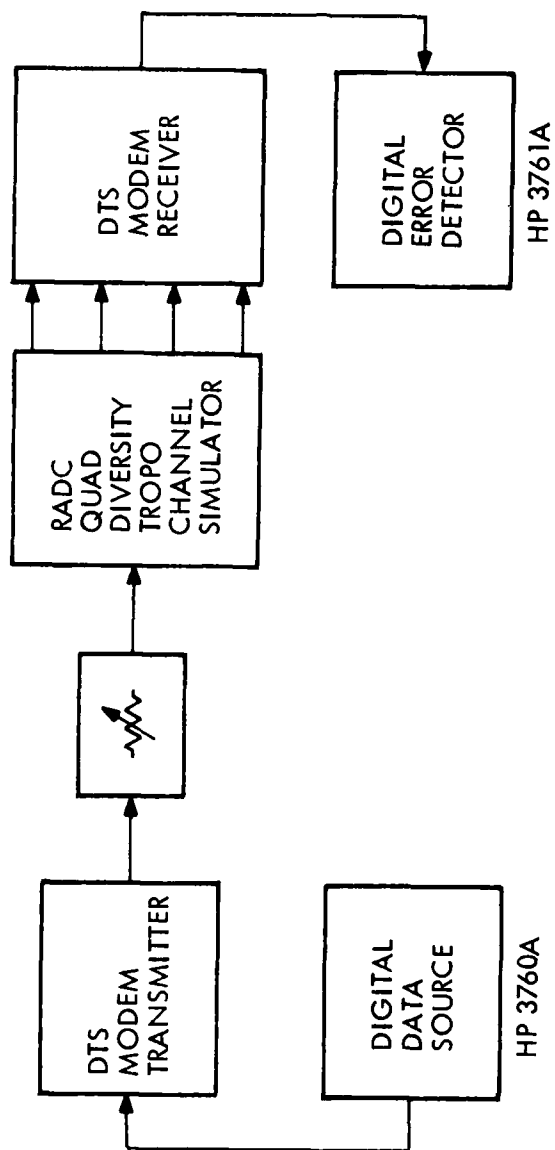


Figure 5-1. Simulator Test Set Up

that the DAR-IV performance is not very sensitive to the fade rates contained in this range. That is, the DAR-IV demodulator employs coherent reference and AGC time constants several orders of magnitude faster than the maximum anticipated fade rates. Only the bit timing recovery loop of the DAR-IV modem displays any sensitivity to fade rate with less than 0.5 dB of performance variation anticipated for the range of fading rates available.

The major performance characteristics of the DAR-IV are thus determined by the multipath delay power spectrum assumed. Unfortunately, there is a scarcity of information, both theoretical and empirical on the multipath characteristics of troposcatter channels. A model for the multipath delay power spectrum has previously been proposed by Bello. This model provides a reasonable description of the multipath profile for a simple, symmetrical, "smooth earth" troposcatter channel when the radio refractive index is known. A range of refractive index values can be used to represent both median and "worst case" propagation conditions.

In computing $Q(\xi)$, it is convenient to deal with a normalized delay variable.

$$\delta = \frac{\xi - D/c}{D/c} \quad (10)$$

which is the percentage departure of the path delay ξ , from the delay corresponding to line-of-sight transmission through a distance equal to the path length D . The quantity c is the speed of light.

Note that due to the shadowing effect of the earth, energy will be scattered for path delays exceeding some minimum path delay greater than D/c . If one assumes zero elevation angles for the antennas, the minimum value of ξ is readily computed to be

$$\delta_0 = \frac{D^2}{8R^2} \quad (11)$$

where R is the earth's radius.

In terms of the normalized delay variable δ , the integral representation of the delay power spectrum for identical antennas at the same height pointing with maximum gain at 0-degree elevation (radio horizons) is found to be

$$Q(\xi) \equiv \hat{Q}(\delta) \sim \frac{1}{\delta^{1+m/2}} \int_{\sqrt{\delta_0/\delta}}^{\sqrt{\delta/\delta_{00}}} \frac{G\left(x\sqrt{2\delta} - \frac{D}{2R}\right) G\left(\frac{\sqrt{2\delta}}{x} - \frac{D}{2R}\right)}{x(x + 1/x)^{m-2}} dx \quad (12)$$

WHERE $G(\cdot)$ is the vertical antenna gain pattern.

This integral expression was evaluated by numerical integration on the digital computer. The antenna gain function was chosen as a symmetrical Gaussian shape which is typical of real antennas for small departures from boresight. The earth's radius must be modified to account for refractive bending of the radio rays. An equivalent earth radius, $R = Ka$, can be defined where a is the true radius and $K = 4/3$ for typical median propagation conditions in overland, temperate climate paths.

The resultant multipath profiles are shown in Figures 5-2, 5-3 and 5-4 for three paths of interest. Figure 5-2 shows the AN/MRC-98 long path, Figure 5-3 shows the AN/TRC-132 path, while Figure 5-4 shows a nominal 250 mile ("smooth earth") path with 28 foot antennas at C-band, or 60 foot antennas at 2 GHz, or 120 foot antennas at 1 GHz. The value $K = 1.33$ represents the median $4/3$ earth's radius. The $K = 1$ value represents the approximate worst month median refractive index of an overland European path. The $K = 0.75$ value is taken as the approximate "worst case" yearly refractive index.

The RADC channel simulator has a tapped delay model of the multipath structure. Up to 16 taps spaced by 0.1 us can be used in the simulation. Table 5-1 provides the tap settings for the six multipath profiles to be simulated.

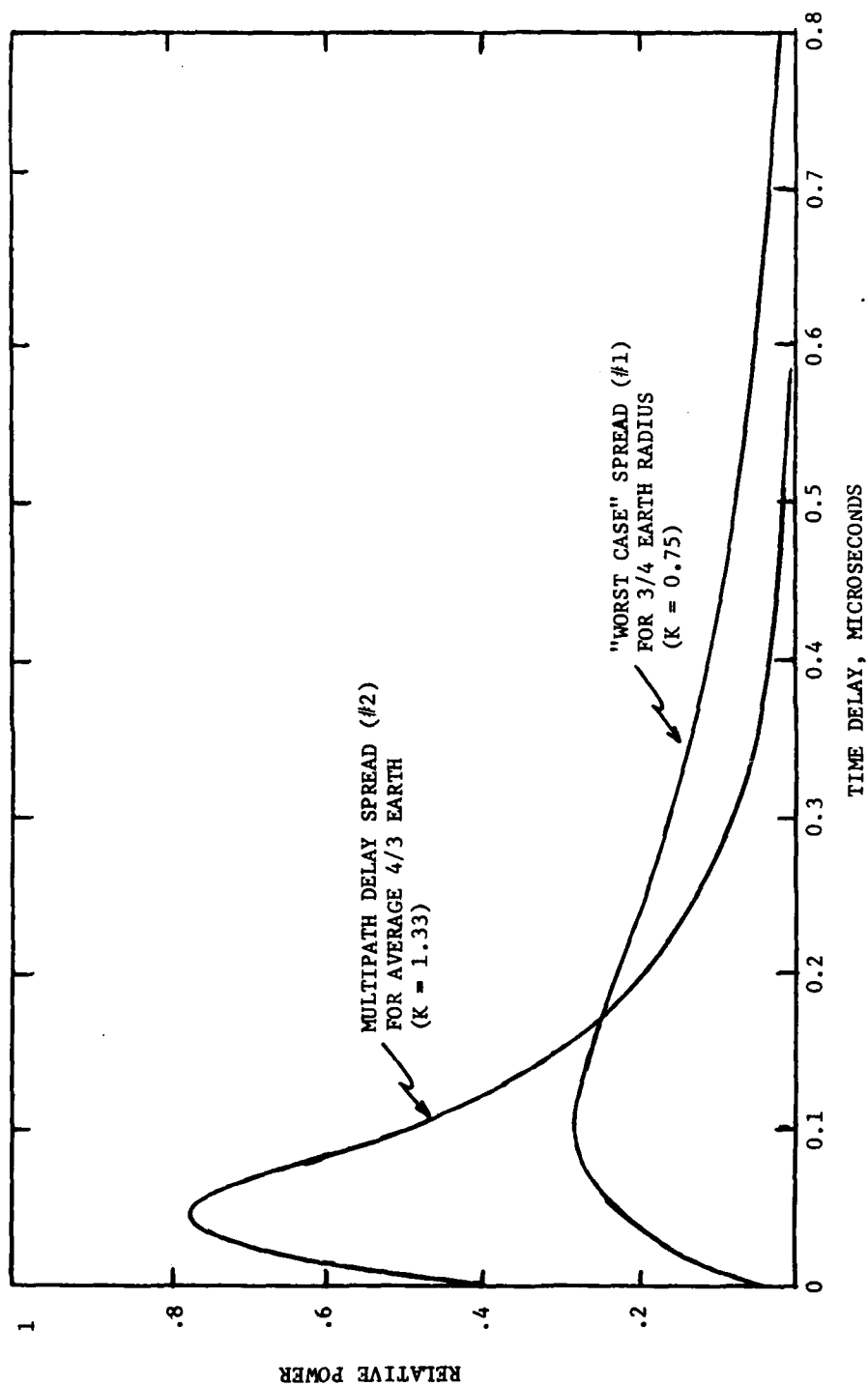


Figure 5-2. Multipath Delay Spreads Employed for Simulation of 168 Mile AN/MRC-98 Test Path (880 MHz)

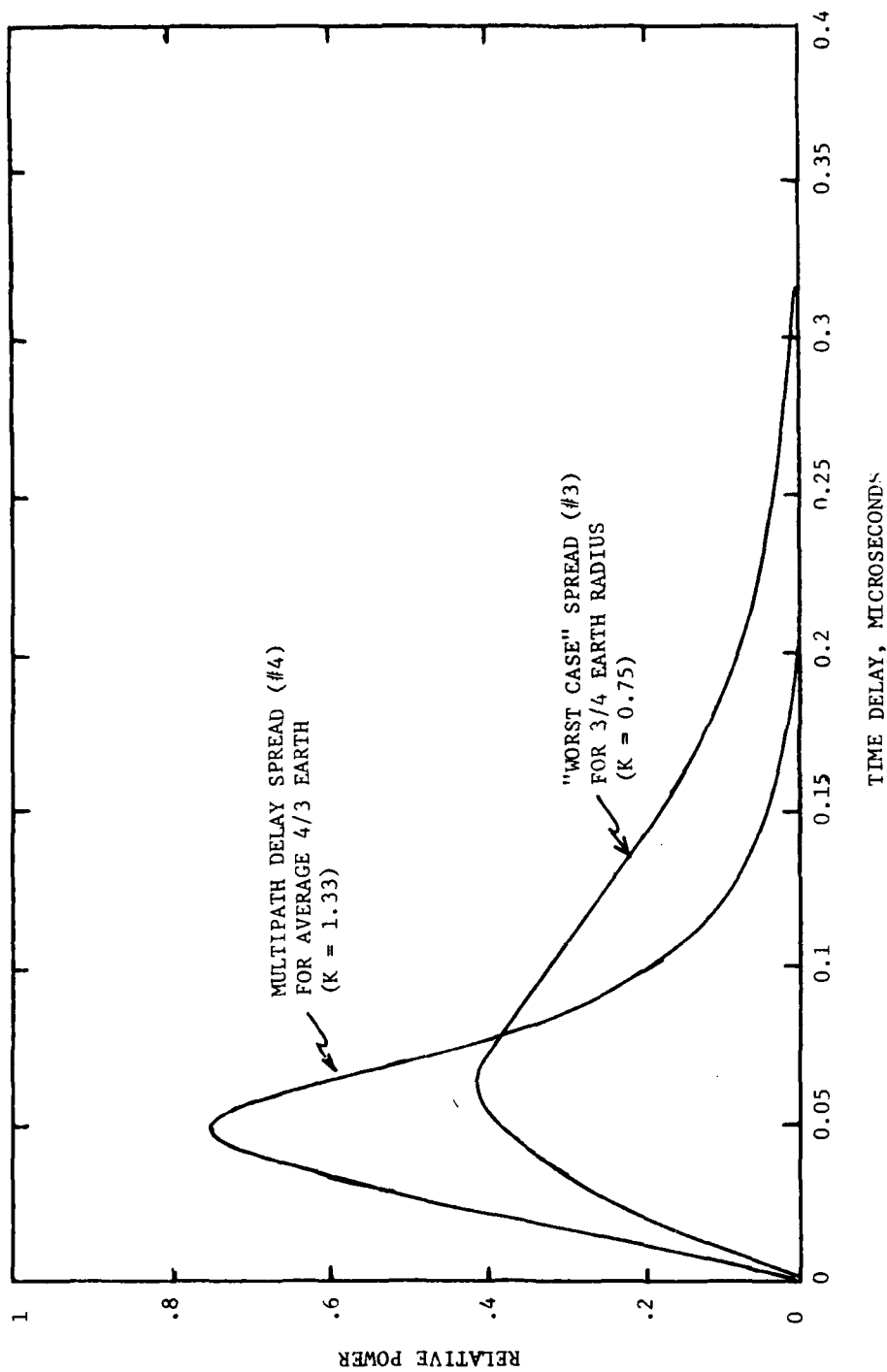


Figure 5-3. Multipath Delay Spread Employed for Simulation of 168 Mile AN/TRC-132 Test Path (4.4 GHz)

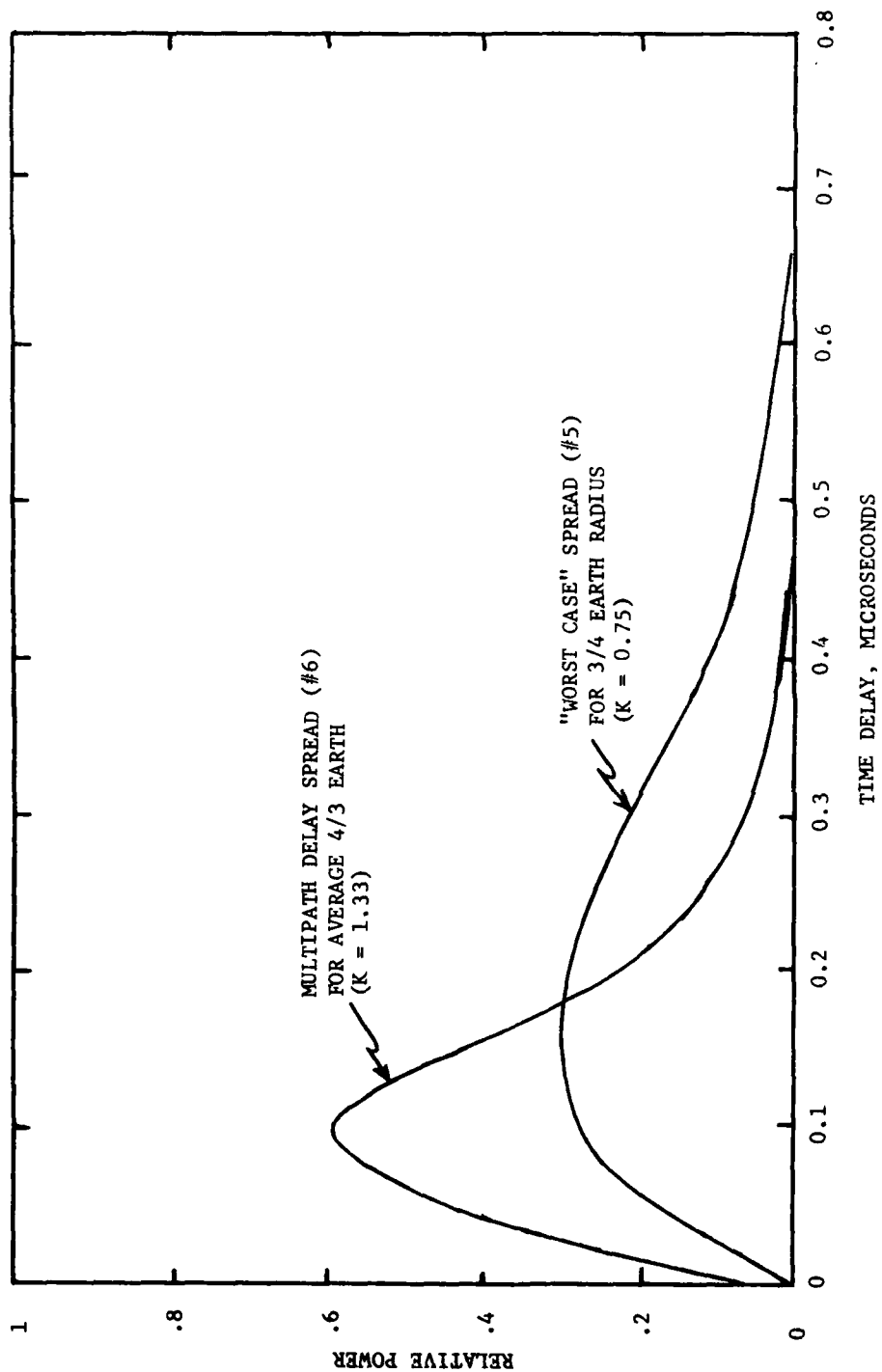


Figure 5-4. Multipath Delay Spreads Employed for Simulation of 250 Mile "Smooth Earth" Path with 0.6° Beamwidth Antennas

TABLE 5-1. SIMULATOR TAP SETTINGS

TAP #	168 MILE AN/MRC-98 PATH		168 MILE AN/TRC-132 PATH		250 MILE 0.6° BEAMWIDTH	
	K=.75	K=1.33	K=.75	K=1.33	K=.75	K=1.33
	PROFILE #1	PROFILE #2	PROFILE #3	PROFILE #4	PROFILE #5	PROFILE #6
1	0	0	0	0	1	0
2	1	5	1	6	0	4
3	2	9	3	13	1	10
4	4	13	7	21	4	17
5	6	16	11	28	8	25
6	8	20	15	35	12	32
7	10	23	20	OFF	16	39
8	12	26	25	OFF	20	OFF
9	13	29	30	OFF	24	OFF
10	15	32	35	OFF	28	OFF
11	17	35	OFF	OFF	32	OFF
12	19	OFF	OFF	OFF	36	OFF
13	21	OFF	OFF	OFF	OFF	OFF
14	23	OFF	OFF	OFF	OFF	OFF
15	25	OFF	OFF	OFF	OFF	OFF
16	27	OFF	OFF	OFF	OFF	OFF

TABLE 5-2. 880 MHZ LONG PATH SIMULATOR TEST

TEST NUMBER	DATA RATE Mbps	DIVERSITY MODE	PROFILE	RECORDED ON FIGURE NUMBER
1	1.75	Quad	#1	5-2 (See Note 1)
2	1.75	Quad	#2	5-2
3	3.5	Dual	#1	5-3
4	3.5	Dual	#2	5-3
5	3.5	Quad	#1	5-3
6	3.5	Quad	#2	5-3
7	7.0	Quad	#1	5-4
8	7.0	Quad	#2	5-4
9	7.0	Quad	#2	5-4

Note 1: Repeated for fade rates of 0.1, 1.0 and 10 Hz.

5.2.3 880 MHz Long Path Simulations, AN/MRC-98

This series of tests is primarily intended to characterize the DAR performance of the over-the-air tests between Youngstown and Verona, New York, using the AN/MRC-98 equipment.

The initial series of measurements was taken at data rates of 1.75 Mb/s, 3.5 Mb/s and 7.0 Mb/s and includes two path profiles - an expected and a "worst case" profile as described in Section 5.2.2.

This series of measurements together with the math model predictions provides the data base necessary for comparison of actual over-the-air results with expected or predicted performance.

The test configuration is depicted in Figure 5-1. The median value of E_b/N_0 is varied by adjustment of the input signal level to the simulator from the DTS transmitter via a variable attenuator.

Table 5-1 summarizes the series of measurements made. Results are plotted directly on Figures 5-5 through 5-9. Plotted profiles on these figures are the theoretical predicted performance for the DAR-IV using the math model and computer simulation. All profiles chosen are considered "representatives".

Test #1 was run at three fade rates to demonstrate the insensitivity of the DTS modem to different fade rates. Two fade rates are shown in Figure 5-6. All following tests were run at the maximum rate for the channel simulator of 10 Hz.

5.2.3.1 Description of 880 MHz Long Path Tests (Table 5-1)

These initial simulator tests form the baseline for the DAR-IV performance on the 168 AN/MRC-98 link. Hence, both the "worst case" and median multipath

profiles (Profiles 1 and 2, respectively) have been chosen for simulation as described in 5.2.2.

Tests 1 and 2 correspond to 1.75 Mbps DAR-IV performance in the quad diversity mode for the two multipath profiles mentioned above. Note from the computer simulated predictions of Figure 5.5 that there is relatively little performance difference in these cases. That is, at 1.75 Mbps, the multipath spread is very short in duration compared to a data symbol. The amount of in-band diversity available is nearly zero for the case of Profile #2 (median) and only slightly greater for Profile #1 (worst case). The approximately 0.5 dB implementation margin of the DAR-IV is not shown in these computer simulation results.

Tests 3 and 4 show the dual diversity performance at 3.5 Mbps for the two previous multipath profiles, while tests 5 and 6 show the corresponding quad diversity performance. The results anticipated are shown in Figures 5-7, and 5-8 from the computer simulation. For multipath Profile #2, the performance is similar to that previously described. For Profile #1 which is more than twice as wide as Profile #2, some irreducible error rate phenomenon is observable in both dual and quad diversity. The "worst case" multipath irreducible BER is approximately 3×10^{-7} for quad diversity.

Tests 7 and 8 represent quad diversity performance at 7 Mbps for Profiles #1 and #2. Notice that in this case, both the median (Profile #2) and "worst case" (Profile #1) multipaths result in irreducible error rate of 4×10^{-6} and 10^{-3} , respectively. This irreducible error rate is due to overlap of adjacent distorted bits. The results are shown in Figure 5-9.

5.2.3.2 Test Results

These initial simulator tests form the baseline for the DAR-IV performance on the 168 mile AN/MRC-98 link. Hence, both the "worst case" and median multipath profiles (Profiles #1 and #2, respectively) were chosen for simulation as described in Section 5.2.3.

Tests 1 and 2 correspond to 1.75 Mbps DAR-IV performance in the quad diversity mode for the two multipath profiles mentioned above. Note from the computer simulated prediction of Figure 5-5, that there is a 4 dB performance difference in these cases. That is, at 1.75 Mbps, the multipath spread is very short in duration compared to a data symbol. The amount of in-band diversity available is small for the case of Profile #2 (median) and only slightly greater for Profile #1 (worst case). The approximately 2 dB implementation margin of the DAR-IV is not shown in these computer simulation results but the simulations do include the effect of the limited loop gain which was $K = 0.93$ for the simulations. Figure 5-5 also shows the measured results for Profiles #1 and #2. It will be noticed that the measured results compare quite favorably with the simulations. The slopes of the curves in both cases match the predictions quite closely and there is about 2 dB offset from theory at 10^{-5} BER for Profile #2. Profile #1 is bettered by about 4 dB due to the intrinsic diversity combining not observed in the computer simulation model due to quantization effects with the short multipath profiles.

Figure 5-6 shows results for fade rates of 0.1 Hz and 1 Hz for Profile #1. At BER higher than 10^{-3} , the results at both fade rates are in close agreement. At BER below 10^{-4} , the 0.1 Hz fade rate appears to produce worse results by several dB. This result can be due to timing offsets created when the bit timing recovery loop tends to follow individual multipath fades (changes in pulse position) at the slow fade rate instead of averaging over a number of positions. With offset timing, the performance will be degraded as a particular fade condition disappears and a new fade occurs with a delay in the opposite direction. At faster fade rates typical of the links of interest, this phenomenon was not observed. Also, at the low BER values and low fade rates, a very long period of time is required to obtain accurate measurements. For example, at 10^{-5} BER, about 10^6 seconds are required per data point for 90 percent measurement confidence. Since the actual measurement times were only on the order of 10^3 seconds, BER values below 10^{-3} for the very low fade rate are suspected.

The 10 Hz fade rate generally agrees with predicted performance at BER of 10^{-5} or below. These tests, as all others, were run with the "Tracking Bandwidth" in the minimum position of X 1/2 to give the maximum accuracy of timing possible. However, because of the time constant of the loop, accuracy in timing is lost at the very slow fade rates as the master oscillator tracks the multipath shift of data. All other tests were run with the simulator in its fastest fade rate of 10 Hz.

Figures 5-7 and 5-8 also show the predicted and measured results for 3.5 Mb/s dual and quad diversity for Profiles #1 and #2. The measured results agree quite closely to the predicted with a 1-2 dB offset due to implementation loss in the modem except in the irreducible error rate region where somewhat larger differences result from small prediction errors. Both dual and quad diversity exhibit an irreducible error rate not seen in the predicted results. This phenomenon has two explanations. First, the predictions assumed a "coherent filter" loop gain of $K = .99$ while the DTS realized an equivalent loop gain of only about 0.92. As a result, severe multipath profiles have a greater effect on the DTS performance due to the simultaneous effects of intersymbol interference and corruption of the coherent reference signal in the matched filter detector. With a larger coherent filter "memory", the distortion in the reference signal is averaged over a longer period and thus reduced. Second, in the computer simulation model, irreducible error rate effects on the order of 10^{-5} or smaller are difficult to predict due to the large number multipath "snapshots" that need to be analyzed for reliable prediction. While an analytical model might be better able to predict irreducible error rate floors, the feedback nature of the DAR, especially when the DFE is employed, dictates the use of simulation analysis for practical results.

Figure 5-9 represents quad diversity performance at 7 Mbps for Profiles #1 and #2. Notice that in this case, both the median (Profile #2) and "worst case" (Profile #1) multipaths result in irreducible error rate of 4×10^{-6} and 10^{-3} , respectively. This irreducible error rate is due to overlap of adjacent distorted bits despite the use of a 50 percent transmitter time gate. The irreducible error

rate floor can be substantially lowered, in theory, by use of an adaptive "tail canceller" as described in the following sections.

Figure 5-9 shows only one curve, that of Profile #2. The DTS at 7.0 Mb/s proved unable to maintain BCI in Profile #1 and as a result showed 0.5 error rate regardless of the value of E_b/N_o . This worse than predicted performance is primarily due to the problems associated with the coherent loop filter. These were discussed previously in detail in Section 3.3.

5.2.4 4.4 GHz Simulations, AN/TRC-132

This series of tests is intended to characterize the DAR-IV performance for the over-the-air tests between Youngstown and Verona, New York using the AN/TRC-132 equipment.

This series of simulator tests will explore fully the characteristics of the DAR-IV. In particular, the effects of performance with and without the adaptive equalizer.

Emphasis is again on quad diversity, and higher bit rate modes of operation. Data was taken for two links with two profiles for each link - an "average" and "worst case". The effects of the adaptive equalizer will be evaluated for each.

Table 5.3 summarizes the series of measurements for this segment of the media simulator testing. As with the preceding tests, the median value of E_b/N_o is varied by adjustment of the output signal levels from the simulator from the DAR-IV transmitter via a variable attenuator. Results are plotted directly on Figures 5-17 through 5-22. Plotted profiles on these figures are the theoretical predicted performance for the DAR-IV using the math model and computer simulation. Refer to Section 5.0 for a description of the profiles used.

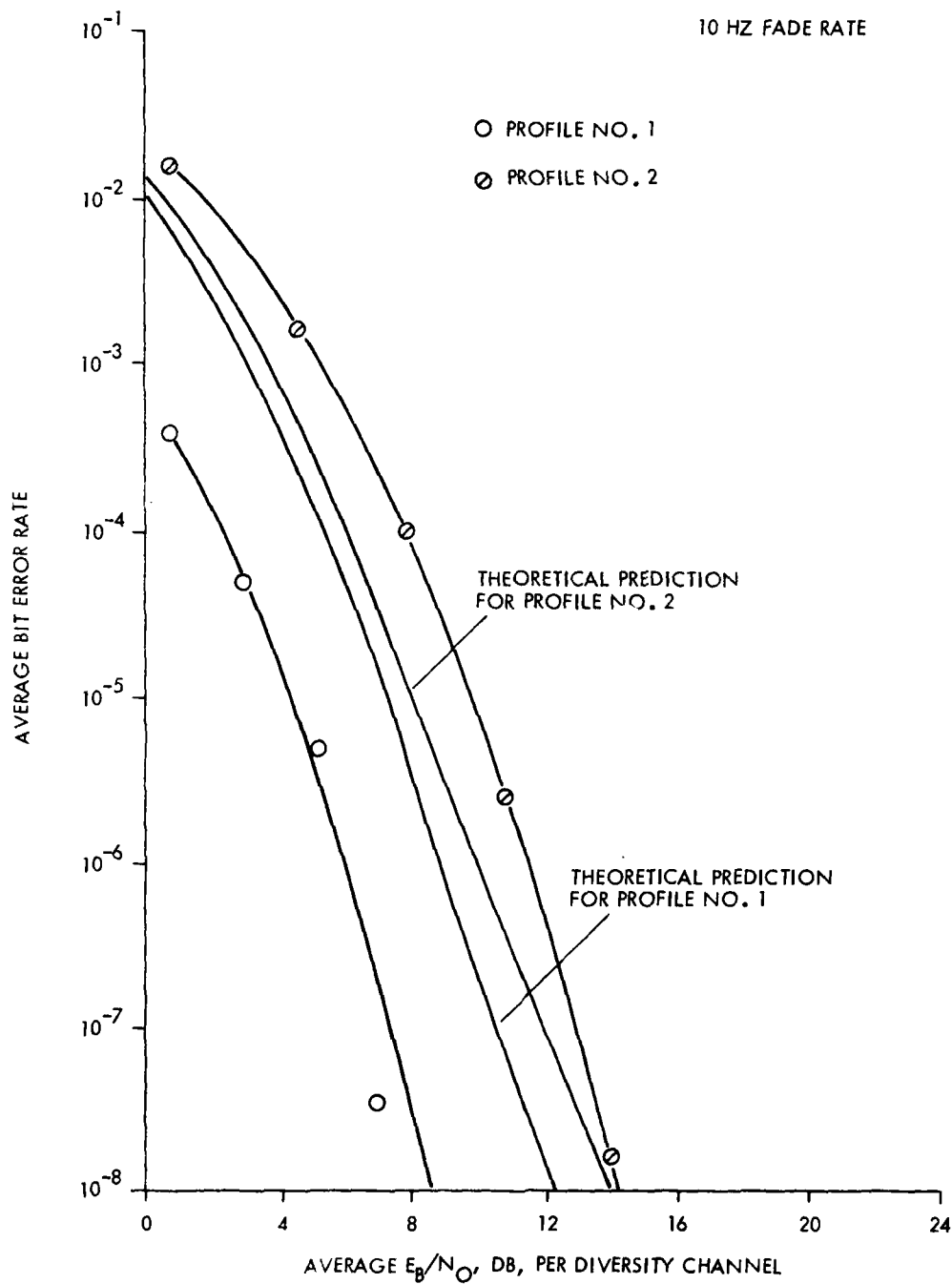


Figure 5-5. AN/MRC-98 Simulator Tests 1.75 Mb/s
Quad Diversity Profiles No. 1 and 2

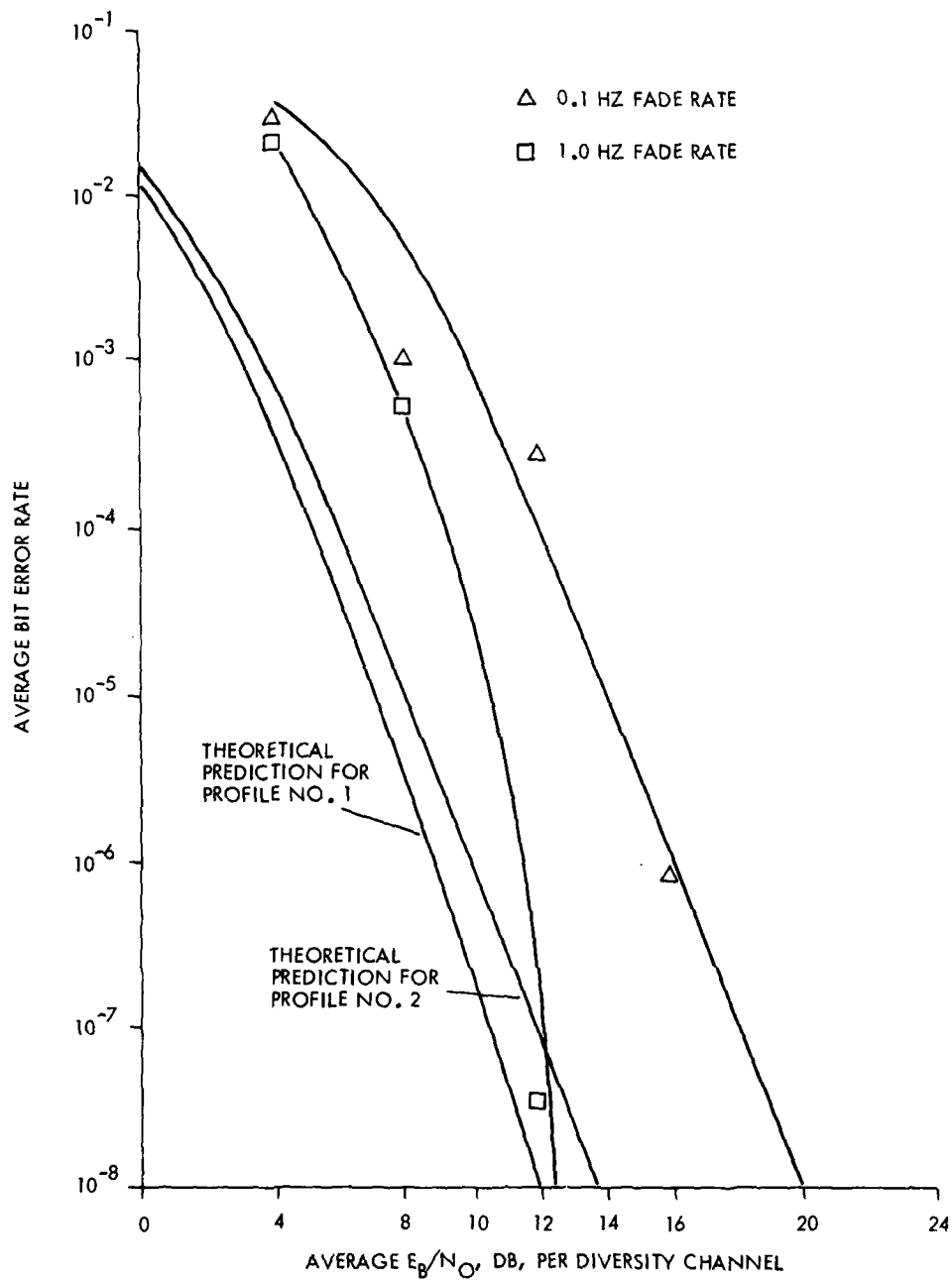


Figure 5-6. AN/MRC-98 Simulator Tests 1.75 Mb/s Quad Diversity Profiles No. 1 at Fade Rates of 0.1 Hz and 1.0 Hz

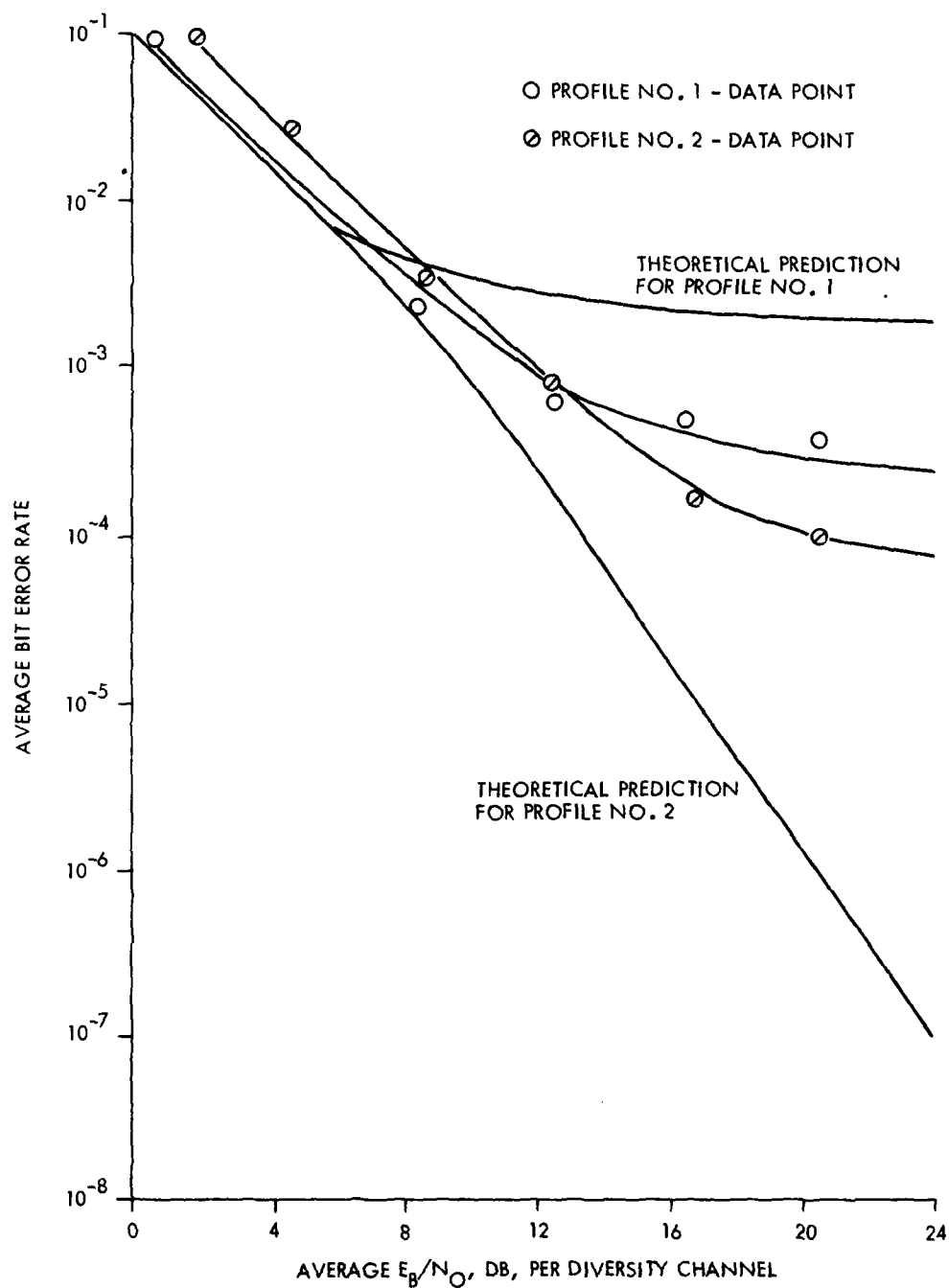


Figure 5-7. AN/MRC-98 Simulator Tests
3.5 Mb/s Dual Diversity

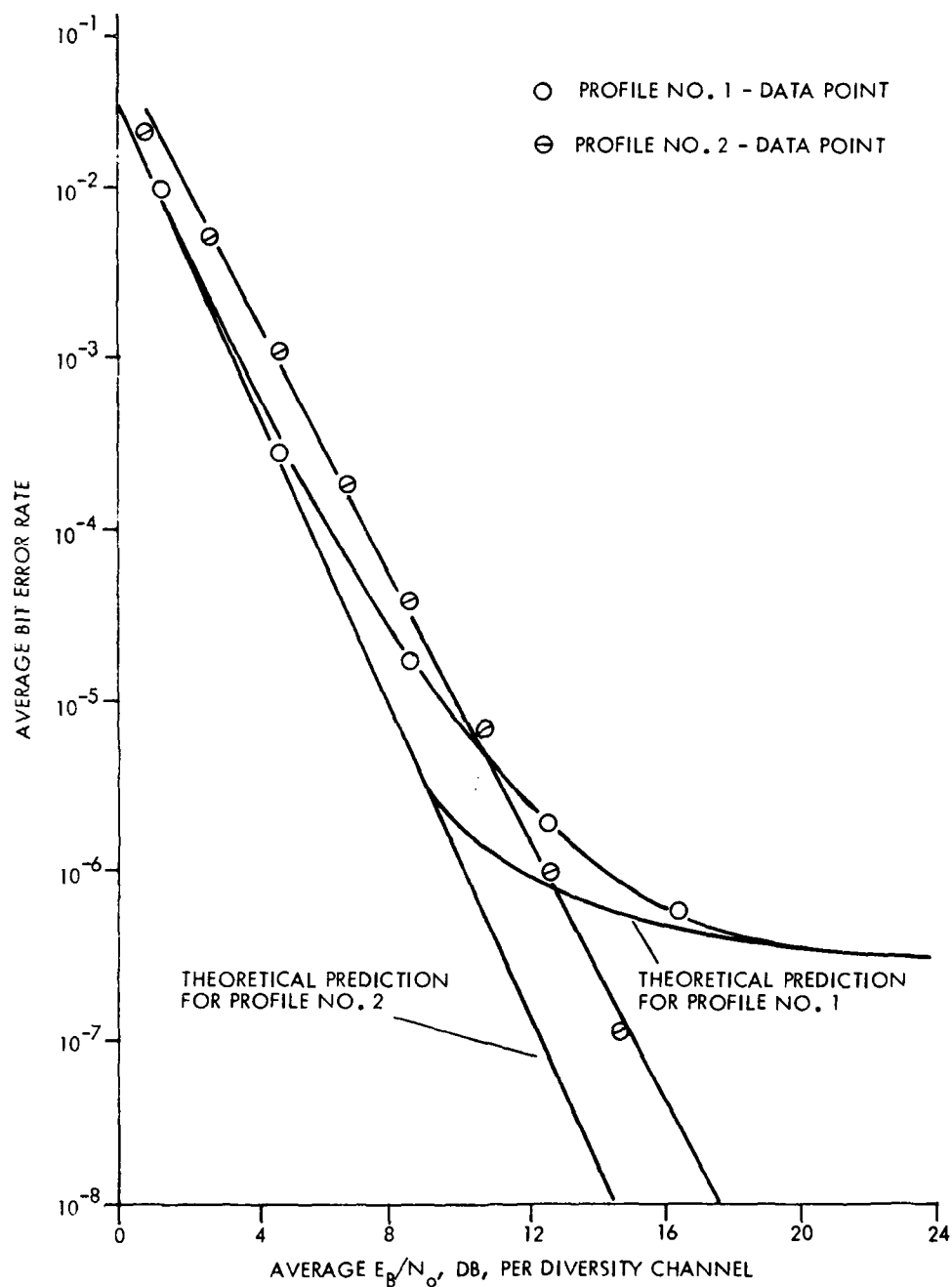


Figure 5-8. AN/MRC-98 Simulator Tests
3.5 Mb/s Quad Diversity

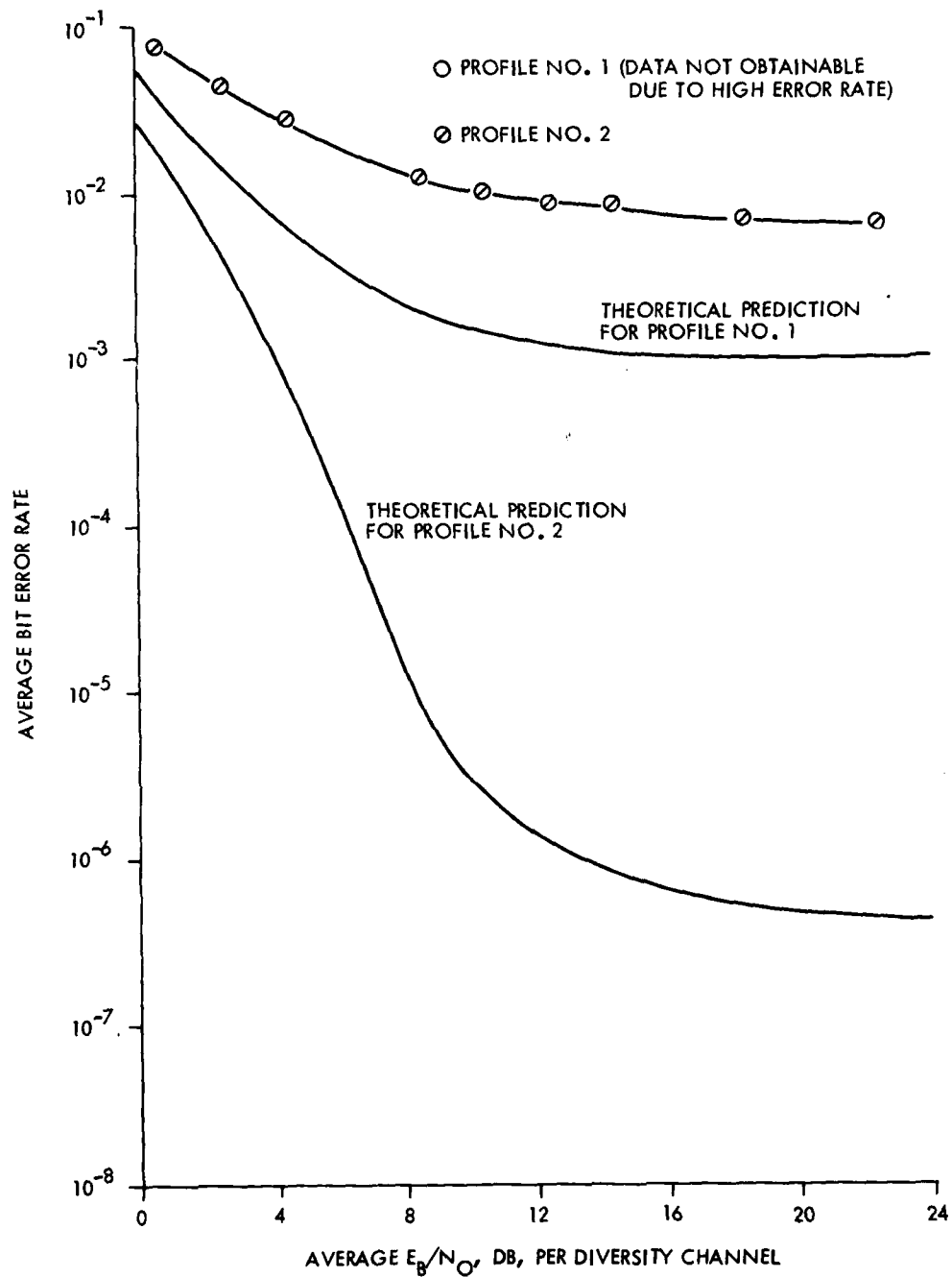


Figure 5-9. Simulator Tests 880 MHz Long Path
7.0 Mb/s Quad Diversity

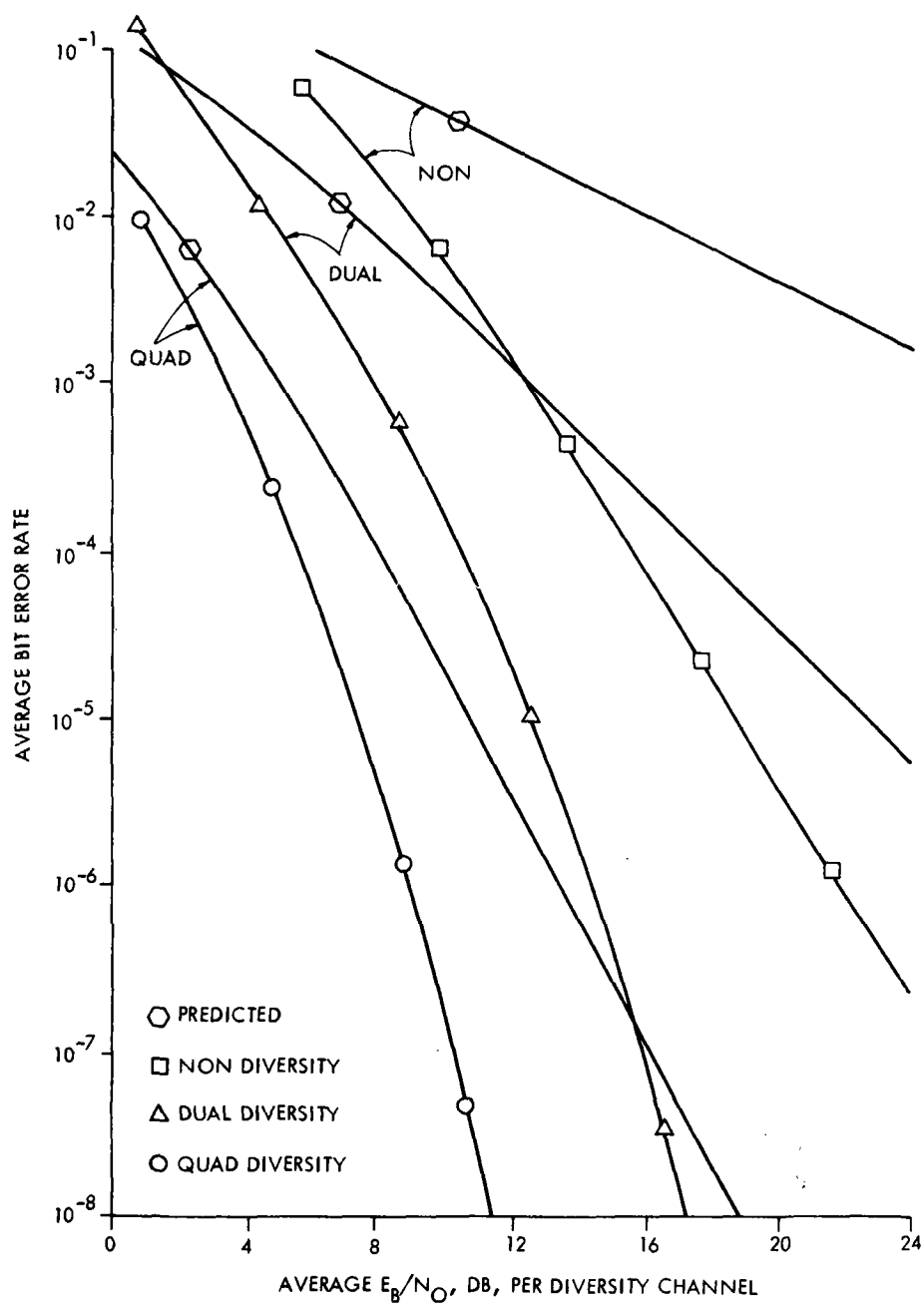


Figure 5-10. Simulator Tests 4.4 GHz Path 1.75 Mb/s
Non, Dual and Quad Diversity Profile No. 3

TABLE 5-3. 4.4 GHZ SIMULATOR TESTS

TEST NO.	DATA RATE MBPS	DIVERSITY MODE	EQUALIZER	PROFILE NO.	RECORDED ON FIGURE NO.
1	1.75	Non	No	3	5-10
2	1.75	Dual	No	3	5-10
3	1.75	Quad	No	3	5-10
4	3.5	Non	No	3	5-11
5	3.5	Dual	No	3	5-11
6	3.5	Quad	No	3	5-11
7	3.5	Quad	No	4	5-12
8	3.5	Quad	No	5	5-12
9	3.5	Quad	No	6	5-12
10	7.0	Non	No	3	5-13
11	7.0	Dual	No	3	5-13
12	7.0	Quad	No	3	5-13
13	7.0	Quad	No	4	5-14
14	7.0	Quad	No	5	5-14
15	7.0	Quad	No	6	5-14
16	7.0	Quad	Yes	3	5-15
17	7.0	Quad	Yes	4	5-15
18	7.0	Quad	Yes	5	5-15
19	7.0	Quad	Yes	6	5-15

5.2.4.1 Simulator Tests Without Tail Cancellor

The tests described in Table 5-3 serve several purposes. Multipath Profiles #3 and #4 are the "worst case" and median profiles for the 168 mile AN/TRC-132 test link. These profiles will serve to establish a baseline for the corresponding over-the-air performance. Multipath Profiles #5 and #6 refer to a 250 mile "smooth earth" path which may be characteristic of long distance DCS path. In this series of tests, a number of tests are repeated with and without the addition of a "tail canceller" circuit.

Tests 1, 2 and 3 show the non, dual and quad diversity performance of the DAR-IV at 1.75 Mbps without tail cancelling. All three tests are performed for the "worst case" multipath profile of the 168 mile AN/TRC-132 link. The large improvement due to diversity is apparent as seen in Figure 5-10. There was no evidence of an irreducible error even at 10^{-8} . The predicted results are somewhat pessimistic in estimating the intrinsic diversity gains for multipath profiles which are small compared to the data rate of interest as previously discussed.

The results of test 4, 5 and 6 are shown in Figure 5-11. The non and dual diversity plots exhibit floors at 10^{-5} and 7×10^{-6} , respectively. Quad diversity exhibits no such floor down to a BER of 10^{-8} . Figure 5-11 also shows all three diversities are better than predicted by more than 2 dB at a BER of 10^{-4} due to the conservative nature of the prediction model as previously described.

Figure 5-12 shows the results of tests 7, 8 and 9 with the results within 1/2 dB of the predicted value in all three cases. Profile #4, test 7 represents the worst case profile for the Youngstown to Verona link using the AN/TRC-132 radios. Tests 8 and 9 correspond to the median and worst case profiles of a 250 miles smooth earth profile for a tactical link.

At the 7.0 Mbps data rate, the DAR without the DFE operating can support only about a 0.12 us multipath delay spread in quad diversity for a 10^{-5} or smaller irreducible BER. The multipath spreads for Profile #3 (worst case 168 mile path) and Profile #5 (worst case 250 mile path), were more than double this amount which prevented maintenance of BCI. Hence, no measured data was available. (See Figure 5-13 for theoretical prediction.) Figure 5-14 shows the measured results for Profiles #4 and #6 which were in a range that can be accommodated by the DAR without DFE. Measured irreducible BER's were higher than predicted primarily due to the limited coherent filter gain achieved in the experimental model. An alternative implementation of the DAR can be constructed to nearly double the amount of multipath that can be tolerated at the 7 Mbps rate without the need for a DFE. Such an implementation has been developed for the AN/TRC-170 tactical troposcatter system and this technique, scaled to 7 Mbps operation, would permit successful operation with Profiles #3 and #5 as discussed further in the conclusion section of this report.

5.2.4.2 Simulator Test with Tail Canceller

As previously discussed, the limited coherent filter gain achieved in the DTS experimental model also limited the improvement obtainable from the "tail canceller" (or DFE). Figure 5-15 shows the predicted results for Profiles #3 through #6 for a DTS with the desired coherent filter gain ($K = 0.99$) and DFE operational. The actual results obtained with the DFE employed were basically the same as those obtained without the DFE. Observation of the integrate and dump output shows that the DFE did indeed greatly reduce the effects of intersymbol interference when the multipath was mild (that is, when irreducible errors were not occurring). However, when multipath conditions were such as to produce intersymbol interference errors, the degradation of the coherent reference signal due to a too short averaging time prevented the DFE from successfully executing its function.

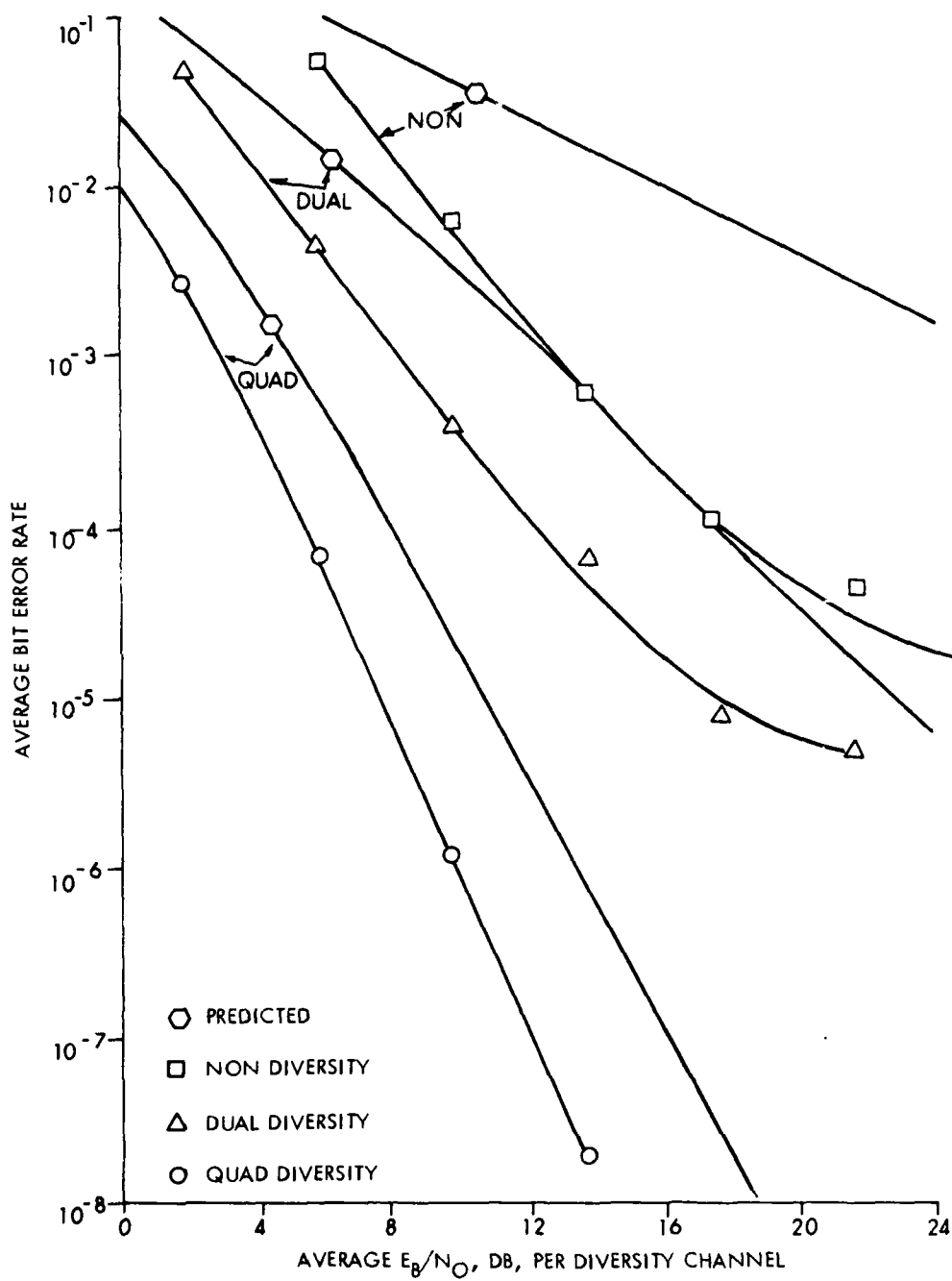


Figure 5-11. Simulator Tests 4.4 GHz Path 3.5 Mb/s
Non, Dual and Quad Diversity Profile No. 3

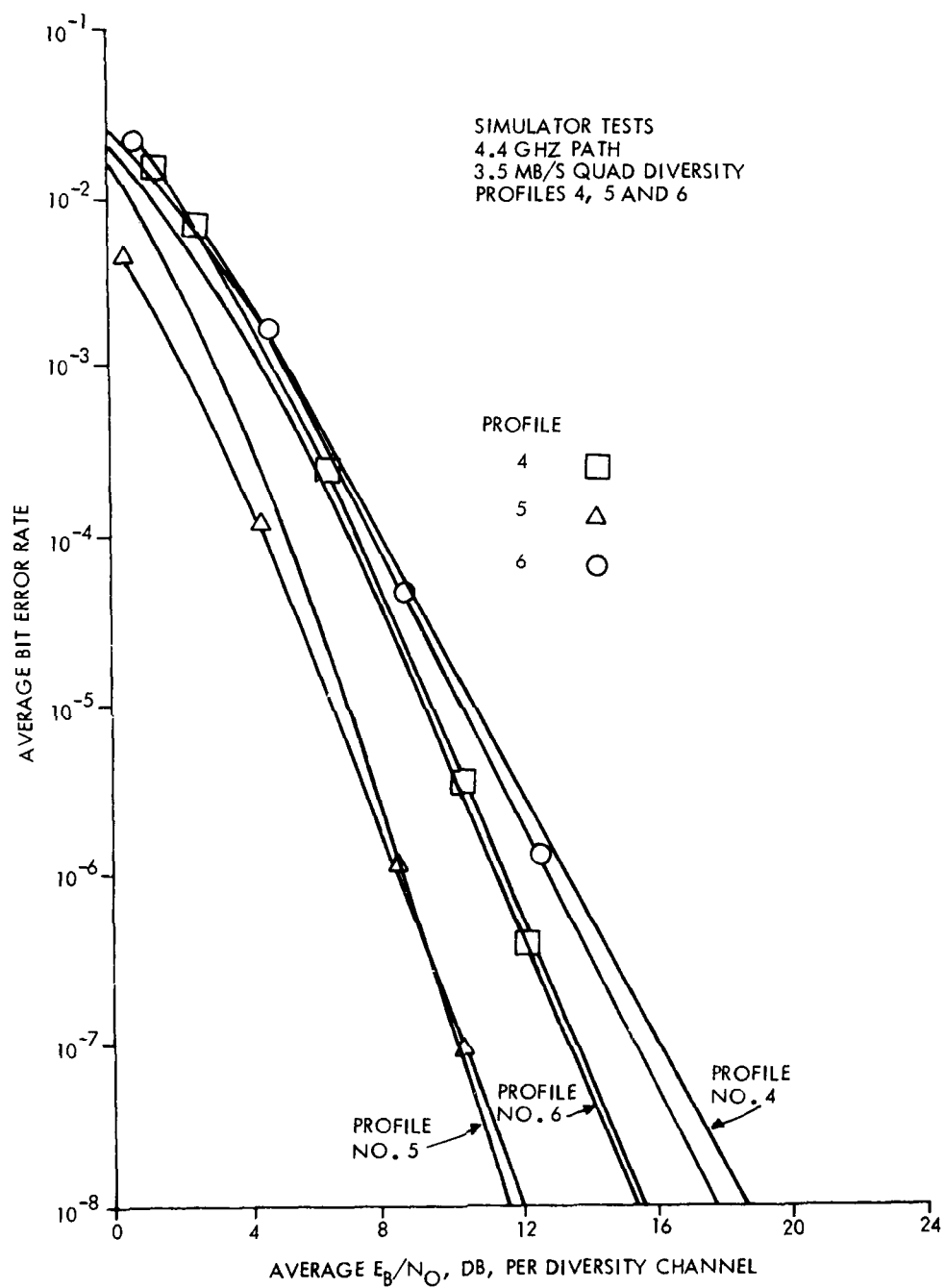


Figure 5-12. Simulator Tests 4.4 GHz Path 3.5 Mb/s Quad Diversity Profiles No. 4, 5 and 6

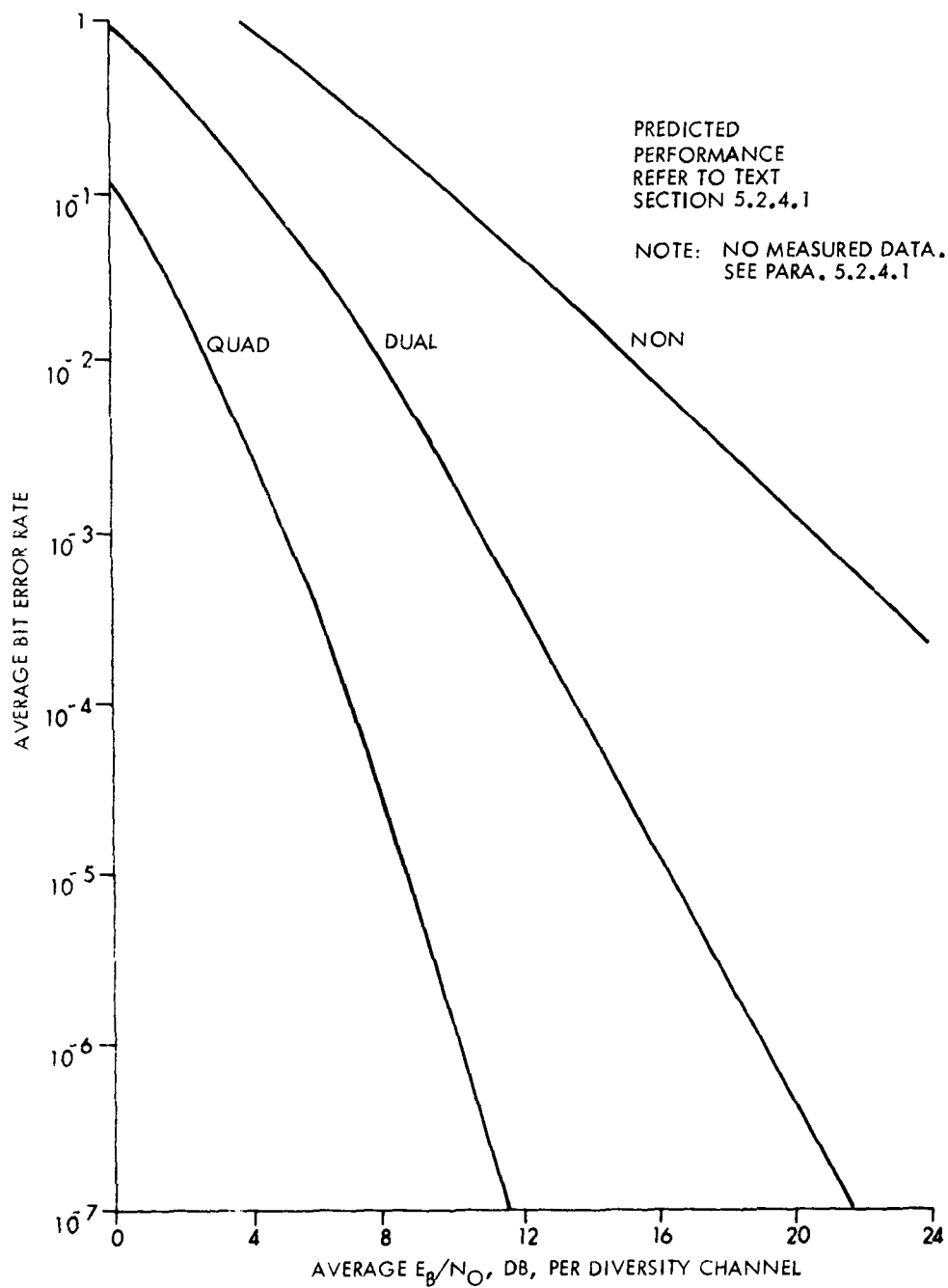


Figure 5-13. Simulator Tests 4.4 GHz Path 7.0 Mb/s Non, Dual and Quad Diversity Profile No. 3

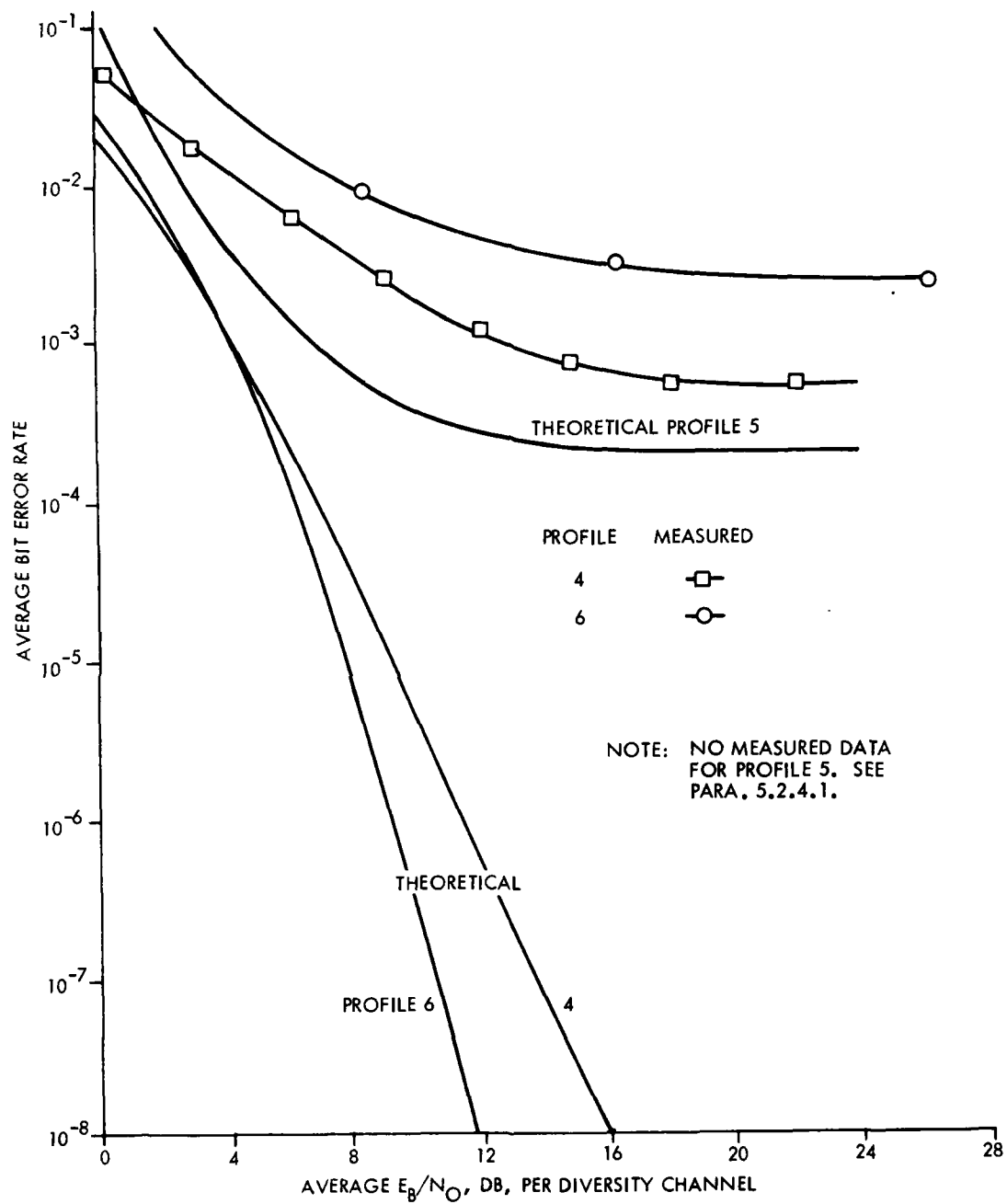


Figure 5-14. Simulator Tests 4.4 GHz Path 7.0 Mb/s Quad Diversity Profiles No. 4, 5 and 6

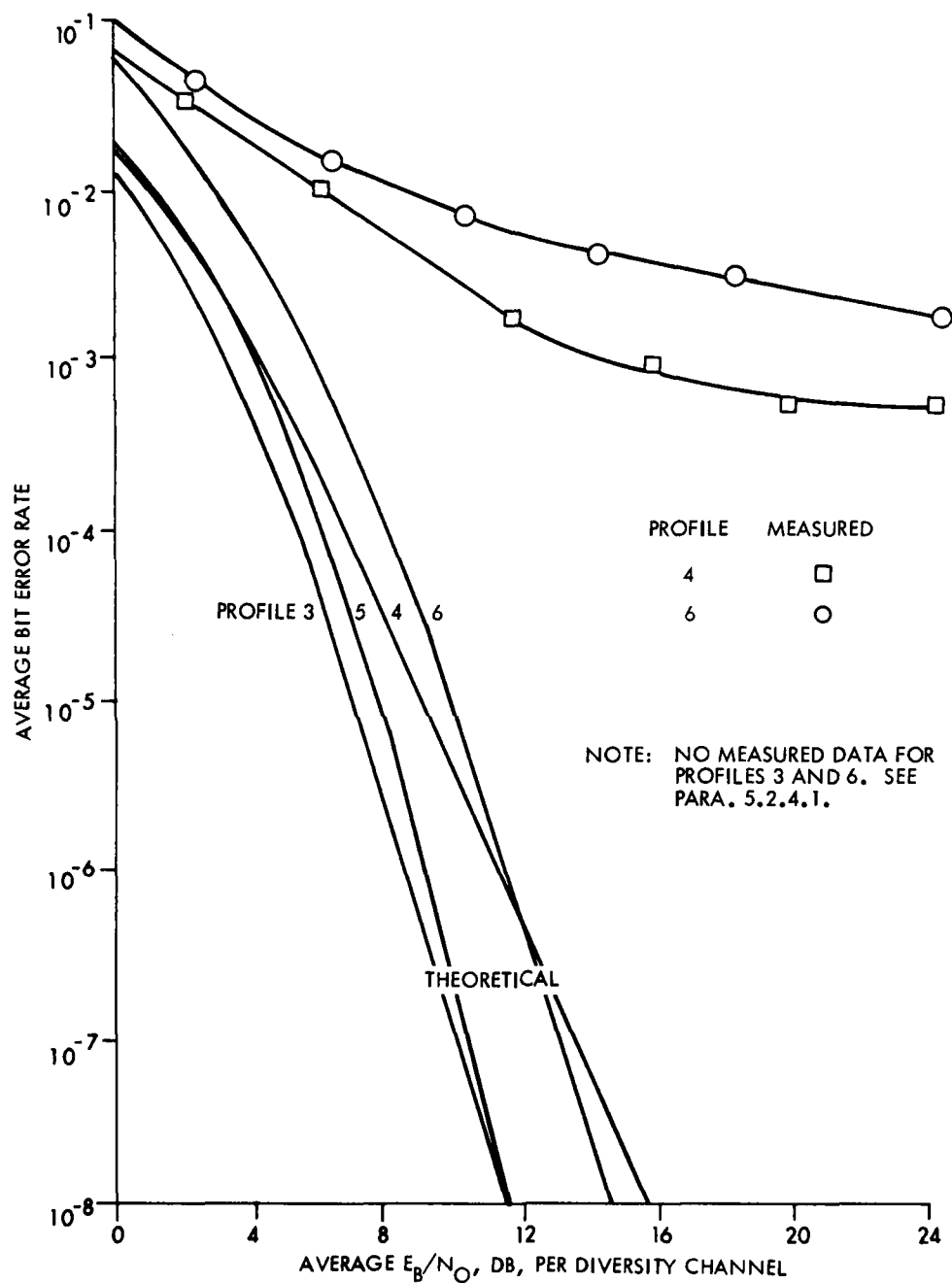


Figure 5-15. Simulator Tests 4.4 GHz Path 7.0 Mb/s Quad Diversity Profiles No. 3, 4, 5 and 6 Equalizer On

5.3 Summary and Conclusions on DCS Simulator Results

On long troposcatter links, the average received signal level tends to fall off as the average multipath dispersion increases. The adaptive matched filter action of the DAR-IV provides an intrinsic diversity performance gain which can potentially offset this average signal level loss and thus may extend the time availability of the link. The maximum data rate that can be supported on a given link depends on the anticipated multipath delay spreads and received signal level.

When the multipath spread equals the bit duration, the dual diversity irreducible BER varies between 10^{-3} and 10^{-6} depending on the DAR-IV transmission bandwidth and choice of pulse shape. For non diversity operation the corresponding irreducible BER would be about two orders of magnitude higher while for quad diversity, the BER would be about two orders of magnitude lower. The normalized multipath of unity (multipath spread X bit rate) for the QPSK DAR-IV signal with 50 percent duty cycle implies that the time gate duration (off time) is equal to the RMS delay spread. Note that when the RMS delay spread is equal to the time gate, the overlap of the adjacent pulses is quite large due to the "tails" of multipath spread. However, the DAR-IV provides serviceable irreducible BER values even under these conditions or intersymbol interference. Actually, it is the large intrinsic diversity gain of the DAR-IV which drastically reduces the onset of the irreducible rate phenomenon.

To set the experimentally measured DAR-IV performance in proper perspective, it is instructive to compare its performance against a non-adaptive, binary FSK modem which has been previously utilized for digital tropo similar to the AN/GRC-143. Since corresponding experimental results are not available for the FSK modem it is necessary to employ theoretical predictions based on the work of Bello and Nelin and described in Chapter 11 of Communication Systems and Techniques by Schwartz, Bennett and Stein. Figure 3-6 of this reference shows the dual diversity SNR degradation of binary FSK with phase continuous transitions (best case) versus a normalized data

rate,

$$d = 1/B_c T \quad (13)$$

where B_c is the correlation bandwidth of the channel. For the corresponding theoretical calculation, the 2σ multipath delay spread is given by

$$2\sigma = \sqrt{8/\pi B_c} \quad (14)$$

and this expression may then be used to link the above results to the normalized multipath spread defined in Figure 5-16.

Figure 5-16 shows the resultant dual diversity FSK E_b/N_o required to maintain 10^{-5} BER versus normalized multipath spread with a 2 dB implementation loss added. For low multipath spread, the performance approaches the flat fading case with a required E_b/N_o of about 27 dB. As the multipath spread increases, the performance degrades since there is no intrinsic diversity mechanism to counteract the intersymbol interference. At a relatively low amount of multipath spread (for the 2.3 Mbps data rate), the FSK modem exhibits an irreducible BER worse than that of 10^{-5} .

The shaded area of Figure 5-16 represents the operational extremes of the present DAR-IV including differences in pulse shape and bandwidth over the range examined. Note the dramatic contrast between the performance of the two types of modems due to the intrinsic diversity advantage of the DAR-IV. This comparison is based on equal transmit power levels and, therefore, implies that the DAR-IV employs a peak-to-average power tradeoff in the Klystron HPA to provide equal average radiated power.

The dashed lines shown in Figure 5-16 indicate the approximate range of normalized multipath spread for an 87 mile AN/TRC-97. Over this range, the simple binary FSK modem cannot provide the required 10^{-5} BER while the DAR-IV requires only 15 to 18 dB or 13 to 16 dB E_b/N_o depending on choice of pulse shape.

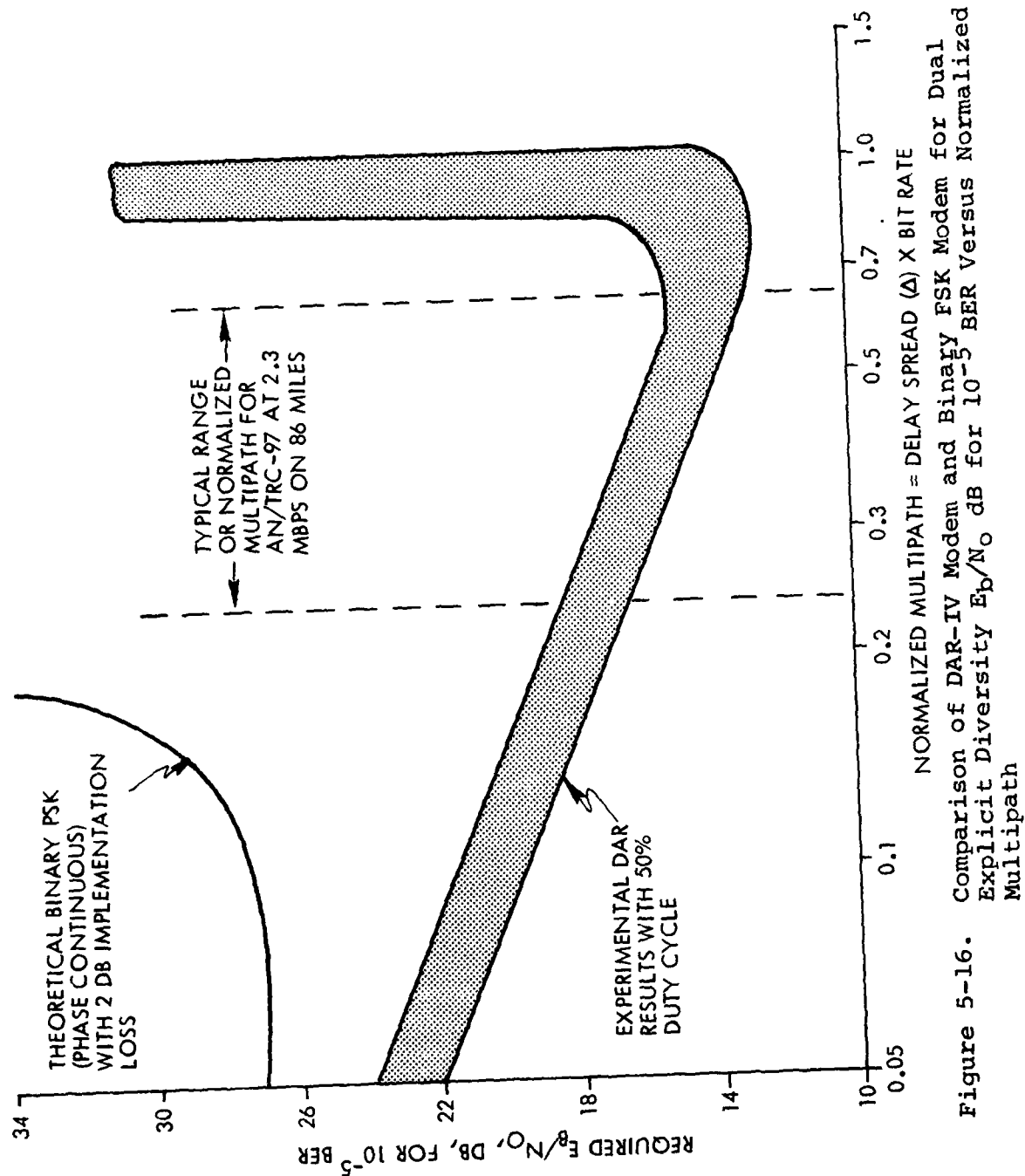


Figure 5-16. Comparison of DAR-IV Modem and Binary FSK Modem for Dual Explicit Diversity E_b/N_0 dB for 10^{-5} BER Versus Normalized Multipath

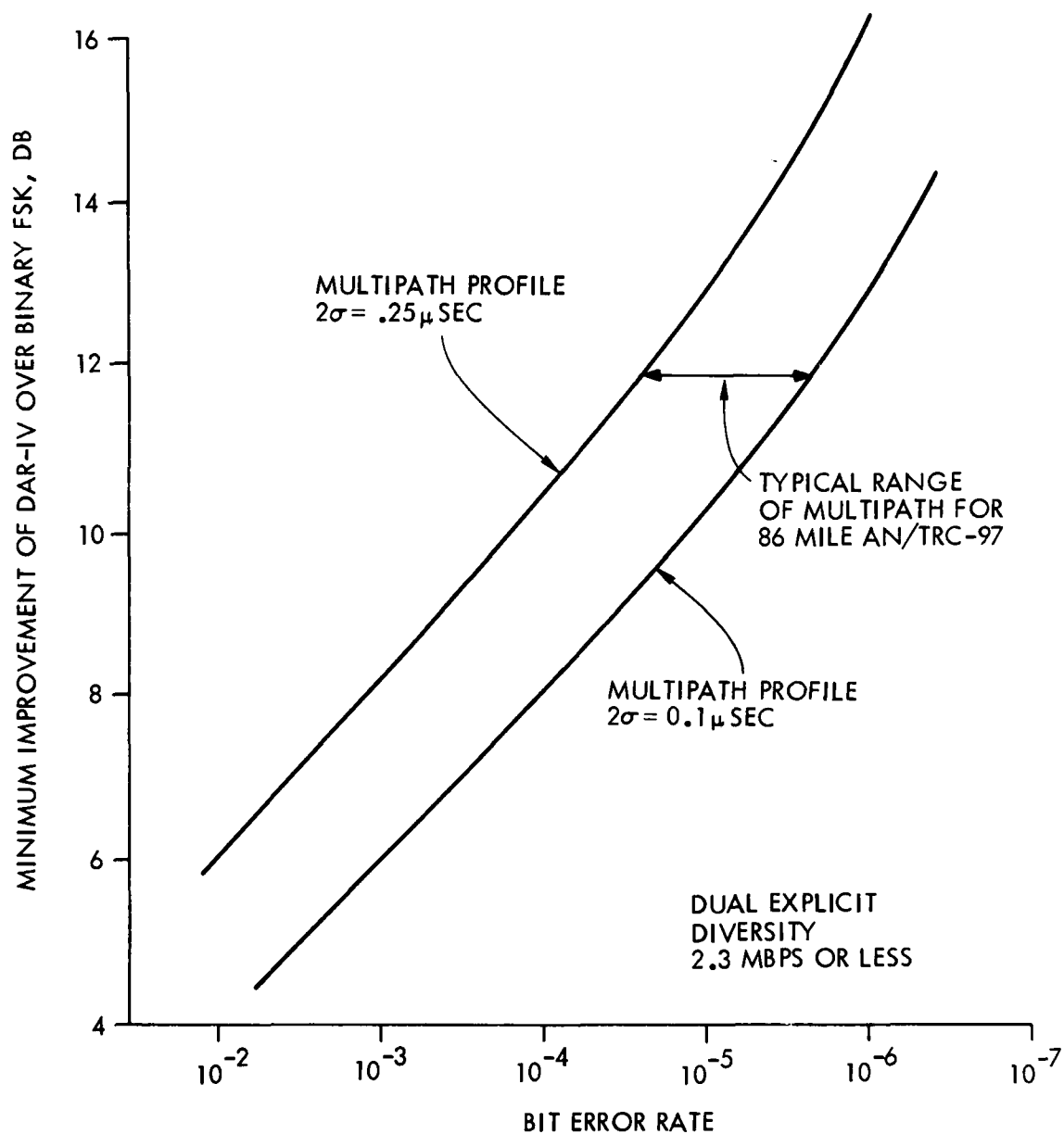


Figure 5-17. Minimum Improvement of QPSK DAR-IV Over Simple Binary FSK Modem with No Sensitivity to Multipath. DAR-IV Improvement is due to Implicit Diversity.

Even if the simple FSK modem did not exhibit an irreducible BER (at much lower bit rates), the DAR-IV would still provide a significant performance advantage. Figure 5-17 shows the resultant average improvement of the DAR-IV over the FSK modem as a function of required average BER. Note that this figure shows the minimum improvement of the DAR-IV relative to the FSK modem and is valid at lower data rates. At megabit rates, the non-adaptive FSK modem exhibits an irreducible BER which prevents it from ever reaching its BER objective. The advantage of using a modem specifically designed to operate in a multipath environment is evident in the results.

The DAR-IV experimental model displayed excellent performance at 1.75 Mb/s and 3.5 Mb/s for most multipath profiles. At 7 Mb/s, the model tended to exhibit premature irreducible BER due to the suboptimum implementation as previously described. It is interesting to compare the performance outside of the irreducible BER region with theory to determine how well the DAR-IV acts as an adaptive matched filter and develop a model for its performance.

The DAR modulation technique described previously employs differentially encoded QPSK modulation with coherent detection. The BER of a QPSK matched filter demodulator is given by

$$\text{BER}_{\text{QPSK}} = 1/2 \operatorname{erfc}(\sqrt{\gamma}) \quad (15)$$

where γ is the E_b/N_0 (energy per bit to noise power density ratio). Differential encoding is necessitated by the acquisition phase ambiguity of the DAR demodulator and tends to double the QPSK BER

$$\text{BER}_{\text{DAR}} = 2(\text{BER}_{\text{QPSK}} - \text{BER}_{\text{QPSK}}^2). \quad (16)$$

Now consider the behavior of this matched filter demodulator on the frequency-flat fading channel. The DAR provides maximal ratio diversity combining and the probability density function for maximal ratio combining of M equal, independent diversity channels is given by [8]

$$P(\gamma) = \frac{1}{(M-1)!} \frac{\gamma^{M-1}}{\Gamma^M} \text{EXP} \left\{ \frac{-\gamma}{\Gamma} \right\} \quad (17)$$

where Γ is the average E_b/N_o per diversity branch. The average BER for the DAR on that flat fading M^{th} order diversity channel is thus given by

$$\overline{\text{BER}} = \int_0^{\infty} \text{BER}_{\text{DAR}} P(\gamma) d\gamma \quad (18)$$

This integral can be easily solved by making the approximation that

$$\text{BER}_{\text{DAR}} = 1/2 \exp(-1.12\gamma) \quad (19)$$

Figure 5-18 shows the ideal QPSK BER as well as that which results due to the addition of differential encoding (solid lines). The above approximation (dashed line) is within about 0.2 dB of the actual DAR performance over the BER region of interest. Making use of this approximation, the above integral solution yields

$$\overline{\text{BER}} \approx 1/2 \frac{1}{(1 + 1.12\Gamma)^M} \quad (20)$$

For an adaptive matched filter demodulator on the tropospheric channel, the overall diversity improvement will be due to both explicit and implicit diversity. Explicit diversity is obtained by establishing independent propagation paths such as separate space diversity receiving antennas or separate in-band frequency diversity obtained by the matched filter action. That is, the adaptive matched filter "matches" the received signal spectrum and basically "weights" each portion of the received spectrum according to its signal-to-noise ratio. The greater the extent of multipath dispersion in the channel, the greater the amount of potential intrinsic diversity for a given radiated bandwidth due to a lower frequency correlation distance. However, as extra orders of intrinsic diversity are obtained, the total average received signal power remains unchanged unlike the case for explicit diversity. If we let $(1 + \alpha)$ equal the order of implicit diversity, then the equivalent system diversity characteristic

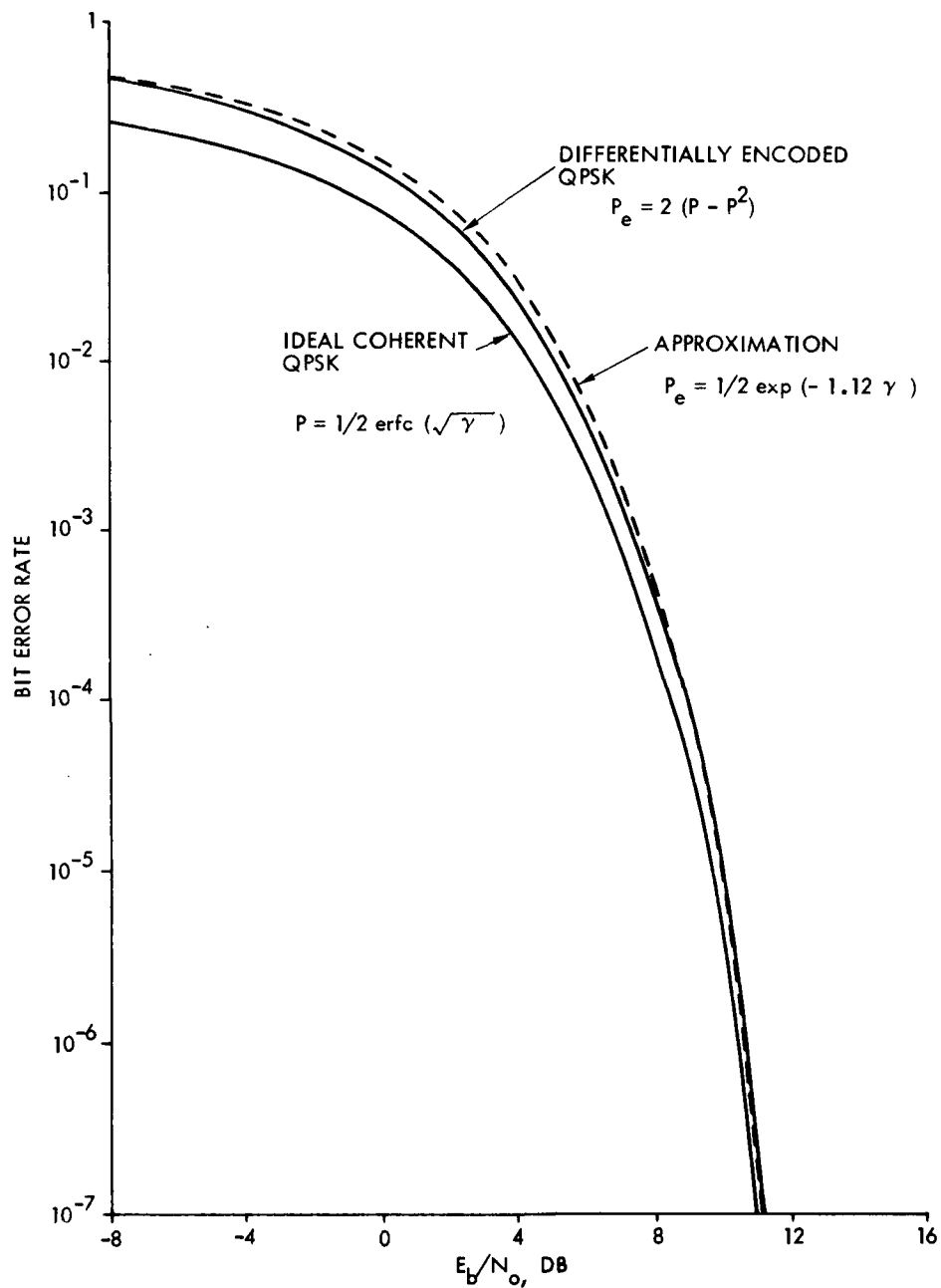


Figure 5-18. Comparison of BER Versus E_b/N_0 for Coherent and Differentially Coherent QPSK Modulation

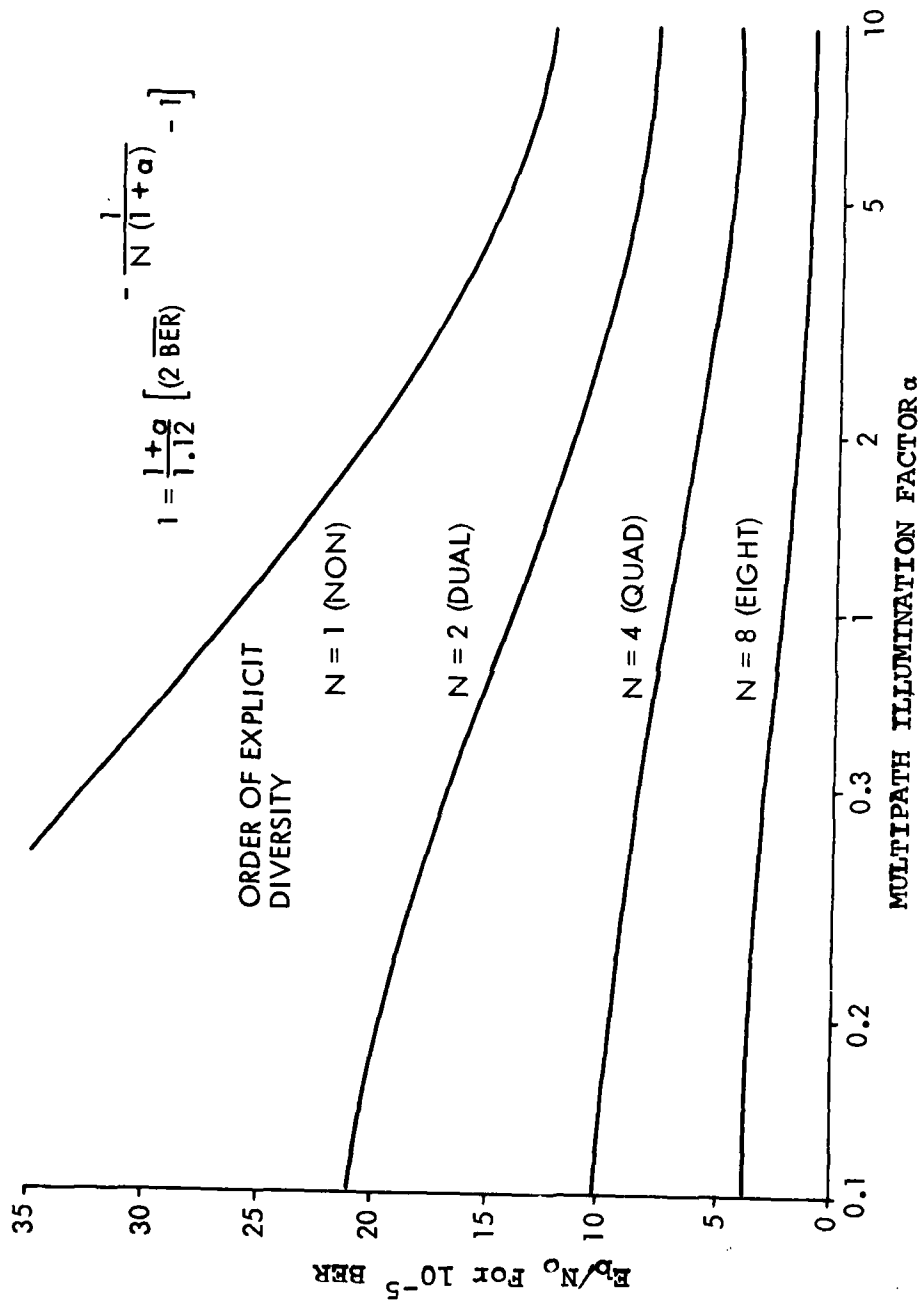


Figure 5-19. Required E_b/N_0 dB for 10^{-5} BER Versus Parameter α

can be defined as

$$M = N (1 + \alpha) \quad (21)$$

The resultant expression for BER is then

$$\overline{\text{BER}} \approx 1/2 \left(\frac{1}{1 + \frac{1.12\Gamma}{1 + \alpha} N(1 + \alpha)} \right) \quad (22)$$

This expression yields the average BER for any average E_b/N_o per explicit diversity branch, Γ , given an order of explicit diversity N and implicit diversity $1 + \alpha$. The expression is accurate to within about 0.2 dB for an ideal adaptive matched filter for low BER. It includes both the flat fading upper limit on BER for $\alpha = 0$ and the non-fading lower limit on BER for $\alpha \gg 1$. This expression is plotted in Figure 5-19 for Γ as a function of α for $\overline{\text{BER}}$ fixed at 10^{-5} . Note that for low orders of explicit diversity, the potential benefit of implicit diversity can be quite large. For example, a single channel (non-diversity) troposcatter system using an adaptive matched filter demodulator with a $\alpha = 1.5$ will perform as well as a dual explicit diversity system that employs a conventional, non-adaptive digital demodulator. The additional intrinsic diversity performance gain of the adaptive filter demodulator thus offers the potential to significantly reduce system cost (order of explicit diversity) without sacrifice of performance compared to conventional digital systems.

To use these curves, it is necessary to first define the multipath illumination factor, α , in terms of RMS multipath delay spread and effective signal bandwidth. The Fourier transform of the multipath delay spread yields the frequency correlation function which describes the correlation between two frequencies of arbitrary spacing. Once one determines the frequency spacing at which two frequencies are sufficiently decorrelated, the value of α is given by the ratio of the signal bandwidth to the frequency correlation distance.

While this procedure to define α appears definite, some judgment is required to determine the frequency correlation coefficient at which adjacent signals can be considered to represent "independent" diversity signals. Consider the correlation properties corresponding to a range of multipath delay power spectra. In each case, let Δ represent the 2 sigma value of the RMS multipath spread and let the "multipath" illumination factor, α , be defined as the ratio of the signals transmitted 3 dB bandwidth, W , to the frequency separation required for a correlation factor of 0.707. It is well known that relatively little diversity gain is lost in the combining of fading signals with cross-correlation coefficients as high as 70 percent.

With this definition of α , its value will depend somewhat, on the shape of the multipath delay spread, $h(\tau)$, as follows:

Exponential

Multipath Spread:

$$h(\tau) = e^{-\frac{2\tau}{\Delta}} U(\tau) \quad (23)$$

Frequency Correlation:

$$u(\omega) = (4/\Delta^2 + \omega^2)^{-1/2} e^{-j \tan^{-1}(\omega\Delta/2)} \quad (24)$$

Multipath Illumination Factor:

$$\alpha = \pi \Delta W \quad (25)$$

Rectangular

Multipath Spread:

$$H(\tau) = \frac{1}{\sqrt{3\Delta}} \quad |\tau| \leq \frac{\sqrt{3\Delta}}{2} \quad (26)$$

Frequency Correlation:

$$u(\omega) = \sin \frac{\sqrt{3}\omega\Delta}{2} / \omega \Delta \quad (27)$$

Multipath Illumination Factor:

$$\alpha = 3.93 \Delta W \quad (28)$$

Gaussian

Multipath Spread:

$$h(\tau) = e^{-\frac{2\tau^2}{\Delta^2}} \quad (29)$$

Frequency Correlation:

$$\mu(\omega) = e^{-\frac{\omega^2 \Delta^2}{8}} \quad (30)$$

Multipath Illumination:

$$\alpha = 1.2 \Pi \Delta \omega \quad (31)$$

Weighted Exponential

Multipath Spread:

$$h(\tau) = \tau e^{-\frac{\sqrt{2}\tau}{\Delta}} \quad (32)$$

Frequency Correlation:

$$\mu(\omega) = 1/(j\omega + \frac{2\sqrt{2}}{\Delta})^2 \quad (33)$$

Multipath Illumination Factor:

$$\alpha = 1.1 \Pi \Delta \omega \quad (34)$$

Double Weighted Exponential

Multipath Spread:

$$h(\tau) = \tau^2 e^{-\frac{2\sqrt{3}\tau}{\Delta}} \quad (35)$$

Frequency Correlation:

$$\rho(\omega) = 1 / (j\omega + \frac{2\sqrt{3}}{\Delta})^3 \quad (36)$$

Multipath Illumination Factor:

$$\alpha = 1.13 \pi \Delta \omega \quad (37)$$

Note that the value of α varies between $3.14 \Delta W$ and $3.93 \Delta W$ depending on the average power density of the multipath delay spread Δ , the resultant order of intrinsic diversity is $1 + \pi \Delta W$ for an adaptive matched filter. This expression is more conservative than the value obtained from a channel with rectangular multipath dispersion density but should match that obtained with exponential dispersion. Still, it would be useful to estimate the "worst case" performance for this model. Clearly, some degradation could be expected due to the finite correlation between adjacent frequency "cells".

The definition of α above implies that when a signal of bandwidth W "illuminates" a channel with multipath delay spread Δ , the resultant order of intrinsic diversity is $1 + \pi \Delta W$ for an adaptive matched filter. This expression is more conservative than the value obtained from a channel with rectangular multipath dispersion density but should match that obtained with exponential dispersion. Still, it would be useful to estimate the "worst case" performance for this model. Clearly, some degradation could be expected due to the finite correlation between adjacent frequency "cells".

The solid lines in Figure 5-20 and 5-21 show the prediction of the math model for 10^{-5} BER. Also shown on the figures are a number of experimentally measured data points. (All data was obtained outside of the modem's region of irreducible error rate phenomenon. The back-to-back modem implementation loss of about 2.5 to 3.5 dB was subtracted from the data points to represent an "ideal" demodulator implementation.) Note that there appears to be good agreement between the data point and the mathematical model with very little dispersion in the data. Note also that the data points all follow closely the math model for uncorrelated frequency "cells". The reason for this apparent lack of degradation due to correlation may be the original choice of 70 percent correlation to define adjacent cells. In fact, still higher correlation may be appropriate for the model which would tend to indicate higher intrinsic diversity with added correlation loss. Since agreement between the experimental data and the

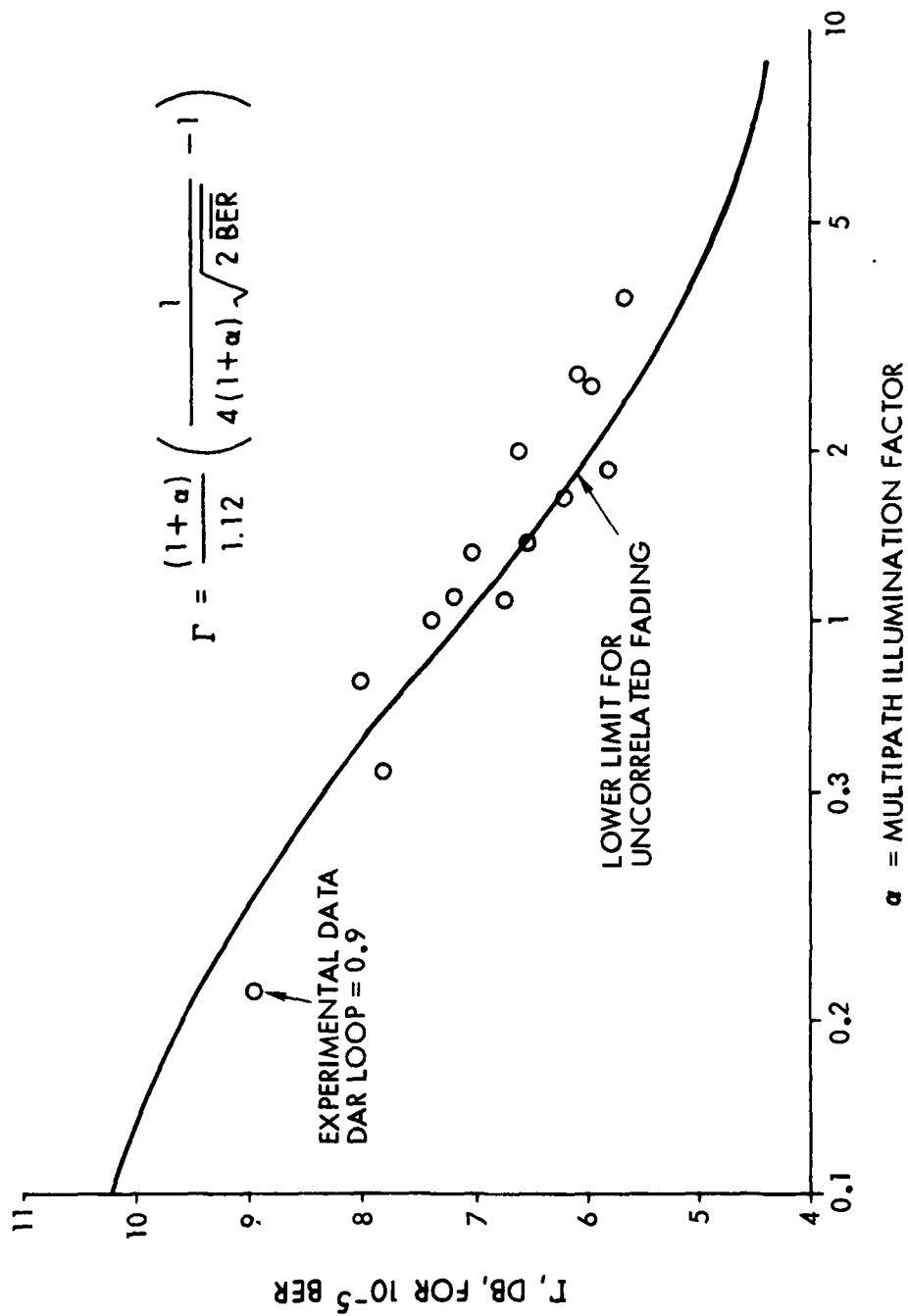


Figure 5-20. Dual Explicit Diversity

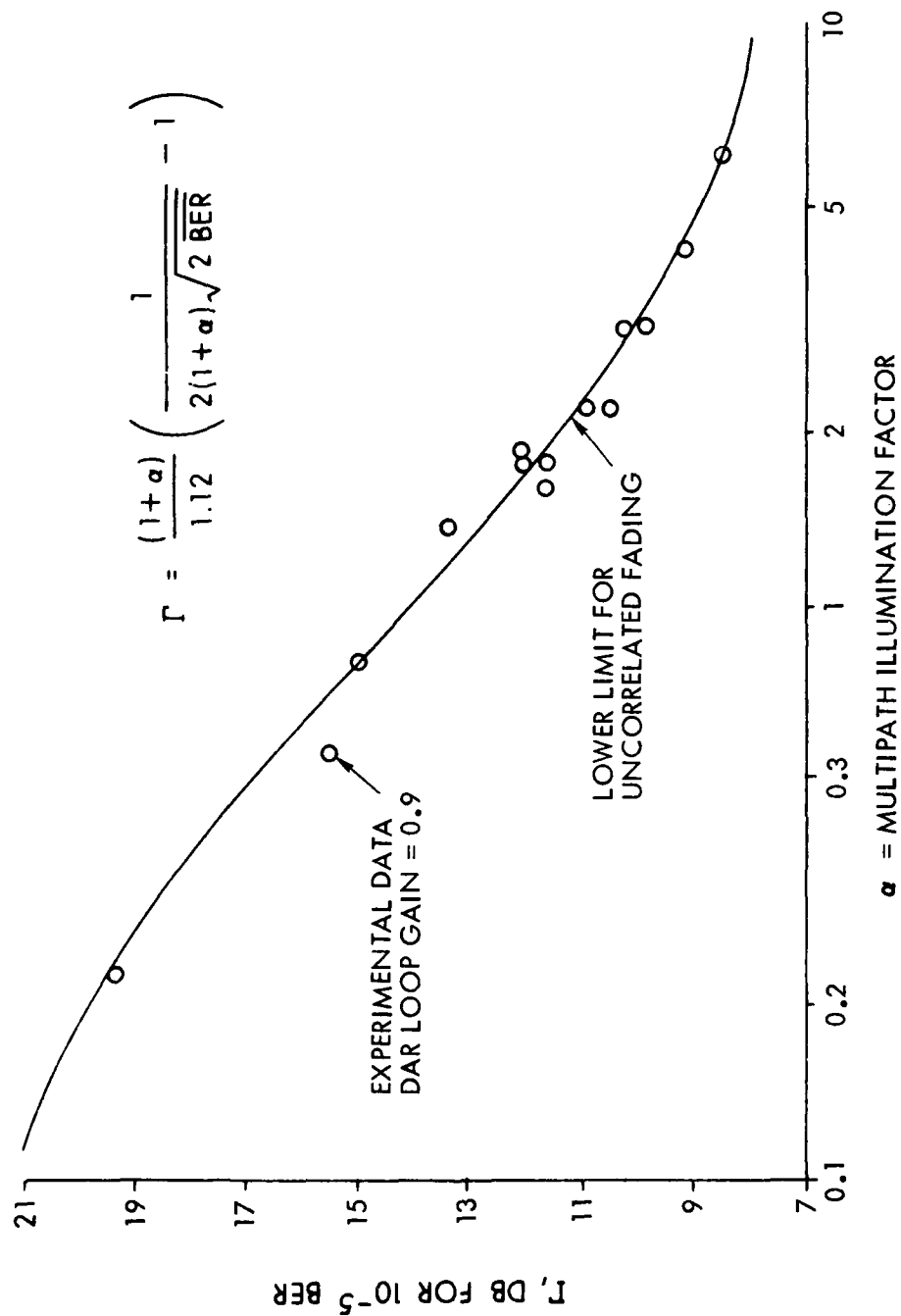


Figure 5-21. Quad Explicit Diversity

model is excellent, no further refinement of the model is needed to provide a useful lower bound on the performance of a digital adaptive matched filter demodulator such as the DAR. However, when the multipath spread is large compared to the data symbol duration of interest, an irreducible BER phenomenon will result in the DAR due to intersymbol interference. The region or irreducible BER and corrections to the above model to account for this phenomenon are given in the following paragraphs.

Figures 5-20 and 5-21 show the agreement between the simple mathematic model described above and a number of experimental data points obtained using a DAR modem at data rates of 1.75, 3.5 and 7.0 Mbps. Various multipath delay spreads were tested at each data rate using the RADC tropo-scatter media simulator facility. However, the data was obtained for combinations of data rate and multipath spread which did not display an irreducible BER phenomenon in the region of 10^{-5} BER.

The mathematical model above assumes negligible intersymbol interference. In the DAR modulation scheme, a time gate is employed on the transmitted QPSK waveform to create an "off-time" between adjacent symbols. At the higher data rates, the DAR typically employs a 50 percent duty cycle waveform. This "off-time" permits the transmitted pulse to be "smeared out" by the multipath propagation without causing excessive overlap of adjacent pulses (or intersymbol interference). For a given data rate and off-time duration, increasing the multipath to a large enough value will eventually cause performance degradation due to intersymbol interference. For large enough intersymbol interference, an irreducible BER phenomenon will result where the intersymbol interference causes bit errors in the absence of noise.

An expression to describe this degradation in performance is difficult to derive analytically. Instead, the DAR modulation technique of adaptive matched filtering was analyzed by computer simulation as previously described. In the region where the intersymbol interference was small (low multipath delay spread), the previously derived mathematical model was

found to be accurate. At large multipath spreads, it was found that the model required correction to account for intersymbol interference.

The transmitted pulse shape employed in the simulation is also a consideration in the correction factor applied. In the simulations performed, a raised-cosine-like pulse shape was employed which results when a 50 percent duty factor QPSK pulse is passed through a five-pole Butterworth filter with a bandwidth equal to approximately 0.9 times the bit rate. This filtering results in a DAR waveform 99 percent power spectral confinement of 1.5 times the bit rate which is the narrowest confinement recommended for use with the DAR technique. It has been shown in the computer simulation that this raised-cosine-like waveform can be passed through a non-linear klystron amplifier with less than 1.2 dB loss due to waveshaping (beyond the 50 percent duty cycle) and still preserve the 1.5 Hertz/bit spectral confinement.

By curve fitting the computer simulation results, the approximate correction factor at 10^{-5} BER for dual explicit diversity was found to be:

$$\text{Correction}_{\text{Dual}} = \begin{cases} (5\lambda - 1) & \text{dB for } \lambda > .2 \\ 0 & \text{for } \lambda \leq .2 \end{cases} \quad (38)$$

where

$$\lambda = R \Delta \sqrt{R/W} \quad (39)$$

and R is the bit rate for a 50 percent duty cycle waveform. In the case of quad explicit diversity, the correction factor was found to be 0.75 (in decibels) of that for dual diversity. At 10^{-5} BER, an irreducible BER phenomenon occurs when $\lambda > .82$ for dual explicit diversity and when $\lambda > .97$ for quad diversity.

In a dual diversity system at 10^{-5} BER, the correction factor varies between 0 dB to 3 dB depending on the extent of multipath dispersion. At high BER, the correction factor is lower. With this correction factor added to the

E_b/N_0 estimate for an ideal QPSK adaptive matched filter, the performance of a band-limited DAR demodulator at 10^{-5} BER is easily estimated. To apply this performance estimate to a real system, it is also necessary to include an allowance for implementation losses. Based on current DAR production activities, it has been found that a 2 dB implementation loss margin can be practically achieved.

The decision feedback equalizer, if successfully implemented, would allow the multipath limits for a given irreducible BER to be extended. However, the DFE requirements greatly complicate the DAR modem implementation making the DFE of dubious value. An alternative modem approach, as developed for the AN/TRC-170, retains the inherent simplicity of the basic DAR but provides the extra multipath protection desired without the use of a DFE and its implementation restrictions. This alternative approach is described in Appendix A and simply consists of exploiting the 50 percent duty cycle of the basic DAR waveform to interleave a second transmission stream at a somewhat offset frequency. The resultant parallel pulse streams (each carrying half the mission traffic) can still fit in the DAR spectral allocation, but can now handle nearly twice the multipath spread since the "effective" data rate is halved. The penalty for this feature is somewhat less intrinsic diversity gain and nearly twice the modem hardware. However, where this feature is needed, the impact of the reduced intrinsic diversity is negligible and the added circuitry is only a duplication of existing basic DAR modem with no stringent requirements of recirculating filter loop gain.

6.0 OVER-THE-AIR TEST RESULTS RADC EXPERIMENTAL RANGE

6.1 General

Over-the-Air test results on the RADC Experimental Range as well as on ACE HIGH links in Europe, described in Section 7, indicated good agreement with predictions and with the Laboratory Simulator results described in the preceding section.

Also, the DAR-IV generally provided reliable digital transmission and significant performance benefits due to efficient utilization of intrinsic diversity. This is particularly true for transmission data rates of 3.5 Mb/s and 1.75 Mb/s. Tests at 7.0 Mb/s did not achieve the full performance expected as noted in earlier sections.

Over-the-Air testing on the RADC Experimental Range was conducted on two links between Youngstown, New York and Verona, New York and between Verona, New York and Ontario Center, New York. Tests on the AN/TRC-97 were run in lieu of testing on the AN/MRC-98 due to unavailability of the AN/MRC-98 equipment.

The AN/TRC-132 tests were run for four weeks starting the last week of May 1978. The modem was set up in Verona for back-to-back verification before the transmitter was forwarded to Youngstown. The AN/TRC-132 equipment was in excellent operating condition. The two transmitters and four receivers, two each operated at 4.5 and 4.69 GHz were phase-locked to 5 MHz Rubidium references. The transmitter power of the AN/TRC-132 was varied in order to obtain different E_b/N_o 's and to maintain the RSL's on both frequencies within 3 dB.

Each test run was ten minutes in length and were run one after another from 8:00 a.m. to 4:30 p.m., Monday through Friday. This yielded approximately 350 data points at the three data rates with Dual or Quad diversity.

Testing on the AN/TRC-97 was done with Verona as the Transmitter and Ontario Center as the Receiver. This series of

tests were extremely successful from a data gathering point of view as a result of the newly installed automatic data gathering/data reduction equipment at the Ontario Center site. After initial installation and debugging, unattended 24 hour day, seven days a week operation was possible. From a statistical point of view this is a significant advantage.

The test site computer at Ontario Center has inputs via LEL's for four independent RSL levels along with the 20 time intervals from the RAKE system. The RSL levels are used on a per channel basis to compute median RSL, path loss, SNR and fade rate. The RAKE was used to obtain an indication of the link's profile for mean path delay, RMS multipath spread and to check the accuracy of the transmitter and receiver Rubidium references. However, the RAKE data obtained is of questionable value.

6.1.1 System Alignment and Calibration

The basic over-the-air system configuration is illustrated by Figures 6-1 and 6-2 for the AN/TRC-132 and the AN/TRC-97, respectively. In the AN/TRC-132 tests the transmitted power was actually varied by adjusting the HPA power. Transmitter power ranged from a maximum of 4 KW down to approximately 25 watts. The low end could only be estimated due to the single span of the power meter.

The AN/TRC-97 tests used constant HPA output and no attenuation at the receiver site. The BER range of 10^{-1} to 10^{-8} was covered by letting the link run continuously around the clock. The RSL median level varied 20 to 30 dB between 4:30 p.m. and 7:00 a.m. with the strongest signals occurring just before sunrise. This capability was attained because of the automated test setup that will run unattended under control of the Hewlett Packard computer-calculator, (refer to Figure 6-2 for the test setup block diagram).

6.2 AN/TRC-132 Over-the-Air Results

6.2.1 General

This series of tests was performed over the Youngstown to Verona RADC Experimental Tropo path. The power

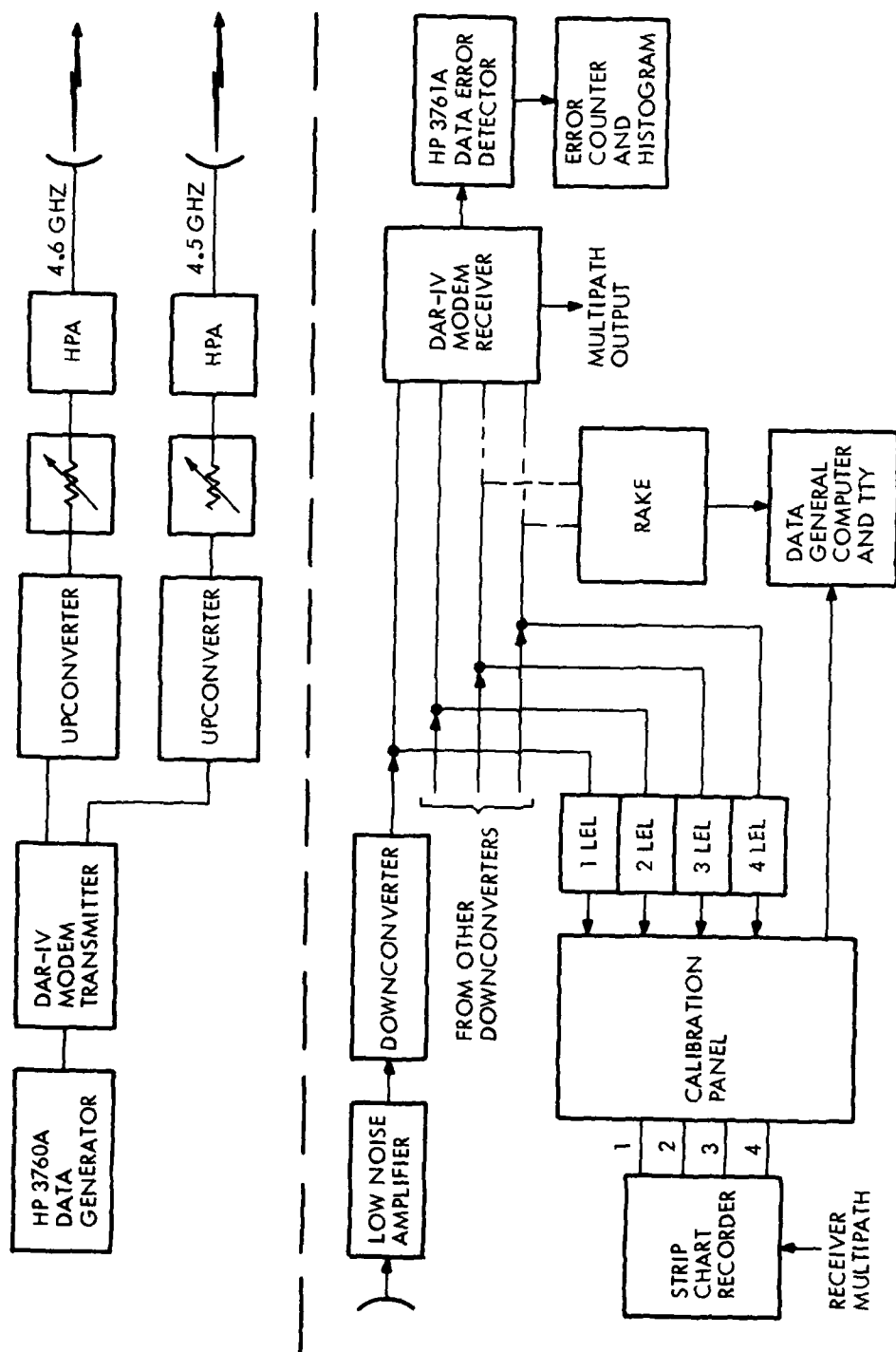


Figure 6-1. AN/TRC-132 Test Configuration

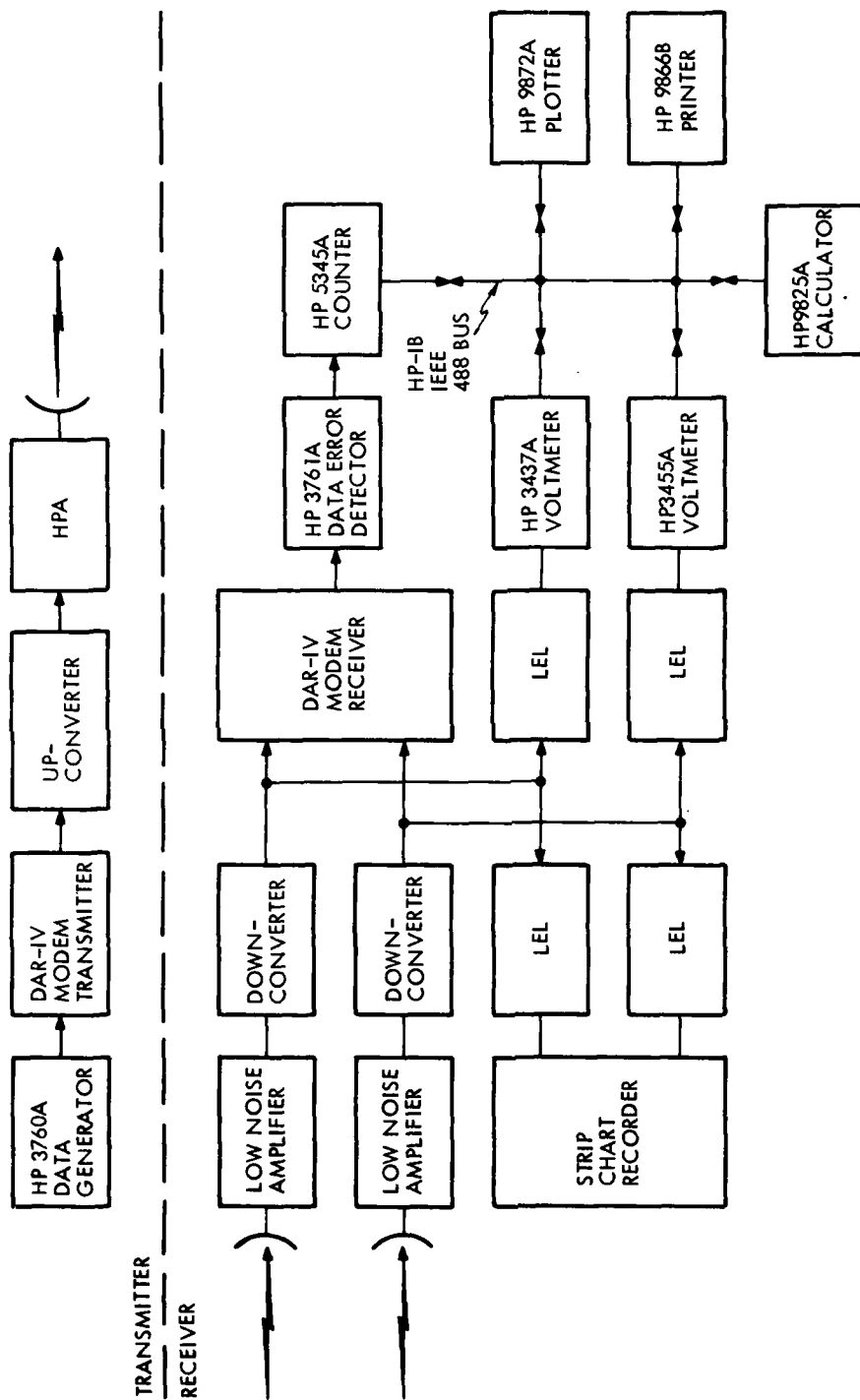


Figure 6-2. AN/TRC-97 Test Configuration

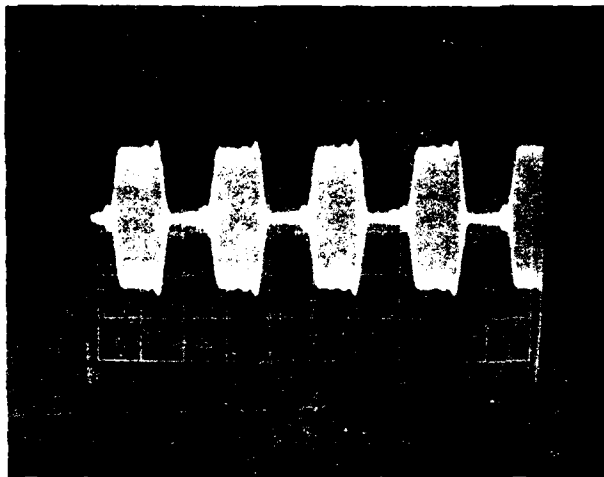
amplifiers were adjusted for optimum performance and broadbanded to provide approximately 7 to 8 MHz 3 dB bandwidth. The AN/TRC-132 operates at C-Band with 28 foot antennas and this link has relatively low multipath spreads. These tests were run during the month of June 1978. During the recording, emphasis was placed on the higher data rates and higher orders of diversity as these are of the most interest to the DCS system.

The objective of the AN/TRC-132 test was to obtain, at least, eight points for each decade of BER from 10^{-1} to 10^{-8} in both dual diversity and quad diversity. Most of the testing with dual diversity was done using Channel 1 and 3 inputs of the modem and Receivers 1 and 3 both of which operated on 4.5 GHz.

Figures 6-3 through 6-7 are photographs of the AN/TRC-132 high power amplifier outputs. These pictures were obtained via a directional coupler and a mixer to down convert the microwave frequencies to 70 MHz. Figure 6-4 is the #1 HPA output taken as above except the transmission rate is 3.5 Mb/s. Even though the time domain waveform is distorted, this has no grave effect on the modem performance because of the phase shift keyed modulation. Figure 6-5 shows the output of #2 HPA at 3.5 Mb/s. This HPA is broadbanded a little better than #1 as shown by the 4 dB difference in the amplitude of the primary side lobes. The power levels of HPA's 1 and 2 are not exactly the same as shown by the lower amplitude of both the time domain and the frequency domain displays. Figure 6-6 shows the 10 MHz bandwidth of HPA #2 at 7.0 Mb/s. The upper and lower side lobes are both filtered out. Figure 6-7 shows the slightly larger bandwidth allowing the first side lobes through even though they are 30 dB down from the main lobe.

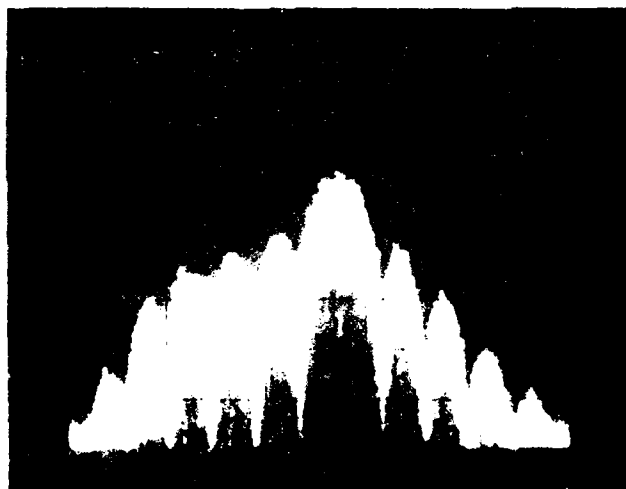
6.2.2 AN/TRC-132 1.75 M Bit Performance

Figure 6-8 and 6-9 plot the data taken relative to theoretical predictions for coherent phase shift keyed modulation (CPSK) for dual and quad diversity. These curves allow for a 3 dB implementation loss. Figure 6-8, which shows the DAR-IV performance for 1.75 Mb/s dual diversity is a good representation of the dual diversity performance with



HOR = 1μ SEC/DIV

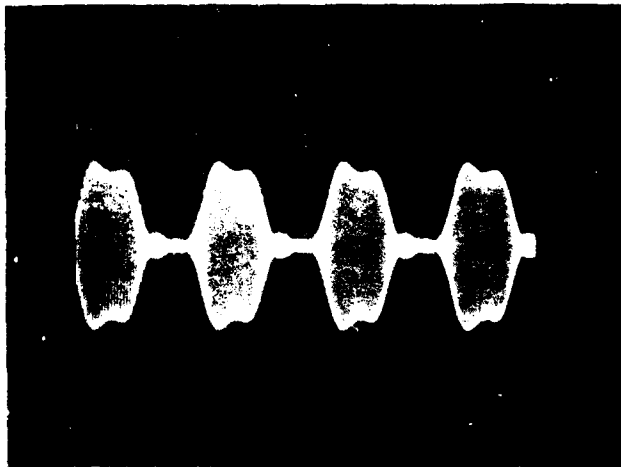
(a) OUTPUT WAVEFORM



HOR = 2 MHz/DIV
VERT = 10 DB/DIV

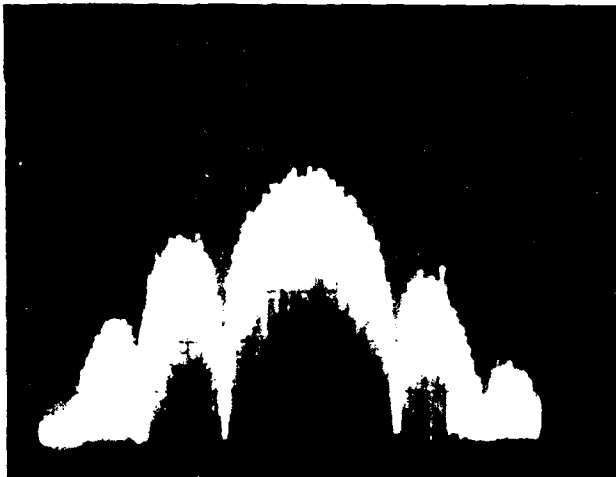
(b) OUTPUT SPECTRUM

Figure 6-3. AN/TRC-132 Transmitter Waveforms PA #1,
1.75 Mb/s, 4 KW O/P



HOR = 0.5μ SEC/DIV

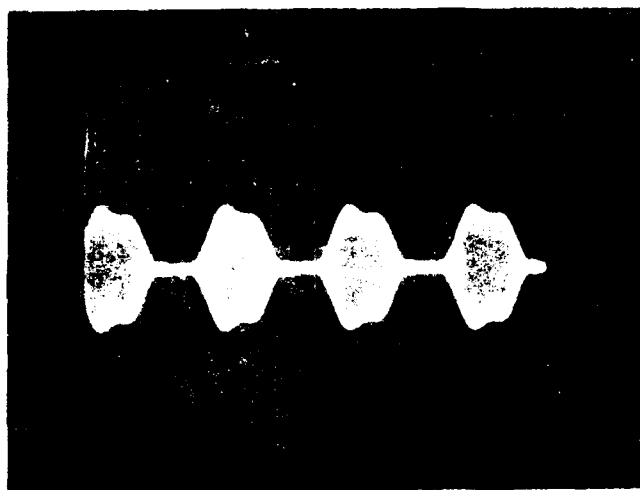
(a) OUTPUT WAVEFORM



HOR = 2 MHz/DIV
VERT = 10 DB/DIV

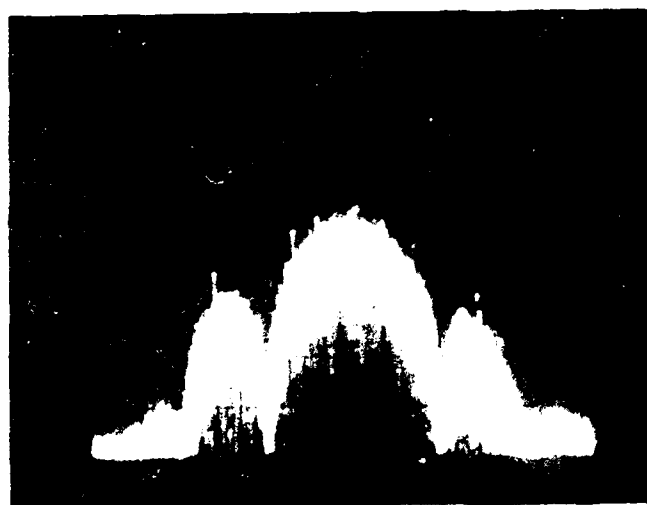
(b) OUTPUT SPECTRUM

Figure 6-4. AN/TRC-132 Transmitter Waveforms PA #1
3.5 Mb/s, 4 KW O/P



HOR = $0.2 \mu\text{SEC}/\text{DIV}$

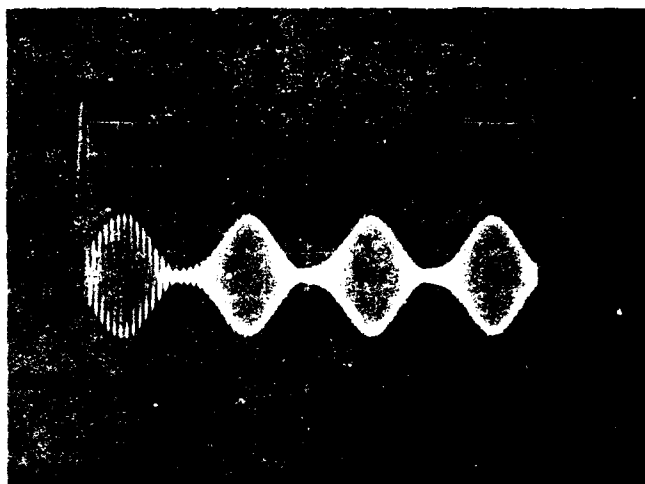
(a) OUTPUT WAVEFORM



HOR = 2 MHz/DIV
VERT = 10 DB/DIV

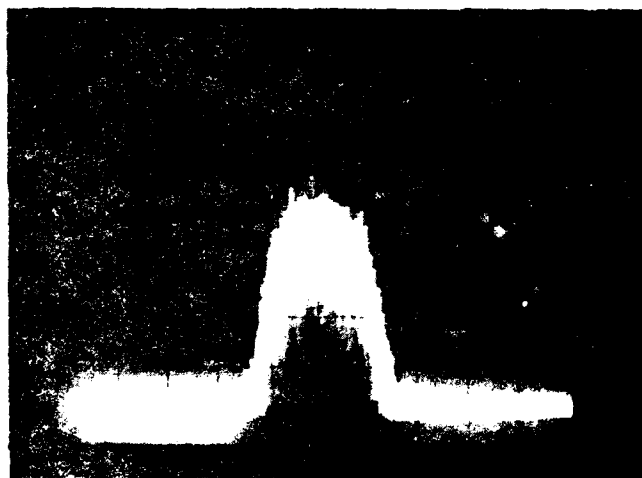
(b) OUTPUT SPECTRUM

Figure 6-5. AN/TRC-132 Transmitter Waveforms HPA #2,
3.5 Mb/s, 4 KW O/P



HOR = 0.1μ SEC/DIV

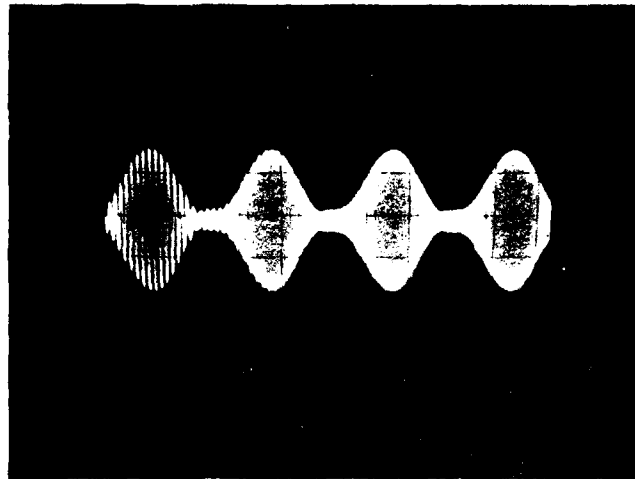
(a) OUTPUT WAVEFORM



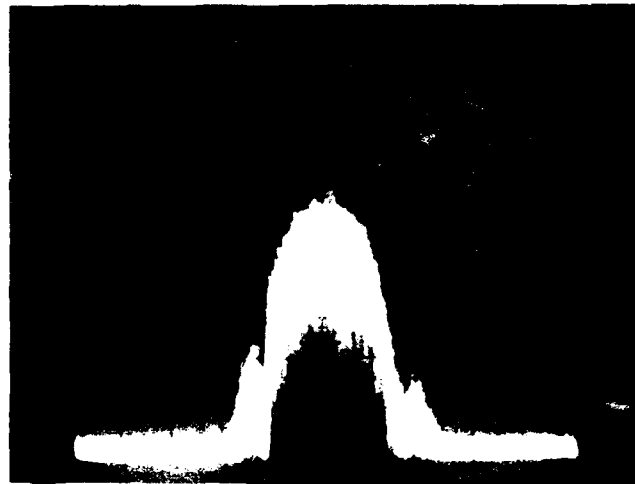
HOR = 5 MHz/DIV
VERT = 10 DB/DIV

(b) OUTPUT SPECTRUM

Figure 6-6. AN/TRC-132 Transmitter Waveforms HPA #2,
7.0 Mb/s, 4 KW O/P



(a)



(b) 5MHz/DIV

Figure 6-7. AN/TRC-132 Transmitter Waveforms HPA #1,
7.0 Mb/s, 4 KW @ 4.69 GHz

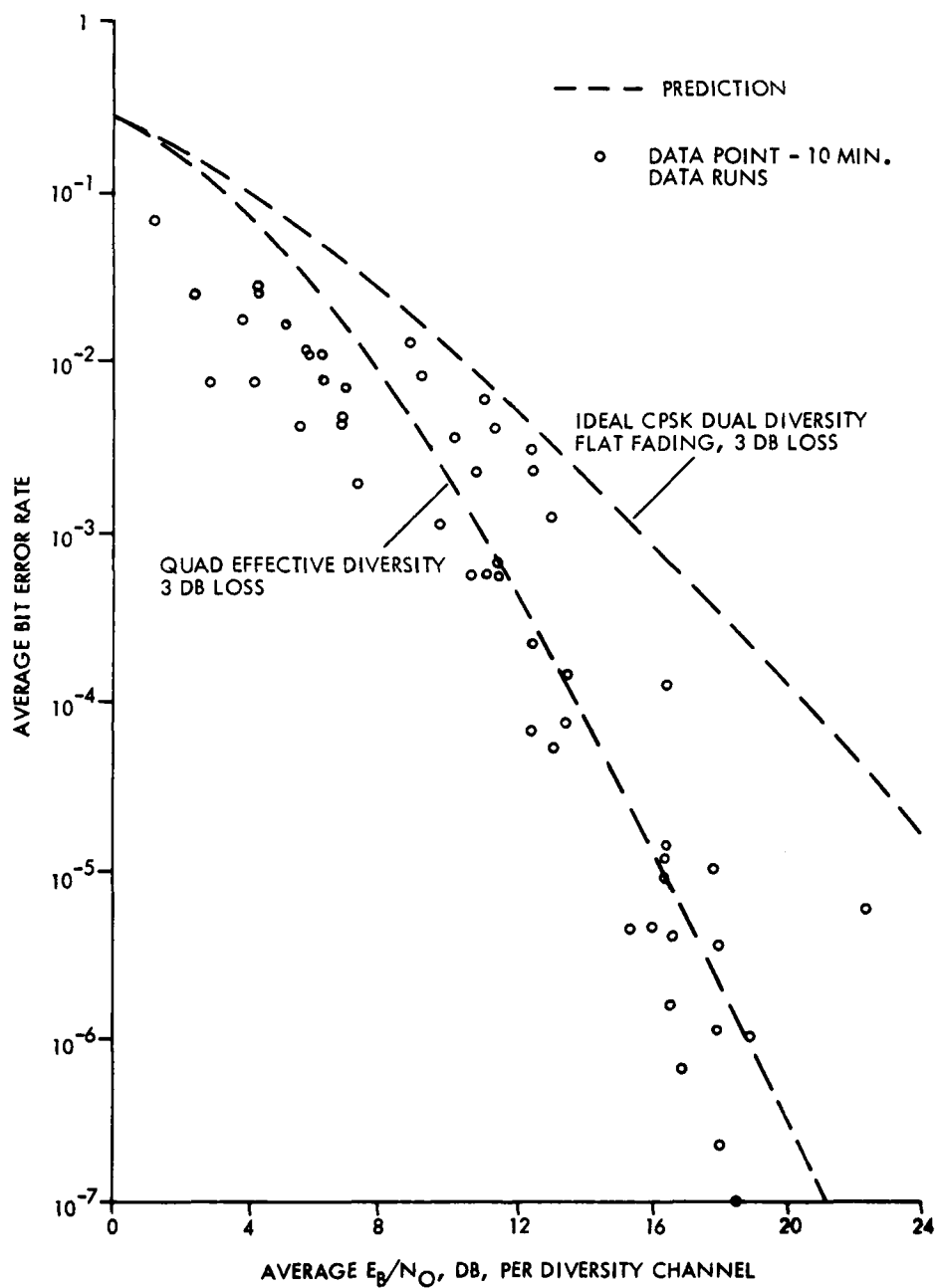


Figure 6-8. "Over-the-Air Tests" AN/TRC-132
Youngstown/Verona 1.75 Mb/s Dual Diversity

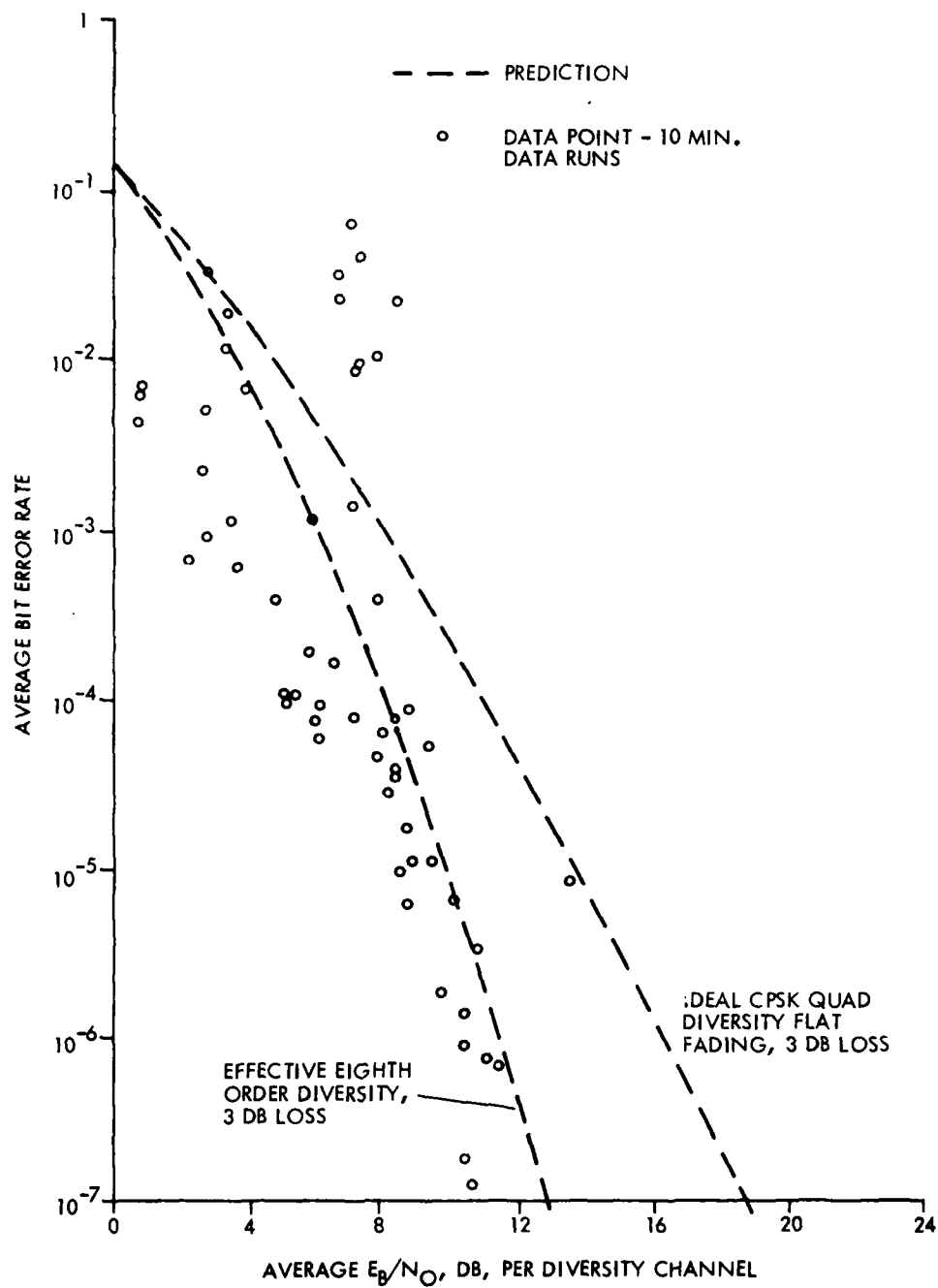


Figure 6-9. "Over-the-Air Tests" AN/TRC-132
Youngstown/Verona 1.75 Mb/s Quad
Diversity

varying levels of intrinsic diversity. The spread in error rate performance shows the significant improvement for increased delay spread. The implicit diversity varies from approximately dual to about sixth order with an excellent collection of data points centered around the fourth order intrinsic diversity prediction.

Figure 6-9, shows similar results for quad diversity. Measured error rates ranged from approximately 10^{-1} to better than 10^{-7} (not shown on the curves). Here the data is clustered around the effective eighth order intrinsic diversity prediction. This data shows a large improvement, on the order of 1 to 4 dB, over similar data taken with the earlier experimental hardware.

6.2.3 AN/TRC-132 3.5 Mb/s Performance

Figures 6-10 and 6-11 are similar plots for the 3.5 Mb/s rate. Figure 6-10 shows the results for 3.5 Mb/s dual explicit diversity. Here we have more of a spread in the data with a general averaging around the effective fourth order intrinsic diversity prediction with Bit Error Rates ranging from 10^{-2} to less than 10^{-8} (not shown on plot). As can be seen, there is no apparent error rate floor. Also, as noted earlier, transmitter power was varied in order to produce varying signal-to-noise ratios for evaluation of the DAR-IV at low signal-to-noise ratios. Hence, actual link performance cannot be directly inferred from the data. This is true of all the AN/TRC-132 measurements.

Figure 6-11 is the comparative data for quad explicit diversity performance. Here the data generally indicates approximate eighth order intrinsic diversity performance with a scattering of data points beyond the theoretical prediction.

6.2.4 AN/TRC-132 7.0 Mb/s Performance

Figures 6-12 and 6-13 are similar plots for 7.0 Mb/s operation for dual and quad diversity operation, respectively. Figure 6-12 shows the 7.0 Mb/s dual diversity

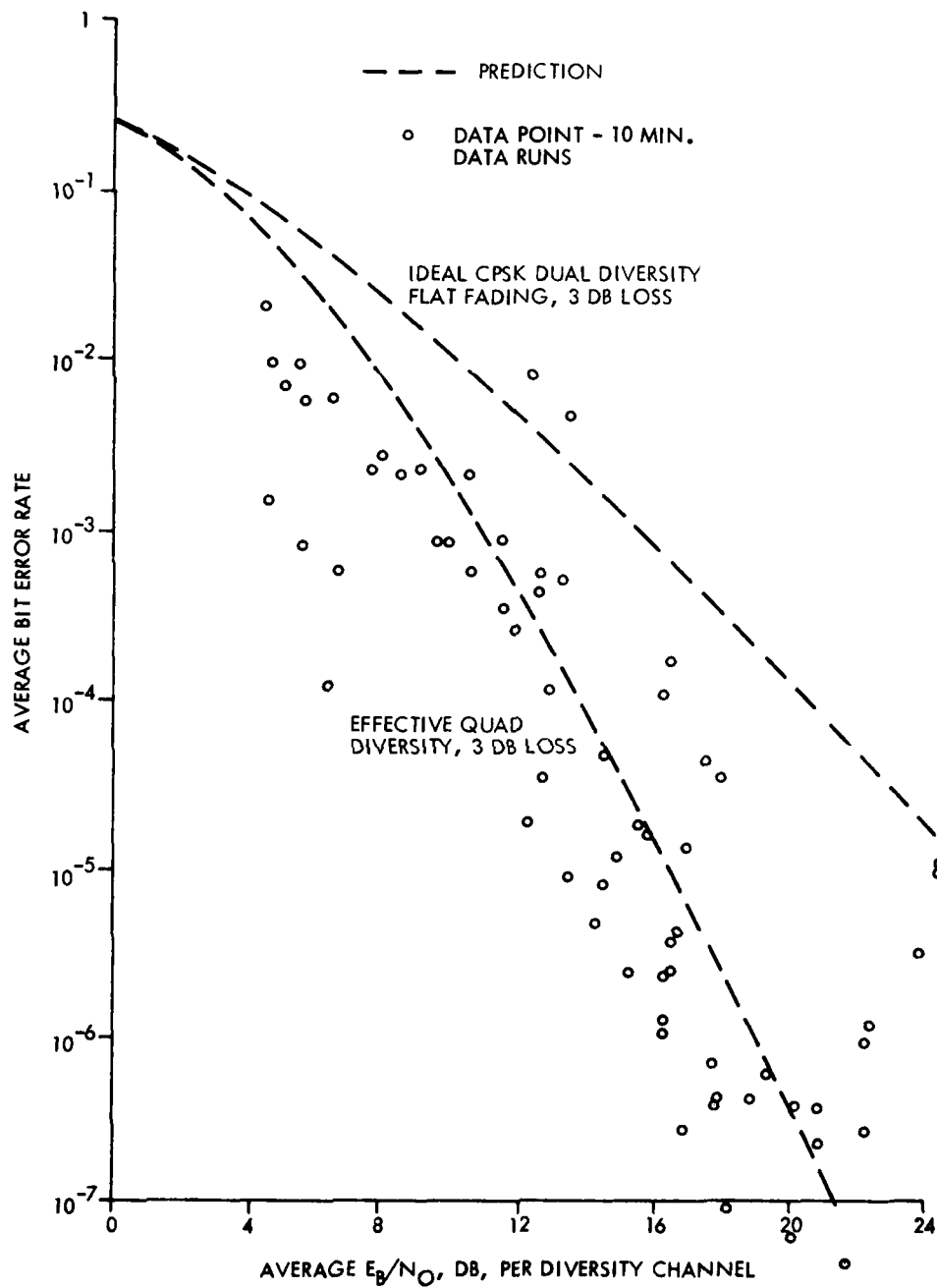


Figure 6-10. "Over-the-Air Tests" AN/TRC-132
Youngstown/Verona 3.5 Mb/s Dual Diversity

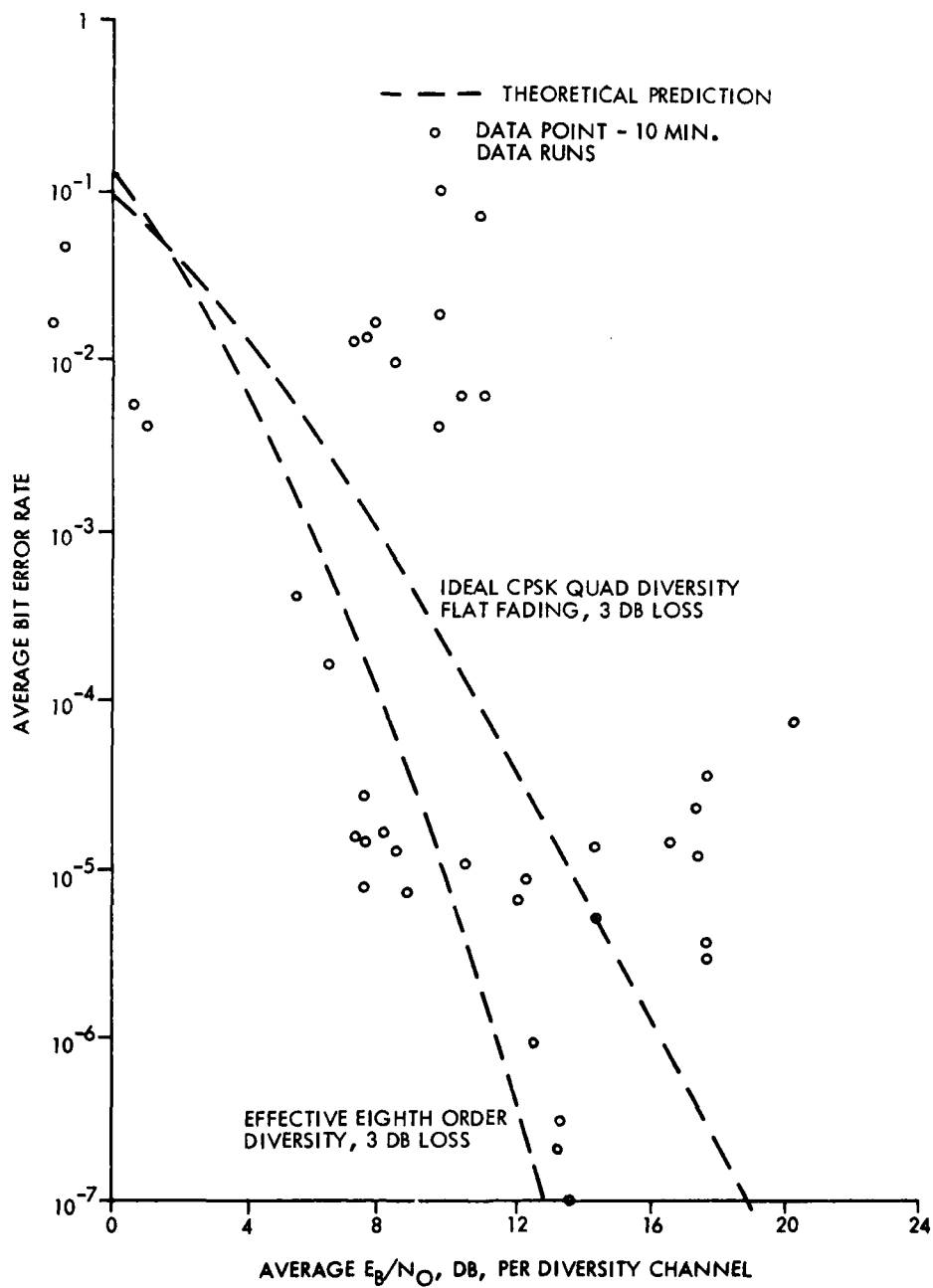


Figure 6-11. "Over-the-Air Tests" AN/TRC-132
Youngstown/Verona 3.5 Mb/s Quad
Diversity

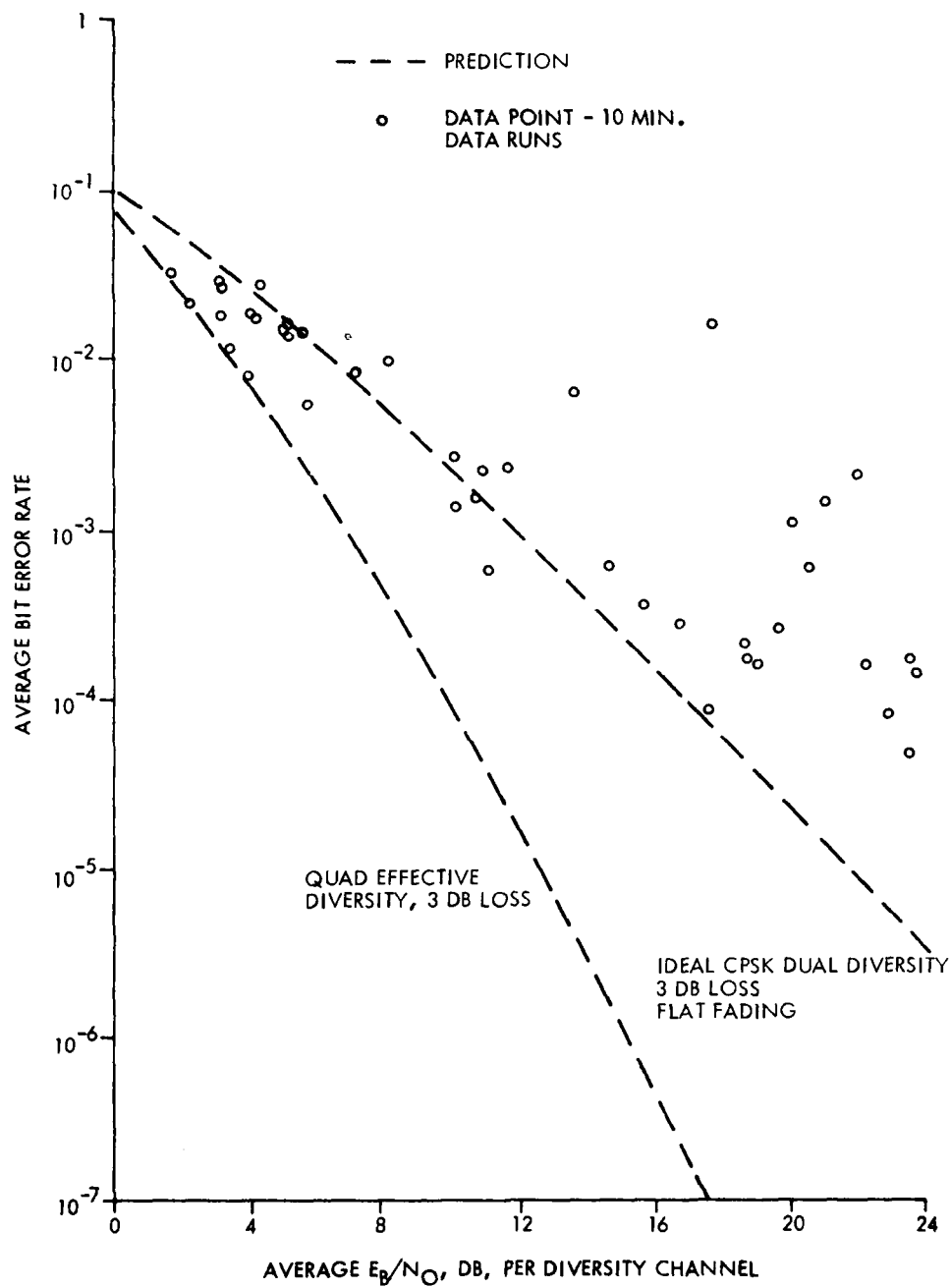


Figure 6-12. "Over-the-Air Tests" AN/TRC-132
Youngstown/Verona 7.0 Mb/s Dual
Diversity

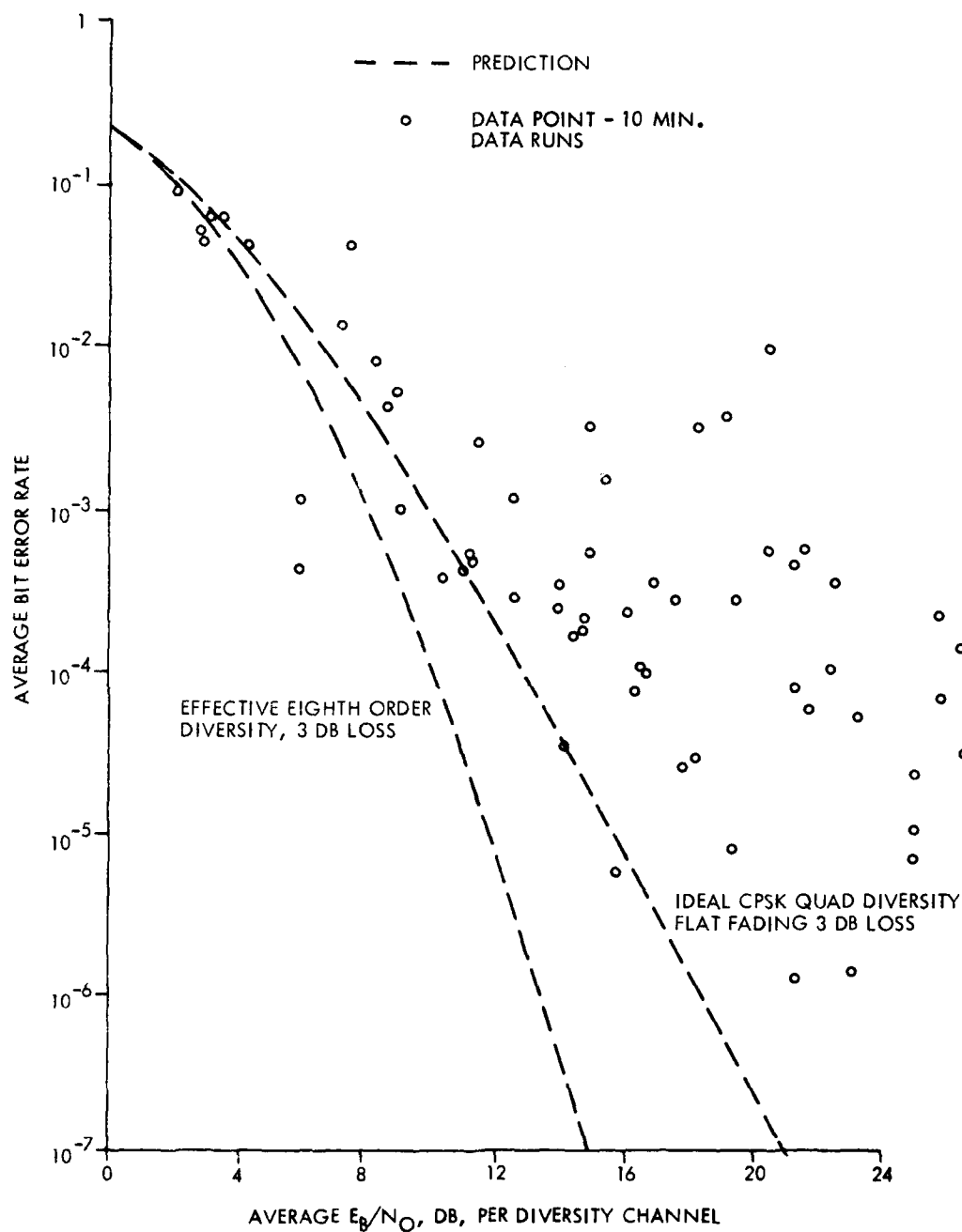


Figure 6-13. "Over-the-Air Tests" AN/TRC-132
Youngstown/Verona 7.0 Mb/s Quad
Diversity

performance. Here we see primarily the effects of insufficient "memory" of the coherent loop filter which effectively nullifies the potential improvement from the adaptive Decision Feedback Equalizer. Further degrading effects are introduced by the bandwidth limitations on both the SAW and the AN/TRC-132 HPA (see Figure 6-6) which in effect reduces the potential intrinsic diversity achievable with the DAR-IV technique.

The quad diversity performance is depicted in Figure 6-13. As with the earlier data, here we see a wide range of signal-to-noise ratios and again the effects of bandwidth limitation and coherent filter memory limitations.

6.3 AN/TRC-97 Over-the-Air Tests

6.3.1 General

This series of tests was extremely successful in that a large data base was obtained which tends to reduce the statistical errors. Furthermore, performance at 1.75 Mb/s and 3.5 Mb/s clearly demonstrates the capability of the DAR-IV for tactical application.

This series of tests was conducted between Verona and Ontario Center with Ontario Center the receiving site. This site has been recently equipped for fully automatic calibration data gathering. As a result, more data would be taken for a given calendar period since testing continued around the clock. These tests were run during July and early August 1978.

As with the AN/TRC-132 data, at least, eight data points per decade of BER from 10^{-1} to 10^{-8} was taken. For these tests both the transmitter and receiver antennas were 8 1/2 foot dishes. A total of 965 test runs were made with run lengths of 5, 10, or 20 minutes each. For each test a data point was automatically plotted on an E_b/N_0 versus BER curve. Also plotted for each test run during working hours, was the RSL distribution. RSL distribution could not be run overnight as the paper had to be changed after each plot.

The modem transmitter was placed inside the Verona test site for convenience in changing data rates. The AN/TRC-97 requires 50 MW into the HPA to obtain full output. This was obtained with the use of a Hewlett-Packard amplifier. Transmit waveform of the modem on the AN/TRC-97 is shown in Figure 6-14. Representative modem waveforms are shown in Figure 6-15. Figure 6-15(a) is the demodulator input signal in the frequency domain. Figure 6-15(b) is the integrated eye for the Q data and the corresponding #2 demodulator input from its IF amplifier. Figure 6-15(c) and (d) are the modem inputs from the two AN/TRC-97 receivers.

Figure 6-16, 6-17 and 6-18 are the plotted results for 1.75, 3.5 and 7.0 Mb/s dual diversity operation. Figure 6-16 shows the 1.75 Mb/s performance and indicates performance close to effective eighth order diversity. Here again we have an excellent distribution of average per channel signal-to-noise ratio for a good evaluation of the DAR-IV technique.

As with the data on the AN/TRC-132 equipment, these results show a substantial performance improvement over the earlier experimental equipment. This improvement is on the order of several dB or more at 10^{-5} error rate. Also, a far more tightly cluster of data points were obtained. This was, of course, due to the very large number of data points that were taken.

Figure 6-17 shows the performance for 3.5 Mb/s dual diversity operation. Here, performance is close to fourth order effective diversity - again with a good distribution of signal-to-noise ratios with a tight grouping of the data points.

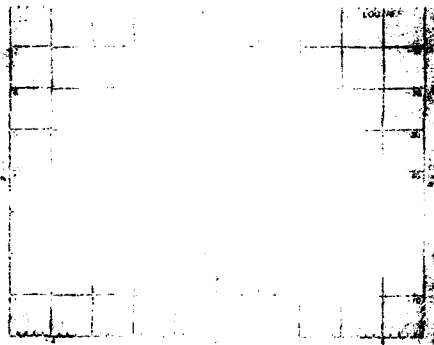
Figure 6-18 shows the 7.0 Mb/s performance. As with the AN/TRC-132 data, performance is limited by the coherent filter memory limitations and is more pronounced for only dual extrinsic diversity.

Samples of the computer printouts for all the data runs and plots are shown in Figure 6-19, 6-20 and 6-21.



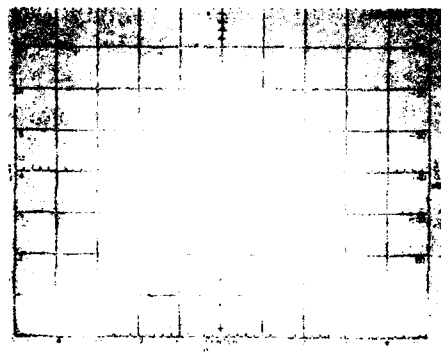
HOR = 5 MHz/DIV

(a) MODEM OUTPUT AT 1.75 MB/S



HOR = 2 MHz/DIV

(b) MODEM OUTPUT AT 1.75 MB/S



HOR = 2 MHz/DIV

(c) AN/TRC-97 ANTENNA OUTPUT
AT 7.0 MB/S

Figure 6-14. DTS Modified Output (For AN/TRC-97 Interface)

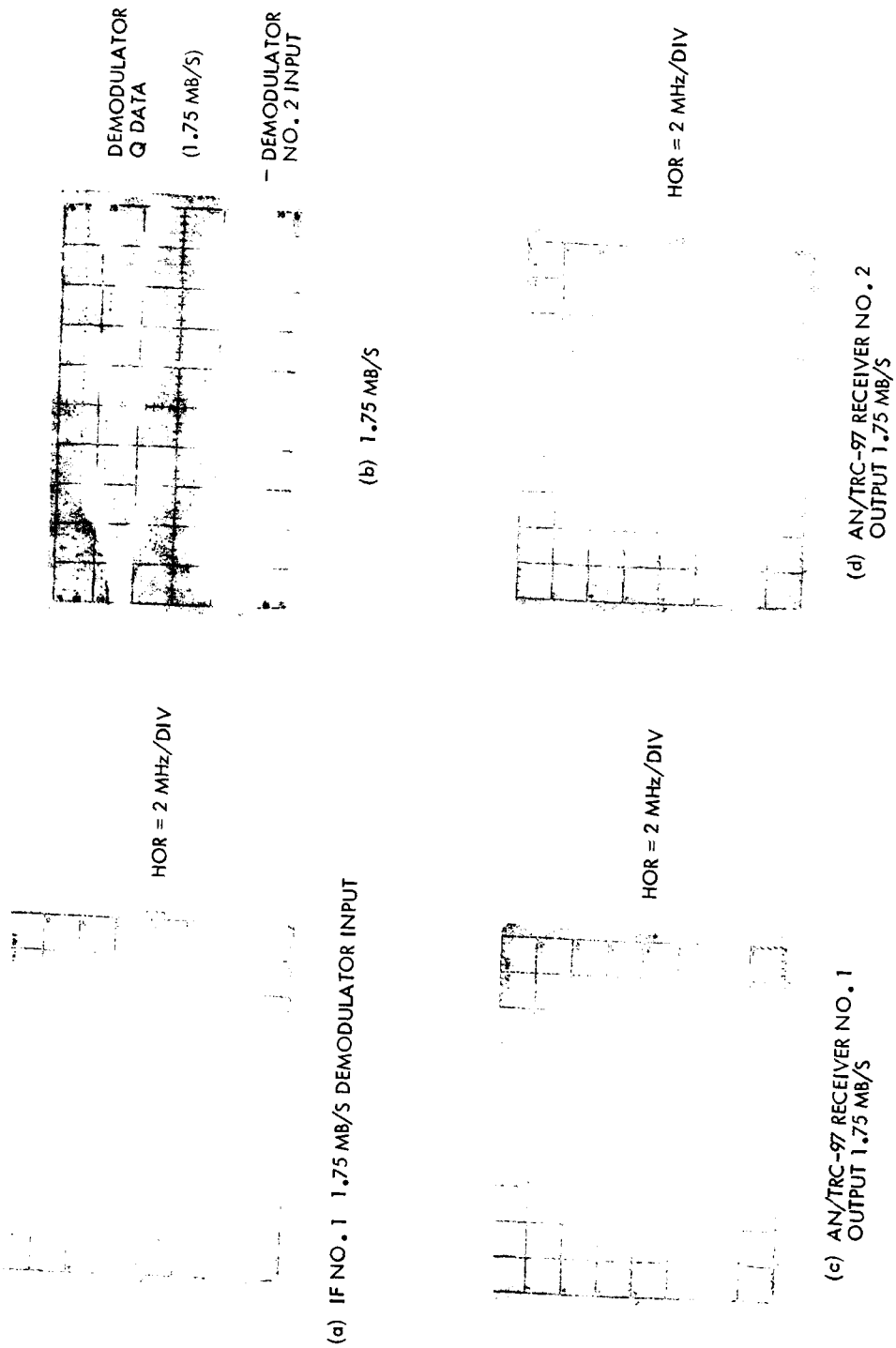


Figure 6-15. AN/TRC-97 Tests Modem Receiver Waveforms

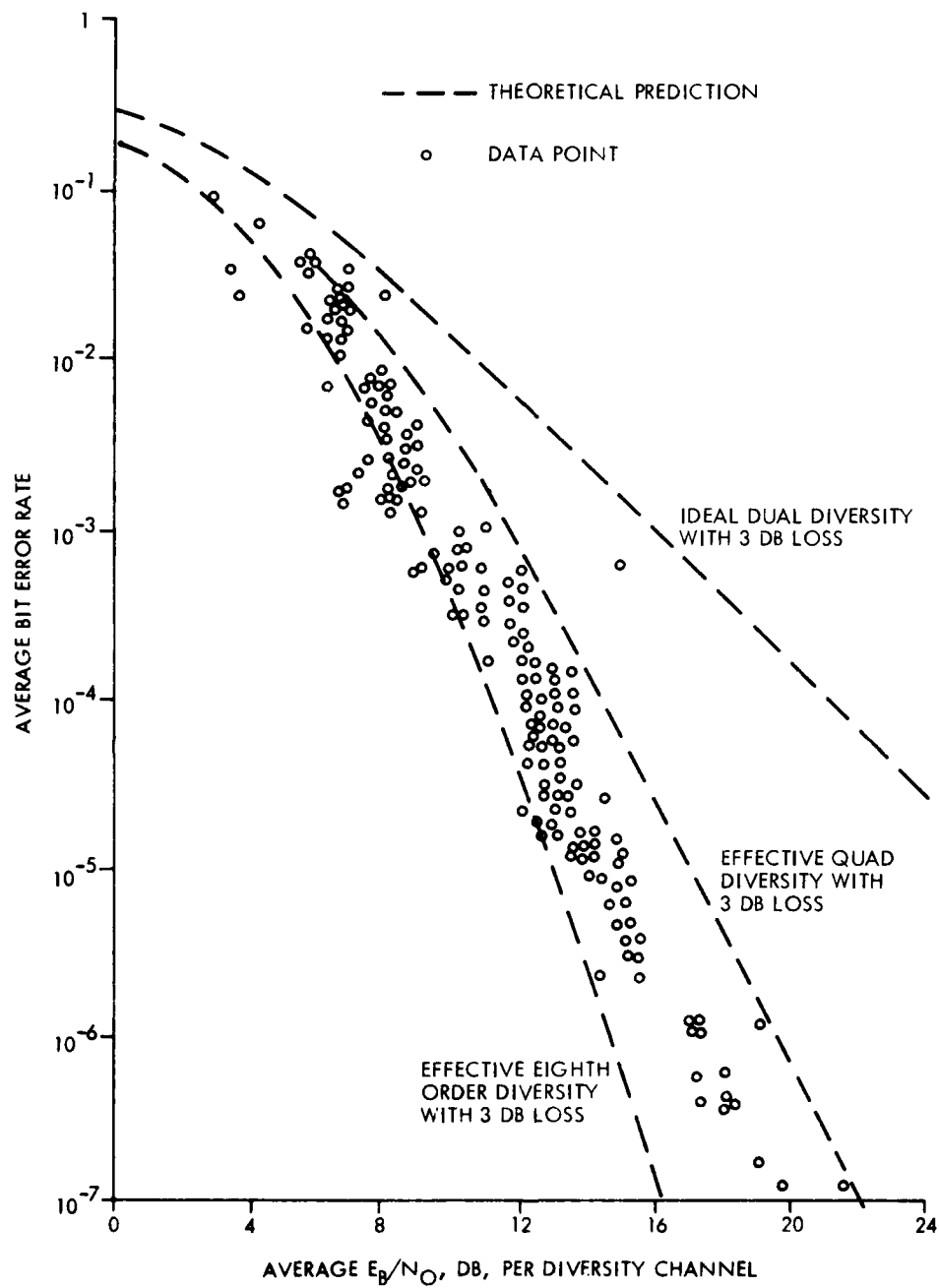


Figure 6-16. "Over-the-Air Tests" AN/TRC-97 Verona/
Ontario Center 1.75 Mb/s Dual Diversity

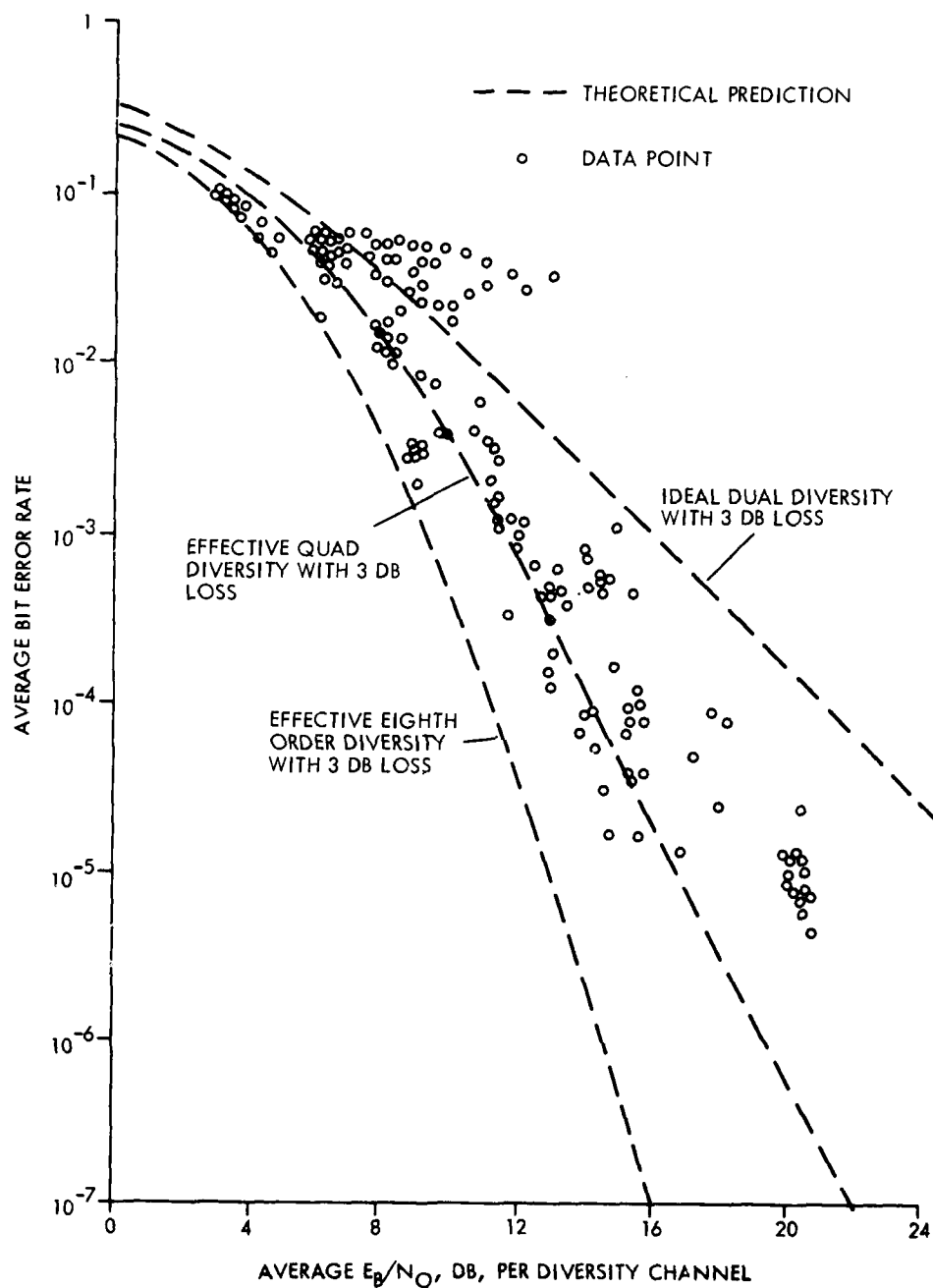


Figure 6-17. "Over-the-Air Tests" AN/TRC-97 Verona/
Ontario Center 3.5 Mb/s Dual Diversity

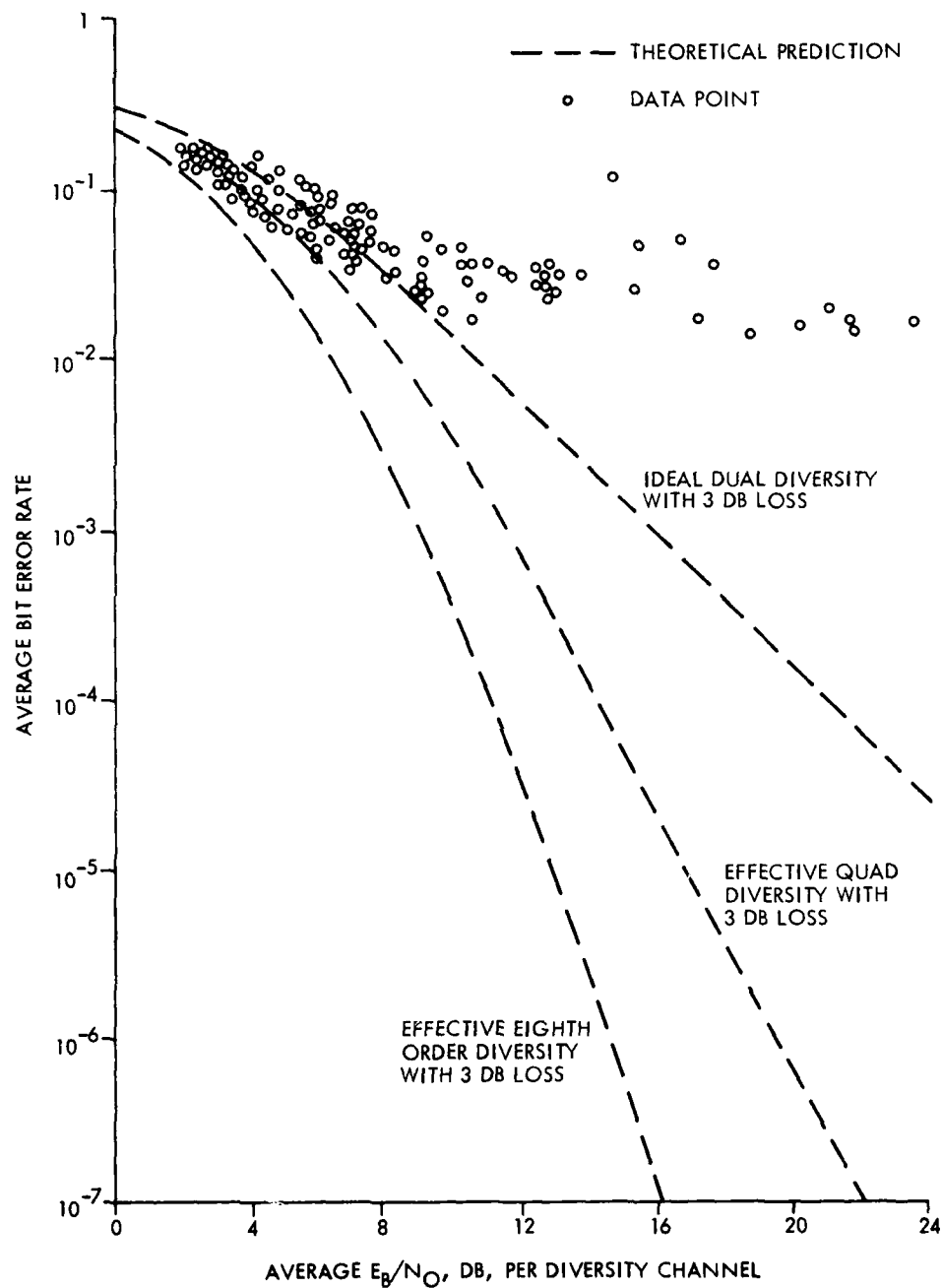


Figure 6-18. "Over-the-Air Tests" AN/TRC-97 Verona/
Ontario Center 7.0 Mb/s Dual Diversity

Figure 6-19 shows the received signal levels for both receivers as well as the calibration voltage of the LEL logarithmic amplifiers. It also records the cumulative distribution of the RSL at each of the 16 levels. The last two columns were to be the error distribution to duplicate the Raytheon EDA. Unfortunately, this portion of the program was not debugged at the time data was being taken. Also printed out are the median RSL's for each received, total errors, BER E_b/N_o and the average median RSL of the receivers. Figure 6-20 is the Histogram and cumulative distribution of the two receiver carrier levels. Figure 6-21 is the computer plot of E_b/N_o versus BER for the evening of 29 July 1978 from 4:30 p.m. to 7:00 a.m.

DAR MODEM ON TRC-97: VERONA TO ONTARIO
 DATE 24 7 78 TEST DURATION (MIN.) 10.00 START TIME
 TEST #364 DATA RATE=1.616MB/S

-DBM	CAL V.	% Rx 1	% CUM	CAL V.	% Rx 2	% CUM	ERR. DIST.	
-105.0	0.150	0.000	0.000	0.114	0.081	0.081	5e-1+1e-1	0
-102.5	0.155	0.289	0.289	0.119	0.526	0.607	1e-1+5e-2	0
-100.0	0.164	2.437	2.726	0.127	2.163	2.770	5e-2+1e-2	0
-97.5	0.177	8.141	10.867	0.188	7.178	9.948	1e-2+5e-3	0
-95.0	0.193	19.104	29.970	0.154	18.200	28.148	5e-2+1e-2	0
-92.5	0.211	28.526	58.496	0.171	25.015	53.163	1e-2+5e-3	0
-90.0	0.231	30.156	88.652	0.190	29.133	82.296	5e-3+1e-3	0
-87.5	0.251	7.067	95.719	0.210	12.170	94.467	1e-4+5e-5	0
-85.0	0.272	1.652	97.370	0.233	3.022	97.489	5e-5+1e-5	0
-82.5	0.289	2.074	99.444	0.254	2.059	99.548	1e-5+5e-6	0
-80.0	0.307	0.556	100.000	0.272	0.452	100.000	5e-6+1e-6	0
-77.5	0.326	0.000	100.000	0.289	0.000	100.000	1e-6+5e-7	0
-75.0	0.347	0.000	100.000	0.307	0.000	100.000	5e-7+1e-7	0
-72.5	0.366	0.000	100.000	0.329	0.000	100.000	1e-7+5e-8	0
-70.0	0.384	0.000	100.000	0.351	0.000	100.000	5e-8+1e-8	0
-67.5	0.399	0.000	100.000	0.369	0.000	100.000	<1e-8	0

TOTAL ERRORS= 1.346E 05 ERROR RATE= 1.389E-04
 FADES/MIN.= 79.40
 MED 1= -93.24DBM MED 2= -92.82DBM AVG.= -93.03 Eb/No= 12.97

DAR MODEM ON TRC-97: VERONA TO ONTARIO
 DATE 24 7 78 TEST DURATION (MIN.) 10.00 START TIME
 TEST #365 DATA RATE=1.616MB/S

-DBM	CAL V.	% Rx 1	% CUM	CAL V.	% Rx 2	% CUM	ERR. DIST.	
-105.0	0.150	0.007	0.007	0.114	0.044	0.044	5e-1+1e-1	0
-102.5	0.155	0.163	0.170	0.119	0.326	0.370	1e-1+5e-2	0
-100.0	0.164	1.452	1.622	0.127	1.748	2.119	5e-2+1e-2	0
-97.5	0.177	5.941	7.563	0.138	5.111	7.230	1e-2+5e-3	0
-95.0	0.193	16.000	23.563	0.154	14.733	21.963	5e-2+1e-2	0
-92.5	0.211	25.778	49.341	0.171	23.163	45.126	1e-2+5e-3	0
-90.0	0.231	32.874	82.215	0.190	30.244	75.370	5e-3+1e-3	0
-87.5	0.251	14.585	96.800	0.210	19.815	95.185	1e-4+5e-5	0
-85.0	0.272	2.970	99.770	0.233	4.763	99.948	5e-5+1e-5	0
-82.5	0.289	0.230	100.000	0.254	0.052	100.000	1e-5+5e-6	0
-80.0	0.307	0.000	100.000	0.272	0.000	100.000	5e-6+1e-6	0
-77.5	0.326	0.000	100.000	0.289	0.000	100.000	1e-6+5e-7	0
-75.0	0.347	0.000	100.000	0.307	0.000	100.000	5e-7+1e-7	0
-72.5	0.366	0.000	100.000	0.329	0.000	100.000	1e-7+5e-8	0
-70.0	0.384	0.000	100.000	0.351	0.000	100.000	5e-8+1e-8	0
-67.5	0.399	0.000	100.000	0.369	0.000	100.000	<1e-8	0

TOTAL ERRORS= 1.020E 05 ERROR RATE= 1.051E-04
 FADES/MIN.= 92.40
 MED 1= -92.45DBM MED 2= -92.10DBM AVG.= -92.27 Eb/No= 13.73

Figure 6-19. DAR Modem on TRC-97: Verona/Ontario

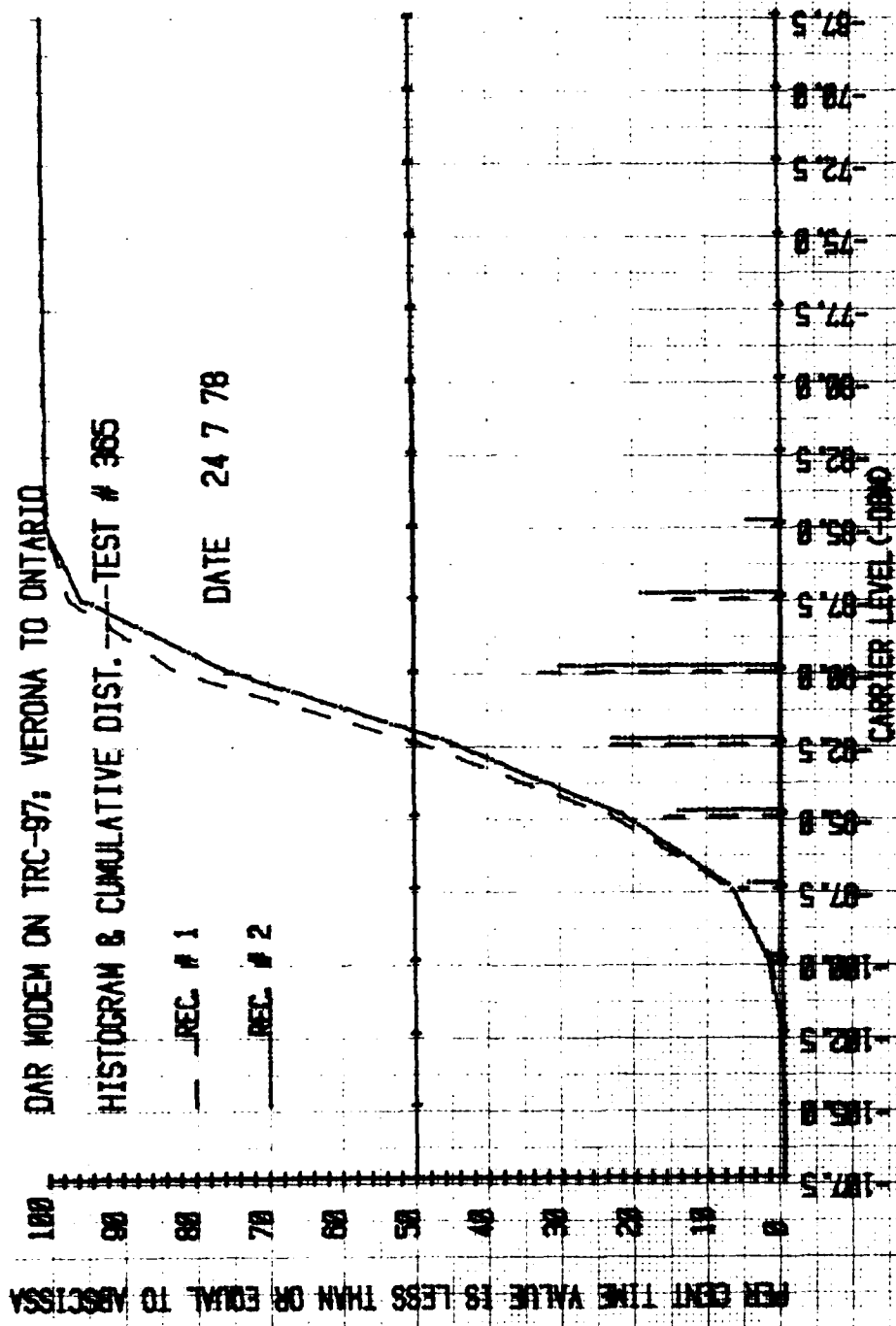


Figure 6-20. DAR Modem on TRC-97: Verona/Ontario

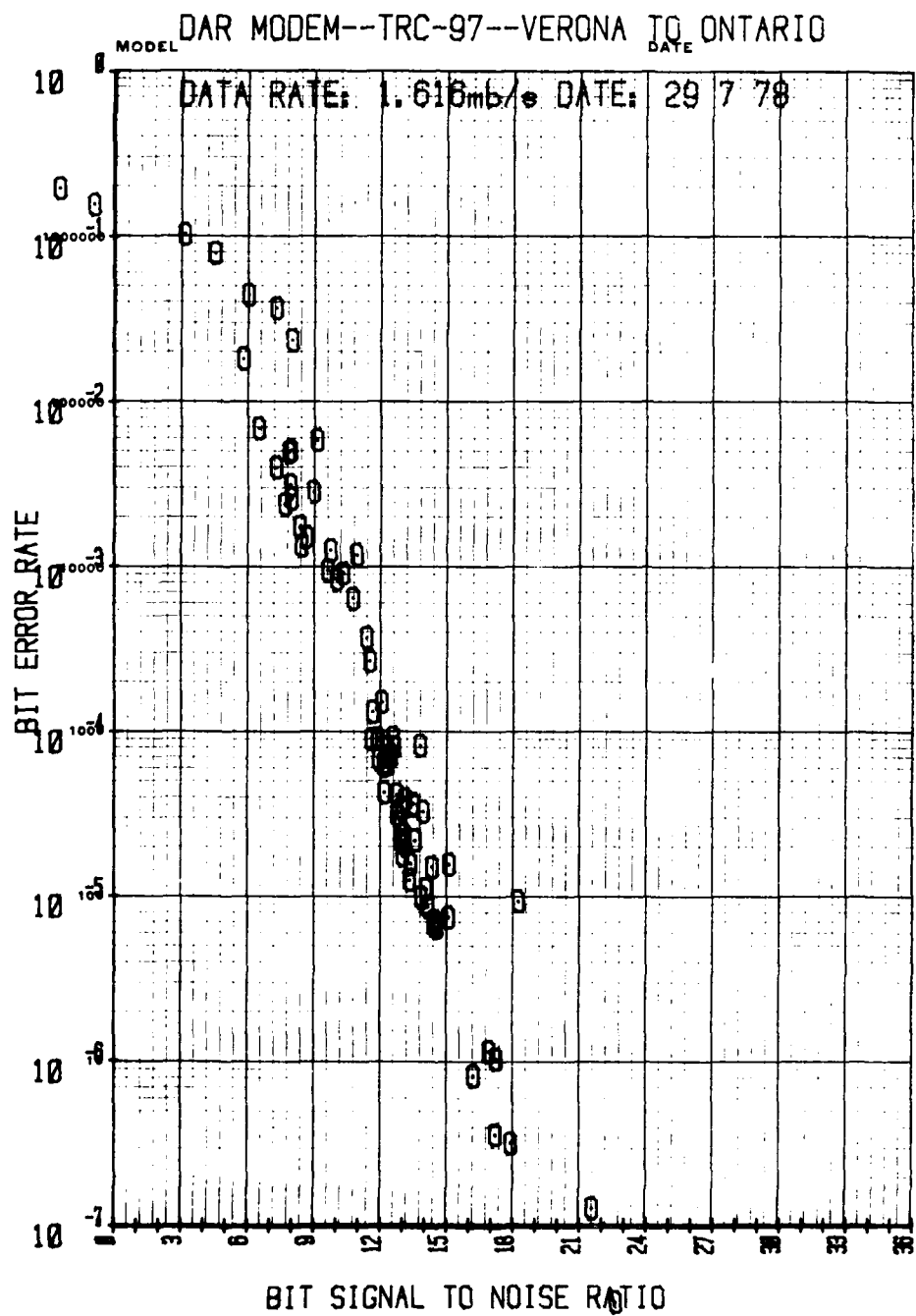


Figure 6-21. DAR Modem TRC-97 Bit Signal-to-Noise Ratio

7.0 OVER-THE-AIR TESTS EUROPE

7.1 General

Further Over-the-Air evaluation was obtained by Raytheon participation in the Combined US/NATO Digital Troposcatter Test Program sponsored by the Defense Communication Engineering Center and SHAPE Technical Enter.

This series of test was also a very successful phase of the program and demonstrated the performance of the DAR-IV on strategic lines of the DCS which represented "severe" and typical links of interest. In virtually all measurements effective data communication performance was maintained.

Testing was conducted for approximately one month each over a 170 km C-band line between Kinsbach and Feldberg, Germany and a 287 km band link between Feldberg, Germany and Dosso Dei Galli, Italy.

The major characteristics of these links are described in Appendix A of the "Combined Digital Troposcatter System Test Plan" by DCEC/SHAPE dated October 1976.

Testing took place during the May-July period 1977.

7.2 Test Results

Test results have been reported in detail in the following two documents: (1) "Digital Modem Technology for Strategic and Tactical Troposcatter Applications" by Walter J. Cybrowski, Communications/ADP Laboratory, EAAECOM and (2) "The Combined US/NATO Digital Troposcatter Test Program" by John L. Osterholz, DCEC.

The following summarizes these test results. Representative data is included in Appendix B. This data is the summary listing of each run and is a direct photo of the summary work sheets prepared by SHAPE/NATO personnel.

7.3 Test Results - Kinsbach (ABHZ) to Feldberg (AEFZ) Link

Data was taken on this ACE high link during August 1978. This is a "C" band link with parameters as shown in Table 7-1.

TABLE 7-1. LINK PARAMETERS

	Kinsbach	Feldberg	Dosso Dei Galli
Altitude	459 M	1470 M	2175 M
Horizon Angle	-0.09°	-0.87/0.06	0.60
Antenna Sizes	3 M		3 M
Path Length	28 KM	385 KM	
Nominal Frequency	4500 MHz	900 KM	
Diversity	Space/Polarization	Space/Frequency	

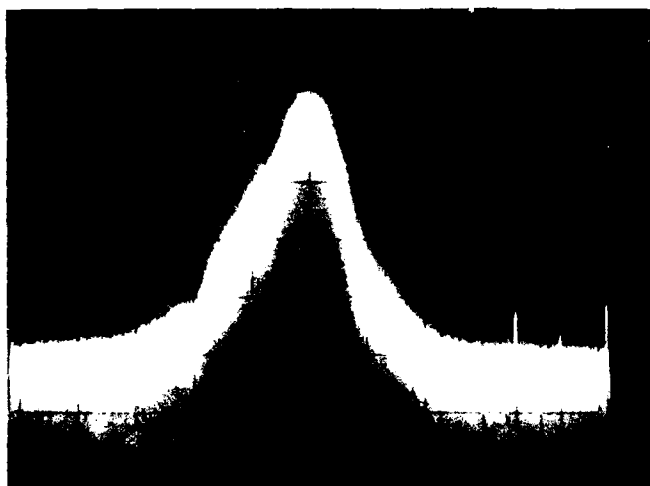
Data was taken at 7.0 Mb/s and 3.5 Mb/s Dual and Quad diversity with several runs of non-diversity taken at 7.0 Mb/s. Run length was generally 20 minutes with overnight runs where possible. Representative Receive Waveforms are shown in Figure 7-1. Data is summarized in Table 7-2.

In almost all cases, the AVG BER was better than 2×10^{-9} .

TABLE 7-2. KINSBACH/FELDBERG DATA SUMMARY

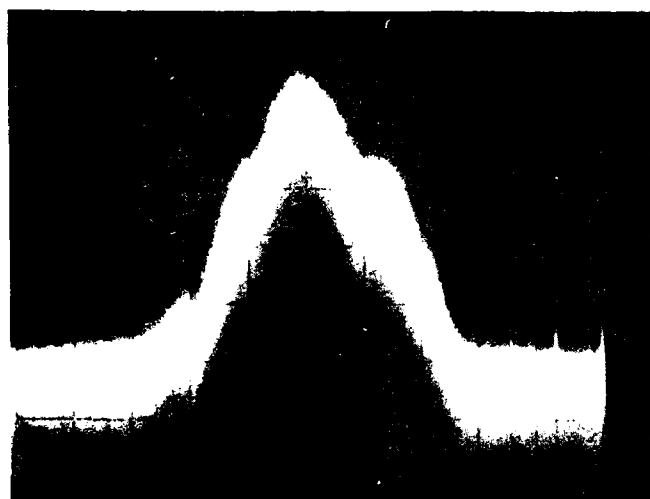
Data Rate	Diversity	# of Runs	BER
7.0 Mb/s	Quad	115	7.6×10^{-10}
7.0 Mb/s	Dual	131	7.3×10^{-7}
7.0 Mb/s	Non	5	2.9×10^{-9}
3.5 Mb/s	Quad	10	10^{-11}
3.5 Mb/s	Dual	8	10^{-11}
3.5 Mb/s	Non	3	10^{-11}

Run data is shown in Appendix A.



HOR = 5 MHz/DIV
VERT = 10 DB/DIV

(a) DIVERSITY RX NO. 1



HOR = 5 MHz/DIV
VERT = 10 DB/DIV

(b) DIVERSITY RX NO. 2

Figure 7-1. Receive Waveforms - Kinsbach/Feldberg
7.0 Mb/s Transmission Rate

7.4 Test Results - Dosso Dei Galli (IDGZ) to Feldberg (AEFZ)

Data on this link was taken in May/June 1978. This is a UHF link with parameters as shown in Table 7-1.

As with the Kinsbach/Feldberg link data was taken at 7.0 Mb/s and 3.5 Mb/s Dual and Quad diversity. For the 7.0 Mb/s quad measurements, most 20 minute data runs, the BER was better than 10^{-6} . For the very small sample of dual diversity 7.0 Mb/s data, BER's ranged from 10^{-3} to 10^{-6} . The much larger sample of 3.5 Mb/s quad diversity measurements yielded BER better than 10^{-6} in almost all cases. Dual diversity 3.5 Mb/s measurements were generally greater than BER's of 10^{-8} . Data is summarized in Table 7-3 and individual run data is summarized in Appendix B.

TABLE 7-3. DOSSI DEI GALLI/FELDBERG DATA SUMMARY

Data Rate	Diversity	# of Runs	BER
7.0 Mb/s	Quad	21	1.6×10^{-3}
7.0 Mb/s	Dual	4	1.0×10^{-3}
3.5 Mb/s	Quad	55	6.8×10^{-7}
3.5 Mb/s	Dual	61	2.3×10^{-7}

APPENDIX A

ADVANCED DIGITAL TROPOSCATTER MODEM TECHNOLOGY

ADVANCED DIGITAL TROPOSCATTER MODEM TECHNOLOGY

M. UNKAUF, N. LISKOV, R. CURTIS and S. BOAK

Raytheon Company, Sudbury, Massachusetts

Abstract

An improved modulator/demodulator (modem) approach is described for megabit digital tropospheric scatter channels. This is an extension of the Distortion Adaptive Receiver (DAR) which provides better bandwidth multipath range and transmission power utilization than earlier versions. By using a pair of frequency offset interleaved pulse streams with a DAR matched to each, operation at higher data rates or longer path lengths is achieved. A computer simulation program is outlined for the detailed performance analysis of the two frequency DAR and sample spectral confinement and bit error rate results are presented.

1.0 Introduction

Previous papers [1-3] have described the theory and operation of an adaptive matched filter modulator-demodulator (modem) concept for the time-variant, dispersive channel. This modem technique, known as the Distortion Adaptive Receiver (DAR) [4], was first developed by USAF/RADC [5] and extensively tested under TRI-TAC, RADC, and ESD [6] sponsorship. The test results showed that the DAR technique could provide high quality digital transmission over tactical grade tropospheric scatter links. However, the DAR technique as previously described in the literature also has several drawbacks in the areas of transmitter power utilization, multipath spread capability, and bandwidth requirements. An alternative implementation of the DAR has been found which improves power utilization and multipath spread capability while retaining its desirable features of high performance and low complexity. A DAR modem of this improved design has been selected for the full-scale development models of the TRI-TAC AN/TRC-170 family of digital troposcatter terminals [7].

The background of the DAR modem is described in Section 2 of this paper. Representative performance characteristics and system limitations are provided. An improved waveform for the DAR modem technique is described in Section 3 which employs a pair of frequency offset, interleaved pulse streams. Finally, Section 4 describes a detailed computer simulation program and sample performance results for the improved approach.

2.0 Background

The DAR modem employs QPSK modulation with adaptive matched filter demodulation. Its basic operation can be understood with reference to Figure 1. At the transmitter, the QPSK symbols are time gated to produce an off-time of Δ μ -seconds between adjacent symbols. If the rms duration of the multipath spread encountered in tropospheric transmission is less than Δ , there may be substantial distortion of the transmitted pulses (due to the multipath propagation) but the amount of intersymbol interference will be small. Since the channel multipath structure changes very slowly compared to the megabit data rates of interest, the received signal can be envisioned as a stream of identically distorted, non-overlapping QPSK symbols. In this case, the optimum receiver consists of an adaptive matched filter which can be realized by multiplying each received QPSK symbol by a locally generated replica (coherent reference signal) and integrating the product over the symbol duration. The sign of the in-phase and quadrature components of the integration yields the desired symbol decision.

The advantage of this approach is that it does not require adaptive equalization at the receiver to correct for intersymbol interference and yields near optimum performance using only an adaptive matched filter. The adaptive matched filter can be realized with relatively low complexity by making use of the decision feedback scheme shown in Figure 2. For simplicity, Figure 2 shows a binary PSK adaptive matched filter implementation but a QPSK version is very similar [1-3]. The distorted received pulse stream is delayed by one symbol and decision feedback is used to remove the original PSK modulation (modulo 2π). The result of this "inverse modulation" is a stream of identically distorted pulses which all have the same phase "state" and which is, therefore, in the form needed for the matched filter reference signal. A coherent broadband recirculating filter is used to enhance the signal to noise ratio of the reference signal and to stabilize the reference against occasional decision feedback errors.

Typical bit error rate performance for the DAR on the troposcatter channel is shown in Figure 3 for several values of rms multipath delay spread. For very low multipath spread, the fading on each diversity channel has a Rayleigh distribution and the performance is indicated by the curve marked

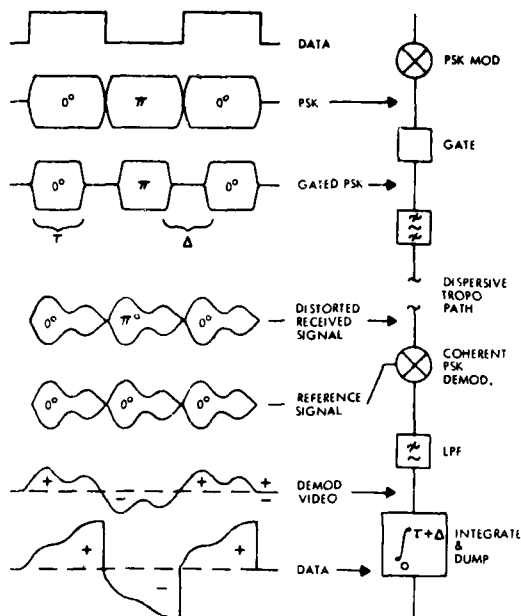


Figure 1 Basic Operation of DAR

"flat fading". As the multipath spread increases (signal distortion increases), the modem performance improves due to a phenomenon called intrinsic diversity which is a sort of in-band frequency diversity. Multipath profiles A, B, and C represent spreads of 0.031, 0.19, and 0.38 μ s, respectively. Note that the performance improves rapidly with increasing multipath spread and, at 10^{-5} error rate, a performance improvement of about 10 dB is realized for multipath profile B. However, as the multipath spread becomes very large (as the path length increases), a point is eventually reached at which the transmitter time-gate is no longer sufficient to eliminate the effects of intersymbol interference. At this point, a phenomenon known as an irreducible error rate occurs which produces an error "floor" as shown by the curve for profile C of Figure 3.

With the previous DAR design, a transmission time gate of 50% was typically employed in a trade-off between transmitter power utilization, bandwidth, and multipath spread capability. The 50% time gate results in a minimum 99% power spectral confinement of about 1.5 Hertz/bit with an inherent 3 dB loss of transmit power for a klystron amplifier (similar to Class A operation). In some applications where large multipath spread is expected, it would be desirable to increase the pulse off-time, Δ . However, the resultant increase in bandwidth and reduction in transmit power for a lower time-gate duty cycle usually cannot be accommodated. An alternative implementation of the DAR is then required known as the two frequency-pulse waveform.

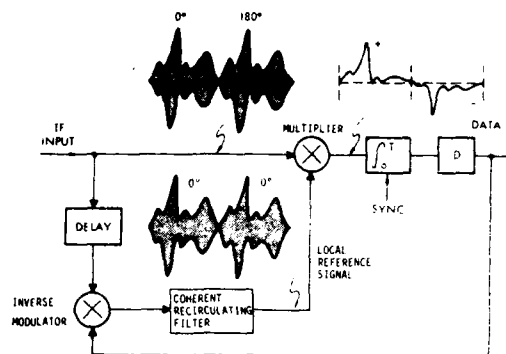


Figure 2 Basic Decision Feedback DAR Demodulator

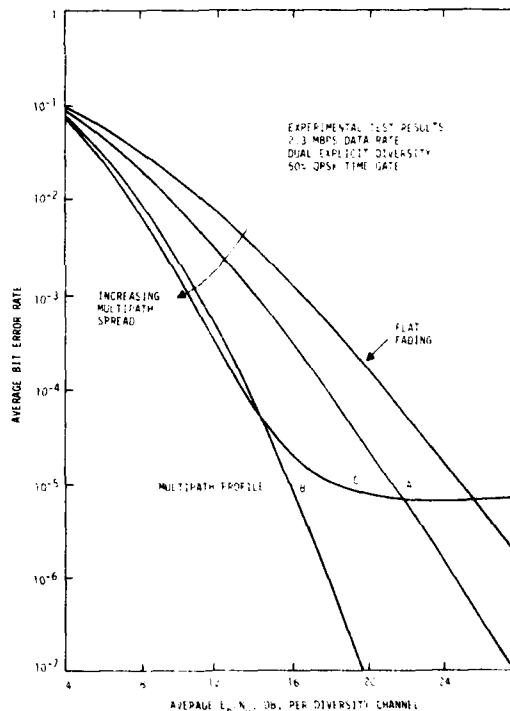


Figure 3 Typical Bit Error Rate Performance of Original DAR

3.0 The Two Frequency Pulse Waveform

The two frequency pulse waveform is simply the time interleaving of two DAR half-duty cycle pulse waveforms, each at a separate frequency. There are two significant advantages over the one frequency waveform. First, the waveform is closer to constant amplitude, thus recovering nearly all of the total 3 dB half duty cycle loss of the single frequency waveform. Second, a total rate R can be divided into rate $R/2$ on each frequency. This, in effect, doubles the guard time and thus doubles the multipath spread tolerance of the waveform. These advantages more than compensate for the loss of intrinsic (in-band) diversity due to using half the band for each independent data signal, so the time-availability is significantly enhanced by the two frequency waveform. In cases where there is sufficient bandwidth available, the full data rate R is sent redundantly on both frequencies, thus retaining the intrinsic in-band diversity. In this case, when the two halves of the band fade independently, the waveform actually provides an explicit dual order of frequency diversity within the band.

The parameters of the waveform were chosen to meet data rates of 2304, 1152, 576, and 288 kbps in 3.5 or 7.0 MHz occupied bandwidth, as shown in Figure 4. In all cases but 1, there was sufficient bandwidth to repeat the same data on both frequencies. For the lower bit rates, phase coding is added within each pulse to provide a spectrum spreading which not only utilizes all the band but has the shape of a comb filter with approximately equal height peaks evenly spaced across the band.

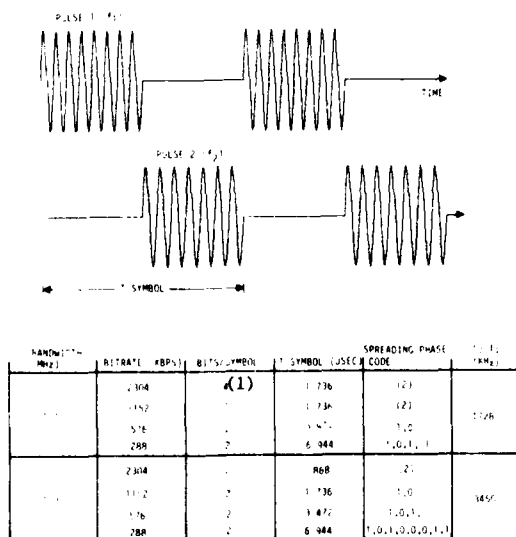


Figure 4 Waveform Illustration and Parameters for Two-Frequency DAR

In order to bandlimit the spectrum of the two frequency waveform, it is necessary to bandlimit each pulse. This is done simply by filtering rectangular pulses. The computer analysis shows that diplexing filters can be chosen so that the bandwidth is confined to that allocated while limiting other effects such as intermodulation, adjacent channel interference, and pulse distortion to tolerable levels.

The simplified block diagram of a transmission system using the two frequency waveform shown in Figure 5 indicates a single RF system but dual DAR modems, with the addition of interleaving/deinterleaving circuits. When redundant data is sent at each frequency, a single data decision is made at the receiver, based on the analog sum of the decision voltages of the dual DAR matched filters.

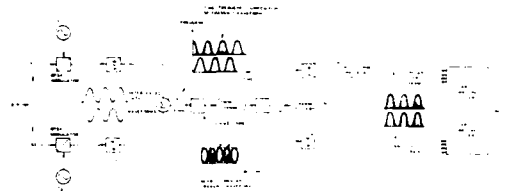


Figure 5 Simplified Block Diagram of Two-Frequency DAR Modem

4.0 Computer Analysis

In order to accurately analyze the performance of digital waveforms in the presence of distortion, a package of computer programs has been developed. The basic element of the computer package is the Fast Fourier Transfer (FFT) which allows efficient conversion between the time and frequency domain. The basic technique for the analysis is to start with a baseband representation of a complex IF modulated probing signal (e.g. a pseudonoise (PN) sequence), pass it through the functional blocks of the system (each of which has a corresponding computer routine), and find the average BER by averaging the BER from each symbol in the probing sequence.

Each functional block is modeled in either the time domain of the frequency domain, whichever is most appropriate, and the FFT is used where necessary. For example, a filter is modeled in the frequency domain and a signal is filtered simply by complex multiplication of its frequency transform by the complex filter transfer function.

An example of time domain modeling is the TWT transfer model which simply maps each time domain input signal voltage sample magnitude to an output voltage sample magnitude by the TWT voltage transfer curve. The phase of the sample is rotated by the AM/PM transfer value.

AD-A080 894

RAYTHEON CO SUDBURY MASS EQUIPMENT DEVELOPMENT LABS
DIGITAL TRANSMISSION SYSTEM.(U)
OCT 79 M UNKAUF, P DANIS, C ALEMEYER

F/8 9/2

UNCLASSIFIED

RADC-TR-79-256

F30602-76-C-0217

NL

3 of 3

AD
A080894



END

DATE

11/1/80

3 - 80

10/1

The use of a PN type probing sequence has some unique advantages. In particular in binary case, the spectrum very closely matches the exact sin x/x modulated spectrum, even with only a few symbols (e.g. 31) in the probing sequence. Also, with as few as 32 symbols (a 31 bit PN with an added zero) all 5 bit subsequences (e.g. every instance of possible intersymbol interference from +1 and +2 symbols from the desired symbols) are represented once. Thus, even with a short sequence, very close to average BER performance can be accurately predicted.

The computer model of the transmitter is shown in Figure 6. Each of two interleaved half duty cycle rectangular symbol QPSK signals are separately filtered, shifted in frequency and then combined. The result is passed through an RF filter, a nonlinear high power amplifier (HPA) model and then filtered again. At that point, the average output power is computed as well as 99 percent spectral occupancy and the radiated spectrum is plotted for comparison to a spectral mask. Examples of the radiated spectrum are shown in Figures 7 - 9 for 2304, 576 and 288 Kbps in 3.5 MHz, 99% bandwidth occupancy. The spreading code for the 576 Kbps case is a diphasic signal so that the four peaks of Figure 8 are corresponding to two separate diphasic signals. The out-of-band falloff spectra is determined by intermodulation. The intermodulation is fairly low because the two frequency pulses are nominally disjoint, but some intermodulation is created at the pulse edges where, due to filtering, both pulses are non-zero. The HPA operating point has been chosen for at least 20 dB margin on the out-of-band spectral mask. About .5 dB more radiated power can be obtained and the 99% bandwidth still confined to 3.5 MHz, if the margin is reduced to zero.

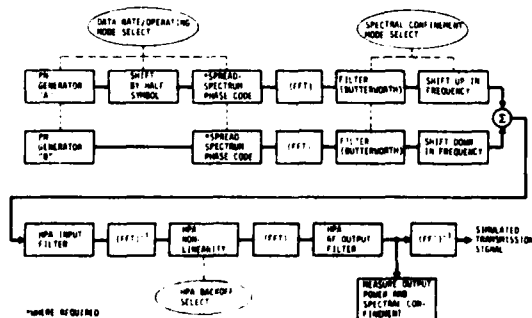


Figure 6 Computer Simulation Model of Two-Frequency DAR Transmitter

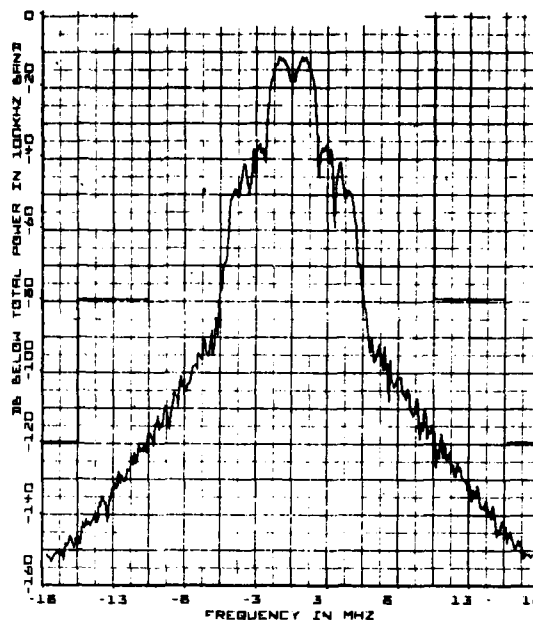


Figure 7 Radiated Spectrum at 2.304 Mbps

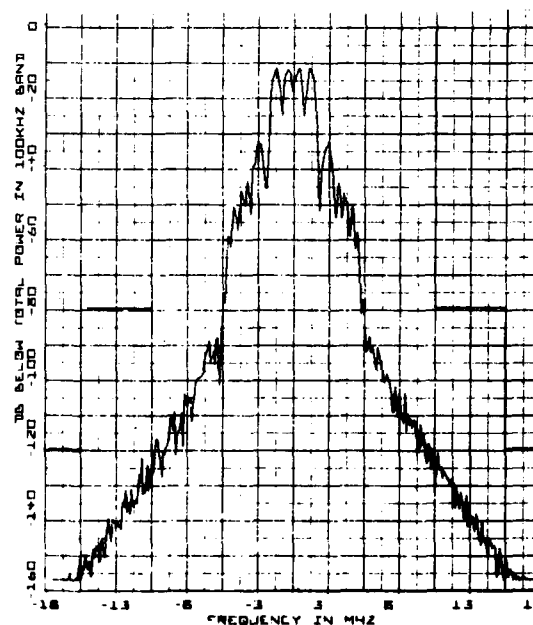
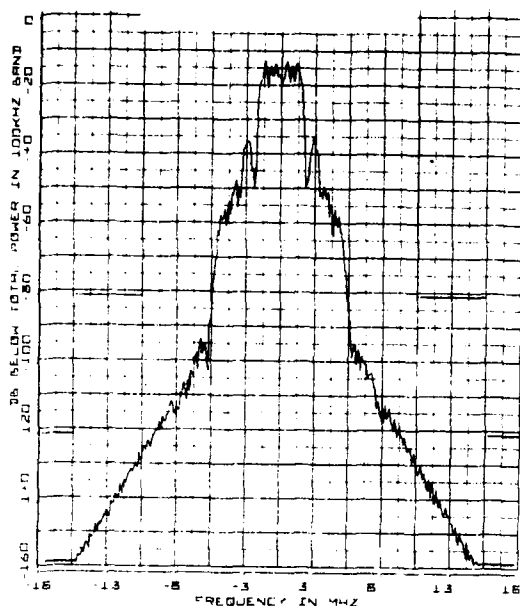
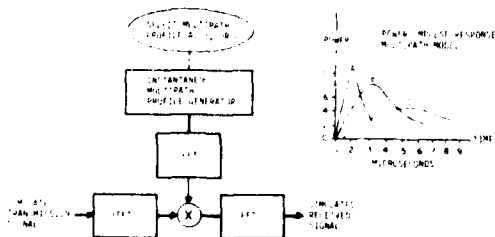


Figure 8 Radiated Spectrum at 576 Kbps



The transmitted signal is passed through the channel by convolving it with a channel "snapshot" impulse response as shown in Figure 10. A channel snapshot is a randomly chosen signal out of the ensemble of signals characterized by the power impulse response with shape A, B or C (see insert in Figure 10). That is, the samples of the snapshot are Rayleigh magnitude distributed complex vectors with uniformly distributed angle. The variance of the Rayleigh distribution for the sample vector at time t is equal to the appropriate power impulse response at that time. The spacing between samples is chosen to adequately follow the shape of the power impulse response, but also to have the same spacing as the samples of the transmitted signal.



For each snapshot the average bit error rate (BER) is computed by averaging the BER for each bit in the probing sequence. Then these results are averaged over a number of snapshots. Since we are interested in a 10^{-5} BER for dual diversity, we need good confidence at $10^{-2.5}$ BER for single diversity. To have 99% confidence that the predicted BER is within a Factor of 2, we should have about $10/10^{-2.5} = 3000$ snapshots. It was found that 500 snapshots gave BER results that were within ± 0.5 dB (2σ) of the 3000 snapshots runs. Since runs were done for many parameter variations, 500 snapshots were used in most cases.

In addition to finding the average BER across the snapshots, a histogram of decision eye openings is obtained. This represents the probability distribution of eye openings for single diversity. Convolution of this distribution with itself gives the distribution for dual diversity. Repeating the same calculation with the dual diversity distribution gives the quad diversity distribution. The BER for dual or quad diversity is then calculated from the appropriate distribution. The advantage of this convolution technique is that with a computation of only N snapshots for single diversity the effect of N^2 snapshots (all eye voltages taken two at a time) for dual diversity and N^4 snapshots for quad diversity is obtained. Without this technique for extrapolating single diversity results to dual or quad, direct computation for either would be prohibitive.

The DAR receiver is simulated as shown in Figure 11. The reference is obtained by averaging over eight symbols after decision feedback to bring each symbol to the reference phase state. This integrating time corresponds to that obtained in practice using a coherent recirculating delay line. After multiplying by the complex reference, the signal is passed through an integrate and dump filter which is modeled in the frequency domain as a $\sin(x)/x$ filter. The optimum clock sampling point is found using one of several techniques (e.g. maximum eye opening, early late gate, best BER clock point) and each symbol is sampled in-phase and quadrature to obtain the bit decision eye voltages. For cases where the data is redundant on the two frequencies, the same probing sequence is used on each frequency and the eye voltages for the same bits are added together to obtain a single eye voltage. The signals are normalized so that an eye voltage of 1 is expected in the ideal case of a perfect channel, zero intersymbol interference and perfect matched filtering. Then the BER for a bit with actual eye voltage x is simply $.5 \operatorname{ERFC}(x/\sqrt{\gamma})$ where γ is E_b/N_0 (energy per bit to noise power density ratio) as a number.

Typical BER results obtained using these analysis techniques are shown in Figures 12 - 14 for 2304 Kbps in 3.5 and 7.0 MHz and 288 Kbps in 3.5 MHz. For each case, 500 channel snapshots were computed, and the worst case dispersion channel profile C was used. Note that there is an improvement of about 3 dB obtained by increasing the bandwidth from 3.5 to 7.0 MHz for quad diversity and even more in dual diversity where an error flooring trend is evident.

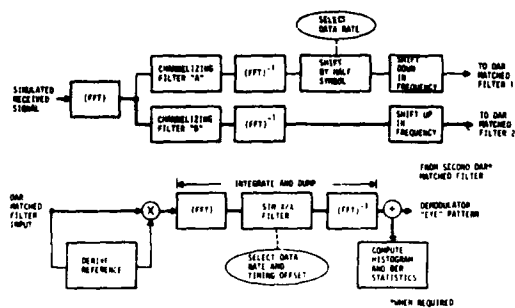


Figure 11 Computer Simulation Model of Two-Frequency DAR Receiver (Profile C)

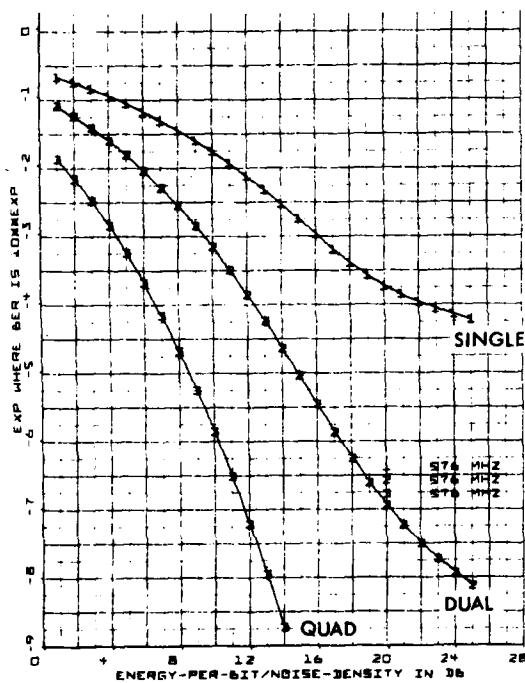


Figure 12 Bit Error Rate Performance at 2.304 MBPS in a 3.5 MHz Spectral Confinement (Profile C)

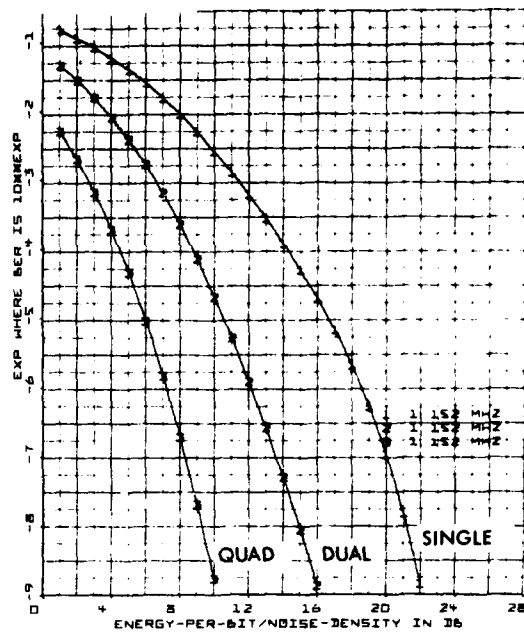


Figure 13 Bit Error Rate Performance at 2.304 MBPS in a 7 MHz Spectral Confinement (Profile C)

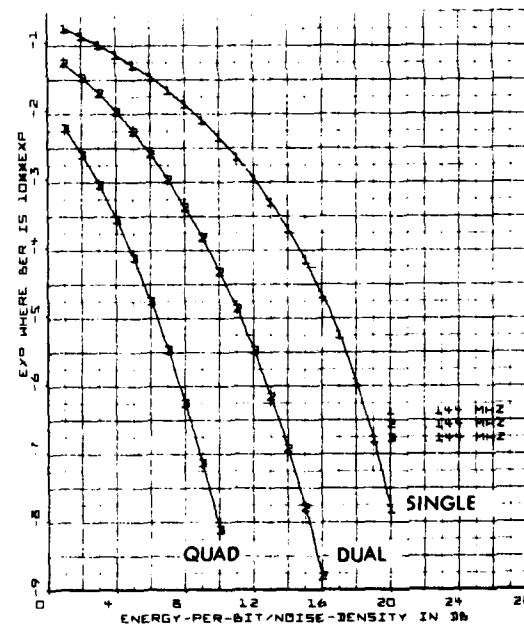


Figure 14 Bit Error Rate Performance at 288 KBPS in a 3.5 MHz Spectral Confinement (Profile C)

5.0 Summary

In typical application to digital troposcatter, the two frequency pulse version of the DAR will provide about a 2 dB performance improvement over the original DAR modem described in the literature.

Where bandwidths on the order of 1.5 Hertz/bit are available, the new approach can provide increased multipath handling capability (increased troposcatter range) and better utilization of transmitter energy. The cost of this two frequency version is about twice the circuitry of the original DAR, but the overall complexity is still low relative to alternative digital modulation schemes of comparable performance. Where bandwidths of 3 Hertz/bit are available, the two frequency approach can be used with negligible increase in the DAR circuitry over the original version. (That is, in the wider bandwidth case, a single DAR matched filter can demodulate the f_1 and f_2 pulses simultaneously after they have been appropriately deinterleaved.) In either case, the applicability of the DAR technique to various digital troposcatter applications is greatly enhanced by this new approach.

6.0 References

1. M. G. Unkauf, "High Speed Digital Troposcatter Technology", 1973 URSI Meeting, Boulder, Colorado, August 22, 1973.
2. M. G. Unkauf, "An Acoustic Surface Wave Modem for the Time-Variant Dispersive Channel", Symposium Record, MRI International Symposium XXIII, New York, N.Y., April 16, 1974 (to be published).
3. M. G. Unkauf and O. A. Tagliaferri, "An Adaptive Matched Filter Modem for Digital Troposcatter" ICC-75 Conference Record, 16-18 June 1975.
4. U. S. Patent #3,794,921 February 26, 1974.
5. RADC Contract F30602-73-C-0273 dated May 15, 1973.
6. ESD Contract F19628-75-C-0103 dated November 18, 1974.
7. ESD Contract F19628-76-C-0195 dated July 1976.

APPENDIX B-1

US/NATO OVER-THE-AIR TESTS

RUN DATA - KINSBACH TO FELDBERG

FLY NUMBER	DATE	DIVER	DATA	RS	CON	TIME	BER	NOTES
				R1	R2			
045	1/8	Q	7	54	53		1.3×10^{-9}	0
046	1/8	Q	7	54	53		1.2×10^{-9}	0
047	1/8	Q	7	54	53		1.0×10^{-9}	0
048	1/8	Q	7	54	53		7.5×10^{-9}	0
049	1/8	Q	7	55	53		1.7×10^{-9}	0
050	1/8	Q	7	56	53		1.1×10^{-9}	0
051	1/8	Q	7	55	50		5.4×10^{-9}	0
052	1/8	Q	7	55	53		8.5×10^{-9}	0
053	1/8	Q	7	57	53		5.4×10^{-10}	0
054	1/8	Q	7	54	53		0	0
055	1/8	Q	7	56	53		5.4×10^{-10}	0
056	1/8	Q	7	56	53		3.1×10^{-10}	0
057	1/8	D	7		53		1.1×10^{-9}	0
058	1/8	D	7		53		2.7×10^{-10}	0
059	1/8	D	7		53		6.7×10^{-10}	0
060	1/8	NON-DIV	7				3.9×10^{-9}	0
061	1/8	D	7	MOTOR LOST - DIVER LEFT THE NIGHT				
062	1/8	D	7		53		9.1×10^{-10}	0
063	1/8	D	7		53		1.3×10^{-9}	0
064	2/8	D	7		53		2.7×10^{-10}	0
065	2/8	D	7		63		0	0
066	2/8	D	7		53		1.3×10^{-9}	0
067	2/8	D	7	54			8.1×10^{-10}	0
068	2/8	D	7	54			4×10^{-10}	0
069	2/8	D	7	54			5.4×10^{-10}	0
070	1/8	D	7	55			1.2×10^{-9}	0
071	2/8	D	7	55			8.1×10^{-10}	0
072	2/8	NON-DIV	7	54			1.3×10^{-9}	0
073	1/8	NON-DIV	7		52		5.6×10^{-10}	0
074	2/8	NON-DIV	7				2.8×10^{-9}	0
075	1/8	NON-DIV	7		53		6.2×10^{-9}	0
076	2/8	D	7		53		5.4×10^{-10}	0
077	2/8	D	7		53		2.2×10^{-9}	0
078	2/8	D	7		53		5.4×10^{-10}	0
079	2/8	D	7		53		6.7×10^{-10}	0
080	2/8	D	7	MOTOR LOST - DIVER LEFT THE NIGHT				

FLY NUMBER	DATE	DIVER	DATA	RS	CON	TIME	BER	NOTES
				R1	R2			
081	2/8	D	7		53			
082	2/8	D	7		53			
083	3/8	D	7		57			
084	3/8	D	7		57			
085	3/8	D	7		58			
086	3/8	D	7		57			
087	3/8	D	7	57	57			
088	3/8	D	7	57	57			
089	3/8	D	7	57	57			
090	3/8	D	7	56	53			
091	3/8	D	7	56	53			
092	3/8	D	7	57	53			
093	3/8	D	7	57	53			
094	3/8	D	7	56	53			
095	3/8	D	7	56	53			
096	3/8	D	7	56	53			
097	3/8	D	7	53	53			
098	3/8	D	7	53	53			
099	3/8	D	7	53	53			
100	3/8	D	7	56	53			
101	3/8	D	7	53	53			
102	3/8	D	7	53	53			
103	3/8	D	7	53	53			
104	3/8	D	7	53	53			
105	3/8	D	7	53				
106	3/8	D	7	53				
107	3/8	D	7	53				
108	3/8	D	7	57				
109	3/8	D	7	53				
110	3/8	D	7	53				
111	3/8	D	7	54				
112	3/8	D	7	54				
113	3/8	D	7	53				
114	3/8	D	7	53				
115	3/8	D	7	53				
116	3/8	D	7	53				

THIS PAGE IS BEING
FROM COPY FORWARDED

B-1-1

D.U.V. NUMBER	DATE	DIVER	DATA SITE	RSL (DBM)				MEAN SNR	BER	NOTES MILES
				Rx1	Rx2	Rx3	Rx4			
153	5/8	Q	7A015	53	53	53	53	45	0	0
154	5/8	Q	7	53	53	53	53	45	0	0
155	5/8	Q	7	53	53	53	52	45	2.7×10^{-10}	0
156	5/8	Q	7	53	53	53	53	45	2.7×10^{-10}	0
157	5/8	Q	7	53	53	53	52	45	0	0
158	5/8	Q	7	53	53	53	-	45	2.7×10^{-10}	0
159	5/8	Q	7	53	53	53	52	45	0	0
160	5/8	Q	7	53	53	53	52	45	5.4×10^{-10}	0
161	5/8	Q	7	53	53	53	52	45	0	0
162	5/8	Q	7	53	53	53	53	45	0	0
163	5/8	Q	7	53	53	53	53	45	0	0
164	5/8	Q	7	53	53	53	53	45	0	0
165	5/8	Q	7	54	53	53	53	45	5.4×10^{-10}	0
166	5/8	Q	7	53	53	53	53	45	2.7×10^{-10}	0
167	5/8	Q	7	56	53	53	53	44	2.7×10^{-10}	0
168	5/8	Q	7	NIGHT	RUN	10 8	4045		2.8×10^{-10}	0
169	6/8	D-143	7	10A2	PLJ5	NIS-4	RUN	23 HOURS	1.6×10^{-7}	32 SAME COMMENT AS RUN 136
170	7/8	D	7		59		57	40	2.7×10^{-10}	0
171	7/8	D	7A035		56		55	43	2.7×10^{-10}	0
172	7/8	D	7		65		63	34	2.2×10^{-9}	1.7×10^{-5} ACTIVE FADING
173	7/8	D	7		57		55	42	1.4×10^{-8}	0
174	7/8	D	7		59		58	40	4.6×10^{-5}	1.7×10^{-5} EXTREMELY ACTIVE FADING
175	7/8	D	7		54		53	45	2.7×10^{-10}	0
176	7/8	D	7		56		55	43	2.7×10^{-10}	0
177	7/8	D	7		54		53	45	0	0
178	7/8	D	7		53		53	45	0	0
179	7/8	D	7		54		53	45	0	0
180	7/8	D	7		53		53	45	2.7×10^{-10}	0
181	7/8	D	7		54		53	45	2.8×10^{-9}	4.3×10^{-3} ACTIVE FADING
182	7/8	D	7		60		57	39	9.2×10^{-9}	0 FADING
183	7/8	D	7		62		56	34	1.2×10^{-6}	4.3×10^{-3} ACTIVE FADING
184	7/8	D-2+4	7	SIGNAL	WRISTED	FIN	SPECTRUM			
185	7/8	Q	7	66	65	65	64	33	2.2×10^{-9}	0 THUNDER STORM REPORTED BY VISUALITY
186	7/8	Q	7	62	59	60	57	39	0	0 ACTIVE FADING
187	7/8	Q	7	63	64	61	62	36	2.7×10^{-10}	0 ACTIVE FADING
188	7/8	Q	7	57	56	57	53	42	2.7×10^{-10}	

THIS PAGE IS DUB OF COPY FROM COPY
FROM COPY FROM COPY TO DUB

B-1-2

2

RUN NUMBER	DATE	DIVER-SITY	DATA RATE	Rx1	Rx2	Rx3	Rx4	BER	LAGS MINUTES
261	10/8	NO-DIV	3.5 Mbps	56				0	0
262	10/8	Q	3.5	56	54	56	54	0	0
263	10/8	Q	3.5	59	57	60	57	0	0
264	10/8	Q	3.5		NO			0	0
265	10/8	Q	3.5	57	56	57	54	0	0
266	10/8	Q	3.5	57	56	57	54	0	0
267	10/8	Q	3.5	57	56	58	56	0	0
268	10/8	Q	3.5	57	55	55	55	0	0
269	10/8	Q	3.5	54	53	53	49	0	0
270	10/8	Q	3.5	58	57	58	56	0	0
271	10/8	Q	3.5	56	53	57	53	0	0
272	10/8	Q	7 Mbps		57	58	58	1.35×10^{-11}	0
273	11/8	D	7	58		58		1.35×10^{-10}	0
274	11/8	D	7	57		57		5.4×10^{-10}	0
275	11/8	D	7	54		54		2.7×10^{-10}	0
276	11/8	D	7	54		53		0	0
277	11/8	D	7	53		53		0	0
278	11/8	D	7	54		54		0	0
279	11/8	D	7 Mbps	55		55		2.7×10^{-10}	0
280	11/8	D	7	54		54		1×10^{-9}	0
281	11/8	D	7	53		53		0	0
282	11/8	D	7	55		56		2.7×10^{-10}	0
283	11/8	D	7	55		56		2.7×10^{-10}	0
284	11/8	D	7	56		56		0	0
285	11/8	D	7	56		56		0	0
286	11/8	D	7	56		53		0	0
287	11/8	D	7	56		53		0	0
288	11/8	D	7	57		56		0	0
289	11/8	D	7	57		56		0	0
290	11/8	D	7	57		55		2.7×10^{-10}	0
291	11/8	D	7	57		56		2.7×10^{-10}	0
292	11/8	D	7	56		56		2.7×10^{-10}	0
293	11/8	D	7	57		56		0	0
294	11/8	D	7	57		56		0	0
295	11/8	D	7	56		56		0	0
296	11/8	D	7	56		56		0	0
297	11/8	D	7	56		56		0	0
298	11/8	D	7	56		56		0	0
299	11/8	D	7	56		56		0	0
300	11/8	D	7	56		56		0	0
301	11/8	D	7	56		56		0	0
302	11/8	D	7	56		56		0	0
303	11/8	D	7	56		56		0	0
304	11/8	D	7	56		56		0	0
305	11/8	D	7	56		56		0	0
306	11/8	D	7	56		56		0	0
307	11/8	D	7	56		56		0	0
308	11/8	D	7	56		56		0	0
309	11/8	D	7	56		56		0	0
310	11/8	D	7	56		56		0	0
311	11/8	D	7	56		56		0	0
312	11/8	D	7	56		56		0	0
313	11/8	D	7	56		56		0	0
314	11/8	D	7	56		56		0	0
315	11/8	D	7 Mbps	55		55		2.7×10^{-10}	0
316	11/8	D	7	55		55		1×10^{-9}	0
317	11/8	D	7	57		53		0	0
318	11/8	D	7	54		53		2.7×10^{-10}	0
319	11/8	D	7	56		53		2.7×10^{-10}	0
320	11/8	D	7	56		53		0	0
321	11/8	D	7	56		53		0	0
322	11/8	D	7	56		53		0	0
323	11/8	D	7	56		53		0	0
324	11/8	D	7	56		53		0	0
325	11/8	D	7	56		53		0	0
326	11/8	D	7	56		53		0	0
327	11/8	D	7	56		53		0	0
328	11/8	D	7	56		53		0	0
329	11/8	D	7	56		53		0	0
330	11/8	D	7	56		53		0	0
331	11/8	D	7	56		53		0	0
332	11/8	D	7	56		53		0	0

RUN NUMBER	DATE	DIVER-SITY	DATA RATE	Rx1	Rx2	Rx3	Rx4	BER	LAGS MINUTES
297	12/8	Q	7 Mbps	55	53	53	53	0	0
298	12/8	Q	7	NO				0	0
299	12/8	Q	7	66	64	64	62	0	0
300	12/8	Q	7	59	57	57	56	0	0
301	12/8	Q	7	57	56	57	56	0	0
302	12/8	Q	7	53	53	53	52	0	0
303	12/8	Q	7	52	47	52	47	0	0
304	12/8	Q	7	53	53	53	52	0	0
305	12/8	Q	7	56	53	54	53	0	0
306	12/8	Q	7	54	53	53	53	0	0
307	12/8	Q	7	55	53	53	53	0	0
308	12/8	Q	7	56	53	53	53	0	0
309	12/8	Q	7	55	53	53	53	0	0
310	12/8	Q	7	56	53	53	53	0	0
311	12/8	Q	7	56	53	53	52	0	0
312	12/8	Q	7	57	53	53	53	0	0
313	12/8	Q	7	56	53	54	53	0	0
314	12/8	Q	7	56	53	53	53	0	0
315	12/8	Q	7 Mbps	55	53	53	53	0	0
316	12/8	Q	7	55	53	53	53	0	0
317	12/8	Q	7	57	53	53	53	0	0
318	12/8	Q	7	54	53	53	52	0	0
319	12/8	Q	7	56	53	53	52	0	0
320	12/8	Q	7	56	53	53	53	0	0
321	12/8	Q	7	56	53	53	53	0	0
322	12/8	D	7	57		56		0	0
323	12/8	D	7	57		56		0	0
324	12/8	D	7	57		56		0	0
325	12/8	D	7	56		54		0	0
326	12/8	D	7	54		53		0	0
327	12/8	D	7	54		53		0	0
328	12/8	D	7	55		54		0	0
329	12/8	D	7	56		53		0	0
330	12/8	D	7	56		53		0	0
331	12/8	D	7	54		53		0	0
332	12/8	D	7	54		53		0	0

THIS PAGE IS NOT FROM

B-1-4

BER	G. TAGES MINUTES
0	0
0	0
0	0
0	0
0	0
0	0
0	0
0	0
0	0
0	0
0	0
1.35×10^{-11}	0
1.35×10^{-10}	0
5.4×10^{-10}	0
2.7×10^{-10}	0
0	0
0	0
0	0
2.7×10^{-10}	0
1×10^{-9}	0
0	0
2.7×10^{-10}	0
2.7×10^{-10}	0
0	0
0	0
0	0
0	0
0	0
0	0
2.7×10^{-10}	0
2.7×10^{-10}	0
2.7×10^{-10}	0
0	0
0	0
3	0
.04 MUDAM LAST BEL	

THIS PAGE IS BEST QUALITY REPRODUCED FROM

朱

RUV NUMBER	DATE	DIVER- SITY	DATA RATE	RSL (DBM)				MEAN SNR	BER	OUTAGES MINUTES	
				Rx1	Rx2	Rx3	Rx4				
333	14/8	D	7	56		55		43	1.0×10^{-9}	0	
334	14/8	D	7	56		53		44	0	0	
335	14/8	D	7	53		53		45	0	0	
336	14/8	D	7	53		53		45	0	0	
337	14/8	D	7	56		56		42	0	0	
338	14/8	D	7	53		53		45	0	0	
339	14/8	D	7	57		57		41	5.4×10^{-10}	0	
340	14/8	D	7	56		55		43	2.1×10^{-8}	0	BER IS SUBJECT AS THE ECU DID NOT SHOW THE ANSWERS!
341	14/8	D	7	55		55		43	5.4×10^{-10}	0	
342	14/8	D	7	53		53		45	5.4×10^{-10}	0	
343	14/8	D	7	53		53		45	2.7×10^{-10}	0	
344	14/8	D	7	53		53		45	8.1×10^{-10}	0	
345	14/8	D	7		53		53	45	2.7×10^{-10}	0	
346	14/8	D	7		53		53	45	5.4×10^{-10}	0	
347	14/8	D	7		53		53	45	2.7×10^{-10}	0	
348	14/8	D	7		53		53	45	1.0×10^{-9}	0	
349	14/8	D	7		53		53	45	0	0	
350	14/8	D	7		53		53	45	0	0	

THIS PAGE IS BEST QUALITY PRACTICE
FROM COPY FURNISHED TO DDC

APPENDIX B-2

US/NATO OVER-THE-AIR TESTS

RUN DATA - DOSSO DEI GALLI TO FELDBERG

RUN #	DATE	DIV	DATA RATE	MEAN SNR				BER	OUTAGES
				1	2	3	4		
655	15 MAY 77	Q	7	RUN TIME					
654	15 MAY 77	Q	7	-75	-75	-75	-75	2.6×10^{-7}	0
653	15 MAY 77	Q	3.5					5.3×10^{-8}	3.6×10^{-3}
652	17 MAY 77	D 2+4	3.5					1.0×10^{-7}	0
651	17 MAY 77	D 2+4	3.5					3.2×10^{-9}	0
650	17 MAY 77	D 2+4	3.5					5.0×10^{-10}	0
649	17 MAY 77	D 1+3	3.5	-73				1.0×10^{-8}	0
648	17 MAY 77	D 1+3	3.5	-72				8.0×10^{-9}	0
647	17 MAY 77	D 1+3	3.5	-75				1.3×10^{-8}	0
646	17 MAY 77	NB 3	3.5					3.2×10^{-7}	.12
645	17 MAY 77	D 1+3	3.5	-76				2.9×10^{-7}	.12
644	17 MAY 77	Q	3.5	-72	-77	-72	-82	0.00001	0
643	17 MAY 77	Q	3.5	-72	-81	-73	-81	0.00001	0
642	16 MAY 77	Q	3.5					4.4×10^{-8}	.0084
641	16 MAY 77	Q	3.5	-70	-65	-70	-65	2.8×10^{-9}	0
640	16 MAY 77	Q	3.5	-70	-65	-70	-65	5.0×10^{-10}	0
639	16 MAY 77	Q	3.5	-70	-65	-70	-65	EQUIPMENT FAILURE TIMING RECOVERY	
638	16 MAY 77	Q	3.5	-70	-65	-70	-65	3.7×10^{-6}	.132
637	16 MAY 77	Q	3.5	-70	-65	-70	-65	1.9×10^{-6}	.18
636	16 MAY 77	Q	7	-72	-65	-72	-65	3.2×10^{-3}	5.94
635	16 MAY 77	Q	7	-73	-65	-71	-65	1.4×10^{-2}	11.52
634	16 MAY 77	Q	7	-67	-65	-67	-65	9.1×10^{-6}	.3
633	16 MAY 77	Q	7	-67	-65	-67	-65	8.4×10^{-6}	.42

RUN #	DATE	DIV	DATA RATE	MEAN SNR		BER	OUTAGES
				1	2		
695	21 MAY 77	D 2+4	3.5				
694	21 MAY 77	D 1+3	3.5				
693	21 MAY 77	D 1+3	3.5				
692	21 MAY 77	D 1+3	3.5				
691	21 MAY 77	Q	3.5				
690	21 MAY 77	Q	3.5				
689	21 MAY 77	Q	3.5				
688	20 MAY 77	D 2+4	3.5				
687	20 MAY 77	D 2+4	3.5				
686	20 MAY 77	D 2+4	3.5				
685	20 MAY 77	D 2+4	3.5				
684	20 MAY 77	D 2+4	3.5				
683	20 MAY 77	D 1+3	3.5				
682	20 MAY 77	D 1+3	3.5				
681	20 MAY 77	D 1+3	3.5				
680	20 MAY 77	D 1+3	3.5				
679	20 MAY 77	Q	3.5				
678	20 MAY 77	Q	3.5				
677	20 MAY 77	Q	3.5				
676	20 MAY 77	Q	3.5				
675	19 MAY 77	D 1+3	3.5				
674	19 MAY 77	D 1+3	3.5				
673	19 MAY 77	D 1+3	3.5				
672	19 MAY 77	D 1+3	3.5				
671	19 MAY 77	D 1+3	3.5				
670	19 MAY 77	Q	3.5				
669	18 MAY 77	Q	3.5				
668	18 MAY 77	Q	3.5				
667	18 MAY 77	Q	7				
666	18 MAY 77	Q	7				
665	18 MAY 77	Q	7				
664	18 MAY 77	Q	7				
663	18 MAY 77	Q	7				
662	18 MAY 77	Q	7				
661	18 MAY 77	Q	7				
660	18 MAY 77	Q	7				
659	18 MAY 77	Q	7				
658	18 MAY 77	Q	7				
657	18 MAY 77	Q	7				
656	18 MAY 77	Q	7				

THIS
FROM

B-2-1

BER OUTAGES

LINE	DATE	DATA RATE	RSL				MEAN SNR	BER	OUTAGES
			1	2	3	4			
675	20 MAY 77	3.5		-75		-80	+225	9.6x10 ⁻⁵	0.00
674	20 MAY 77	3.5	-73		-73		+34	0.00x10 ⁻⁵	0
673	20 MAY 77	3.5	-74		-72		+31	0.00x10 ⁻⁵	0
672	20 MAY 77	3.5	-72		-72		+33	0.00x10 ⁻⁵	0
671	20 MAY 77	3.5	-72	-77	-73	-85	+28	0.00x10 ⁻⁵	0
670	20 MAY 77	3.5	-72	-78	-73	-85	+28	0.00x10 ⁻⁵	0
689	20 MAY 77	3.5	-72	-77	-73	-85	+28	0.00x10 ⁻⁵	0
688	20 MAY 77	3.5						8.8x10 ⁻⁵	.10
687	20 MAY 77	3.5		-75		-74	+20	0.00x10 ⁻⁵	0
686	20 MAY 77	3.5		-77		-86	+26	1.8x10 ⁻⁸	0
685	20 MAY 77	3.5					+26	0.00x10 ⁻⁵	0
684	20 MAY 77	3.5		-77		-81	+26	0.00x10 ⁻⁵	0
683	20 MAY 77	3.5	-71		-70		+34	0.00x10 ⁻⁵	0
682	20 MAY 77	3.5	-68		-68		+37	0.00x10 ⁻⁵	0
681	20 MAY 77	3.5	-68		-67		+37	0.00x10 ⁻⁵	0
680	20 MAY 77	3.5	-68		-67		+37	0.00x10 ⁻⁵	0
679	20 MAY 77	3.5	-70	-77	-71	-82	+28	0.00x10 ⁻⁵	0
678	20 MAY 77	3.5	-78	-77	-72	-82	+28	0.00x10 ⁻⁵	0
677	20 MAY 77	3.5	-78	-77	-72	-81	+28	0.00x10 ⁻⁵	0
676	20 MAY 77	3.5	-77	-77	-72	-81	+28	0.00x10 ⁻⁵	0
675	10 MAY 77	3.5						4.9x10 ⁻³	1x10 ⁻⁵
674	10 MAY 77	3.5	-69		-69		+37	0.00x10 ⁻⁵	0
673	10 MAY 77	3.5	-73		-72		+33	0.00x10 ⁻⁵	0
672	10 MAY 77	3.5	-73		-72		+33	0.00x10 ⁻⁵	0
671	10 MAY 77	3.5	-73		-72		+33	0.00x10 ⁻⁵	0
670	10 MAY 77	3.5	LOST PA #1 R-00350 ADDED (RSL)						
669	18 MAY 77	3.5						9.2x10 ⁻⁴	.36
668	18 MAY 77	3.5	-70	-80	-67	-83	+27	0.00x10 ⁻⁵	0
667	18 MAY 77	7	-72	-82	-67	-84	+25	0.00x10 ⁻⁵	0
666	18 MAY 77	7	-72	-82	-67	-85	+25	2.3x10 ⁻⁸	.06
665	18 MAY 77	7	-70	-80	-67	-84	+27	2.3x10 ⁻⁷	.12
664	18 MAY 77	7	-72	-80	-67	-84	+26	3.4x10 ⁻⁸	0
663	18 MAY 77	7	-70	-78	-67	-84	+27	2.7x10 ⁻²	0.42
662	18 MAY 77	7	-72	-77	-67	-85	+27	2.4x10 ⁻⁸	0
661	18 MAY 77	7	-70	-78	-67	-85	+27	1.9x10 ⁻⁷	0
660	18 MAY 77	7	-70	-77	-67	-85	+27	6.3x10 ⁻⁷	.12
659	18 MAY 77	7	-72	-77	-67	-85	+27	4.2x10 ⁻⁷	.12
658	18 MAY 77	7	-72	-77	-67	-86	+26	1.9x10 ⁻⁷	0
657	18 MAY 77	7	-72	-77	-67	-86	+26	5.3x10 ⁻⁸	.12
656	18 MAY 77	7	-72	77	-67	-86	+26	3.5x10 ⁻⁷	0

THIS PAGE IS BEST QUALITY PRACTICE
FROM COPY FURNISHED TO DDC

R. #	DATE	DIV	DATA RATE	KSL				MEAN SNR	BER	OUTAG'S
				1	2	3	4			
775	5 JUN 77	Q	3.5	-75	-74	-74	-75	+20	1.1×10^{-9}	0
774	4 JUN 77	Q	3.5	-75	-75	-75	-75	+33	2.7×10^{-11}	0
773	3 JUN 77	Q	3.5	-73	-75	-76	-78	+30	5.4×10^{-6}	0
772	2 JUN 77	Q	3.5						2.2×10^{-6}	0.04
771	1 JUN 77	Q	3.5	-74	-77	-72	-80	+27	6.5×10^{-6}	1.1
770	31 MAY 77	Q	3.5	-72	-77	-72	-80	+35	1.3×10^{-7}	18
769	30 MAY 77	Q	3.5	-81	-73	-69	-78	+35	3.5×10^{-9}	0
768	29 MAY 77	Q	3.5	-67	-73	-67	-77	+34	2.3×10^{-7}	18
767	28 MAY 77	Q	3.5	-68	-73	-68	-78	+33	1.5×10^{-9}	0
766	27 MAY 77	Q	3.5	-67	-73	-68	-78	+33.5	1.5×10^{-7}	12
765	26 MAY 77	Q	3.5	-71	-74	-71	-80	+33	1.5×10^{-6}	3
764	25 MAY 77	Q	7	TERMINATED RUN CONDITIONS TOO SEVERE						
763	24 MAY 77	Q	7	-68	-77	-67	-83	+28	7.6×10^{-5}	2.1
762	23 MAY 77	Q	3.5						2.7×10^{-6}	4.1
761	22 MAY 77	Q	3.5	-63	-71	-64	-74	+37	0.000000	0
760	21 MAY 77	Q	3.5	-62.5	-73	-60	-73	+38	5×10^{-10}	0
759	20 MAY 77	Q	3.5	-64	-72	-64	-72	+37	1.1×10^{-9}	0
758	19 MAY 77	Q	3.5	-64	-72	-67	-72	+36	1.1×10^{-9}	0
757	18 MAY 77	Q	3.5	-70	-74	-70	-76	+33	5.8×10^{-8}	0
756	17 MAY 77	D 1+3	3.5						40×10^{-8}	9.2×10^{-3}
755	16 MAY 77	Q	3.5	-72	-81	-68	-80	+37	2.2×10^{-9}	0
754	15 MAY 77	Q	3.5	-74	-78	-72	-80	+29	7.5×10^{-9}	0
753	14 MAY 77	Q	3.5	-77	-80	-72	-80	+28	4.8×10^{-9}	0
752	13 MAY 77	Q	7	-70	-75	-72	-80	+37	5.5×10^{-4}	2.9
751	12 MAY 77	Q	7	-70	-79	-68	-80	+31	1.9×10^{-5}	1.2
750	11 MAY 77	Q	7	-70	-79	-70	-80	+30	6.7×10^{-7}	6
749	10 MAY 77	Q	3.5	-68	-77	-76	-78	0	0.000000	0
748	9 MAY 77	D 1+3	3.5						1.8×10^{-8}	0
747	8 MAY 77	D 1+3	3.5	-73		-72		+32.5	5.4×10^{-8}	0
746	7 MAY 77	D 1+3	3.5	-73		-72		+32.5	1.5×10^{-9}	0
745	6 MAY 77	D 1+3	3.5	-73		-72		+32.5	2.2×10^{-8}	0
744	5 MAY 77	D 1+3	3.5	-72		-70		+34	1.8×10^{-8}	0
743	4 MAY 77	Q	3.5	-74	-75	-69	-77	+31	0.000000	0
742	3 MAY 77	Q	3.5	-72	-74	-68	-77	+32	0.000000	0
741	2 MAY 77	Q	3.5	-72	-74	-69	-77	+32	3.2×10^{-8}	0
740	1 MAY 77	Q	3.5	-69	-72	-69	-78	+33	3.0×10^{-9}	0
739	30 APR 77	D 2+4	3.5						2.3×10^{-7}	0.43
738	29 APR 77	D 2+4	3.5						8.8×10^{-7}	0.064
737	28 APR 77	D 2+4	3.5		-78		-80	+26	7.3×10^{-8}	0
736	27 APR 77	D 2+4	3.5		-78		-82	+25	5.7×10^{-8}	0

R. #	DATE	DIV	DATA RATE	KSL	
				1	2
775	5 JUN 77	Q	3.5		
774	4 JUN 77	D 1+3	3.5		
773	3 JUN 77	D 2+4	3.5		
772	2 JUN 77	D 2+4	3.5		-72
771	1 JUN 77	D 2+4	3.5		-72
770	31 MAY 77	Q	3.5		
769	30 JUN 77	D 1+3	3.5	-64	
768	2 JUN 77	D 1+3	3.5	-67	
767	2 JUN 77	D 1+3	3.5	-66	
766	2 JUN 77	D 1+3	7	-68	
765	2 JUN 77	D 1+3	7	-60	
764	2 JUN 77	D 1+3	7	-63	
763	2 JUN 77	D 1+3	7	-63	
762	2 JUN 77	D 1+3	3.5	-62	
761	1 JUN 77	D 1+3	3.5	-66	
760	1 JUN 77	D 1+3	3.5	-66	
759	1 JUN 77	D 1+3	3.5	-66	
758	1 JUN 77	D 1+3	3.5	-66	-6
757	1 JUN 77	D 1+3	3.5	-65	-6
756	1 JUN 77	D 1+3	3.5	-66	-6
755	31 MAY 77	D 2+4	3.5		
754	31 MAY 77	D 2+4	3.5		-78
753	31 MAY 77	D 2+4	3.5		-80
752	31 MAY 77	D 2+4	3.5		-79
751	31 MAY 77	D 2+4	3.5		-75
750	31 MAY 77	Q	3.5	-67	-73
749	31 MAY 77	Q	3.5	-68	-73
748	30 MAY 77	D 1+3	3.5		
747	30 MAY 77	D 1+3	3.5	-66	
746	30 MAY 77	Q	3.5	-76	-77
745	30 MAY 77	Q	3.5	-76	-77
744	29 MAY 77	Q	3.5		
743	28 MAY 77	Q	3.5		MODERN LOS
742	27 MAY 77	Q	3.5		
741	27 MAY 77	D 1+3	3.5	-73	
740	27 MAY 77	D 1+3	3.5	-68	
739	27 MAY 77	D 1+3	3.5	-67	
738	27 MAY 77	D 1+3	3.5	-67	
737	27 MAY 77	Q	3.5	-75	-75
736	27 MAY 77	Q	3.5	-75	-76

BER	OUTAGES
1.1x10 ⁻⁹	0
2.7x10 ⁻⁹	0
5.4x10 ⁻¹⁰	0
2.2x10 ⁻⁶	.064
6.5x10 ⁻⁶	1.1
1.3x10 ⁻⁶	.18
3.5x10 ⁻⁹	0
2.3x10 ⁻⁷	.18
1.5x10 ⁻⁹	0
1.5x10 ⁻⁷	.12
1.5x10 ⁻⁶	.3
7.6x10 ⁻⁵	2.1
2.7x10 ⁻⁶	.41
0.000005	0
5x10 ⁻¹⁰	0
1.1x10 ⁻⁹	0
1.1x10 ⁻⁹	0
5.8x10 ⁻⁸	0
40x10 ⁻⁸	9.2x10 ⁻³
2.2x10 ⁻⁹	0
7.5x10 ⁻⁹	0
4.8x10 ⁻⁹	0
5.5x10 ⁻⁴	2.9
1.9x10 ⁻⁵	1.2
6.7x10 ⁻⁷	.6
0.000001	0
1.8x10 ⁻⁸	0
5.4x10 ⁻⁸	0
1.5x10 ⁻⁹	0
2.2x10 ⁻⁸	0
1.8x10 ⁻⁸	0
0.000001	0
0.000001	0
2.2x10 ⁻⁸	0
3.0x10 ⁻⁹	0
2.3x10 ⁻⁷	.045
8.8x10 ⁻⁷	.064
7.3x10 ⁻⁸	0
5.7x10 ⁻⁸	0

RUN #	DATE	DIV	DATA RATE	RSL				MEAN SNR	BER	OUTAGES
				1	2	3	4			
775	5 JUN 77	Q	3.5						9.3x10 ⁻⁶	7.6x10 ⁻⁴
774	4 JUN 77	D 1+3	3.5						6.8x10 ⁻⁶	.021
773	3 JUN 77	D 2+4	3.5						4.9x10 ⁻⁶	.02
772	2 JUN 77	D 2+4	3.5		-72		-70	+34	5.4x10 ⁻¹⁰	0
771	3 JUN 77	D 2+4	3.5		-72		-69	+35	6.3x10 ⁻⁸	0
770	2 JUN 77	Q	3.5						1.8x10 ⁻⁹	0
769	2 JUN 77	D 1+3	3.5	-64		-66		+34	0.000001	0
768	2 JUN 77	D 1+3	3.5	-67		-64		+40	5x10 ⁻¹⁰	0
767	2 JUN 77	D 1+3	3.5	-66		-65		+40	0.000001	0
766	2 JUN 77	D 1+3	7	-68		-67		+37.5	7x10 ⁻⁴	1.2
765	2 JUN 77	D 1+3	7	-60		-68		+45	8.1x10 ⁻⁷	.25
764	2 JUN 77	D 1+3	7	-63		-68		+40	3.1x10 ⁻⁷	2.05
763	2 JUN 77	D 1+3	7	-63		-66		+41	3.6x10 ⁻⁴	.7
762	2 JUN 77	D 1+3	3.5	-62		-67		+40	0.000001	0
761	1 JUN 77	D 1+3	8.5						1.1x10 ⁻⁸	2.05x10 ⁻³
760	1 JUN 77	D 1+3	3.5	-66		-66		+39	2.7x10 ⁻⁹	0
759	1 JUN 77	D 1+3	3.5	-66		-65		+39.5	7.8x10 ⁻⁹	0
758	1 JUN 77	D 1+3	3.5	-66		-66		+39	9.1x10 ⁻⁹	0
757	1 JUN 77	D 1+3	3.5	-65		-67		+39	5.4x10 ⁻¹⁰	0
756	1 JUN 77	D 1+3	3.5	-66		-67		+38.5	0.000001	0
755	31 MAY 77	D 2+4	3.5						2.7x10 ⁻⁸	2.9x10 ⁻³
754	31 MAY 77	D 2+4	3.5		-78		-78	+30	5.4x10 ⁻⁹	0
753	31 MAY 77	D 2+4	3.5		-80		-80	+28	1.4x10 ⁻⁸	0
752	31 MAY 77	D 2+4	3.5		-79		-79	+29	2.0x10 ⁻⁸	0
751	31 MAY 77	D 2+4	3.5		-75		-80	+27.5	1.1x10 ⁻⁷	0
750	31 MAY 77	Q	3.5	-67	-73	-67	-77	+34	1.9x10 ⁻⁸	0
749	31 MAY 77	Q	3.5	-68	-73	-68	-77	+32.5	2.7x10 ⁻⁹	0
748	30 MAY 77	D 1+3	3.5						6.3x10 ⁻⁸	.017
747	30 MAY 77	D 1+3	3.5	-66		-67		+38.5	0.000001	0
746	30 MAY 77	Q	3.5	-76	-77	-78	-78	+33	0.000001	0
745	30 MAY 77	Q	3.5	-76	-77	-78	-78	+33	5.4x10 ⁻⁹	0
744	29 MAY 77	Q	3.5						4.4x10 ⁻⁹	0
743	28 MAY 77	Q	3.5	MODEM LOST TIMING						
742	27 MAY 77	Q	3.5						1.3x10 ⁻⁸	.0025
741	27 MAY 77	D 1+3	3.5	-73		-75		+37	2.3x10 ⁻⁸	0
740	27 MAY 77	D 1+3	3.5	-68		-68		+37	2.0x10 ⁻⁸	0
739	27 MAY 77	D 1+3	3.5	-67		-68		+37.5	2.8x10 ⁻⁸	0
738	27 MAY 77	D 1+3	3.5	-67		-67		+38	1.3x10 ⁻⁸	0
737	27 MAY 77	Q	3.5	-75	-75	-73	-78	+33	3.2x10 ⁻⁹	0
736	27 MAY 77	Q	3.5	-75	-76	-73	-78	+33	5.4x10 ⁻¹⁰	0

B-2-2

THIS PAGE IS FOR QUALITY PROGRAMS
FROM COPY 2 & RETURNED TO DDC

4